ABSTRACT

Title of thesis: HYPERSONIC APPLICATION OF FOCUSED SCHLIEREN AND DEFLECTOMETRY

Colin VanDercreek, Master of Science, 2010

Thesis directed by: Associate Professor Kenneth Yu
Department of Aerospace Engineering

A non-intrusive diagnostic capability for determining the hypersonic shock and boundary layer structure was developed, installed, and successfully tested at the AEDC Hypervelocity Tunnel 9. This customized diagnostic involves a combination of a focused schlieren system, which relies on creating multiple virtual light sources using a Fresnel lens and a source grid, and a deflectometry system, which uses the focused schlieren and a photomultiplier tube. It was used for obtaining spatially resolved images of density gradients with a depth of focus less than one centimeter, while allowing high frequency measurements of density fluctuations. The diagnostic was applied in investigating the second mode instability waves present in the boundary layer of a sharp-nosed cone submerged in a Mach 10 flow. The waves were successfully imaged and their frequencies were measured even though the flow density was below 0.01 $\frac{kg}{m^3}$ and the frequencies over 200 kHz. This adds a new capability to hypersonic testing.

HYPERSONIC APPLICATION OF FOCUSED SCHLIEREN AND DEFLECTOMETRY

by

Colin Paul VanDercreek

Thesis submitted to the Faculty of the Graduate School of the
University of Maryland, College Park in partial fulfillment
of the requirements for the degree of
M.S. in Aerospace
Engineering
2010

Advisory Committee:
Associate Professor Kenneth H. Yu, Chair
Associate Professor Chris Cadou
Professor Mark Lewis

© Copyright by
Colin VanDercreek
2010

Dedication

To Badger

Acknowledgments

I would like to thank the extremely knowledgeable and dedicated staff of Tunnel 9, especially Mike Smith for their support and assistance. My advisor Dr. Yu has been very helpful by giving me excellent advice on improving my research. Additionally, I would like to thank AFOSR, Purdue University, and Dr. Settles group at Penn State University for their support and assistance.

Table of Contents

List of Tables

List of Figures

List of Abbreviations

n	Index of Refraction
k	Gladstone-Dale coefficient
ρ	Density
ϵ	Angle of deflection
n_0	Refractive index of surrounding medium
α	The smallest ratio between the change in illumination due to a disturbance and the initial illumination
E	Image illumination
a	Light source image height above cut-off
ϵ_m	Smallest detectable angle of deflection
S	Distance from disturbance to knife edge
f	Focal length
L	Distance from source grid to imaging lens
l	Distance from region of interest to imaging lens
l'	Distance from imaging lens to imaging plane
L'	Distance from imaging lens to cut-off grid
w	Resolution
λ	Wavelength of light
b	Spacing between opaque lines in the cut-off grid
A	Aperture of imaging lens
DS	Depth of sharp focus
DU	Depth of unsharp focus
R	$\frac{l}{A}$
θ	Angle of ray bundle from individual source slit
a_2	Distance between center lines of adjacent slits
ϕ	Number of pairs of cutoff gridlines that blend together to form a schlieren image
x	Distance from plane of interest
N	Number of opaque and transparent line pairs
Ω	Ohms
L_F	Fresnel Lens
L_S	Schlieren Lens
L_R	Relay Lens
f_{LF}	Focal length of Fresnel Lens
f_{LS}	Focal length of schlieren Lens
f_{LR}	Focal length of relay Lens
γ	Ratio of specific heats
L^*	Distance from shock to cavity base
R_{air}	Ideal gas constant for air
T_o	Stagnation Temperature

AEDC	Arnold Engineering Development Center
AFOSR	Air Force Office of Scientific Research
PIV	Particle Image Velocimetry
LDI	Laser Differential Interferometry

Chapter 1

Introduction

Sustained hypersonic flight is critical to the future of aerospace technology. Currently, re-entry vehicles such as spacecraft [1] are the dominant application of hypersonic aerodynamics. As technologies mature, hypersonic vehicles will increasingly be relied on for low cost access to space and rapid global transportation. However there are many issues, such as transition prediction and thermal management, preventing sustained hypersonic travel from being practical. The accuracy of the prediction of the hypersonic flow over a vehicle is critical to designing an efficient vehicle [2]. Accurate prediction of where transition occurs is a critical area of research and is necessary to design hypersonic vehicles more effectively [3]. Knowledge of the transition location is important because it has a significant effect on the vehicle's lifting properties and the amount of heat transfer into a vehicle. Current hypersonic vehicle designs are conservative when it comes to thermal protection due to the uncertainty surrounding the prediction of transition. Increasing thermal protection adds more weight to the vehicle. With a more accurate understanding of the aerodynamics, vehicles can be optimized to reduce weight, increase performance, and reduce operational cost. In order to develop new theories and computational models, experimental data is critical. The focused schlieren and deflectometry diagnostic tools developed in this thesis will be a non-intrusive and flexible new capability for

acquiring hypersonic wind tunnel data to help improve the understanding of flow properties in order to improve hypersonic vehicle designs.

1.1 Motivation

Wind tunnel testing is a critical part of the development and advancement of aerospace technologies [4]. Hypersonic wind tunnel testing is an important tool for investigating boundary layer transition and other hypersonic flow phenomena. Tunnel 9, located in White Oak Maryland and part of the United States Air Force's Arnold Engineering Development Center, is on the forefront of hypersonic wind tunnel testing. In order to maintain its technical edge, Tunnel 9 is constantly developing new diagnostic tools, such as focused schlieren and deflectometry, to meet its customers evolving requirements. A major focus of Tunnel 9's work is to improve the understanding of flow physics in order to validate their customer's computational tools. Developing tools, such as focused schlieren and deflectometry, to gather new data on hypersonic boundary layer transition is important to advancing knowledge in this research area.

Knowing where transition occurs in a hypersonic boundary layer is extremely important because the magnitude of heat transfer increases by approximately a factor of five [5] in the turbulent boundary layer. Second mode instability waves are a boundary layer phenomena that plays a key role in predicting the onset of transition [2, 6–8]. Measuring the amplitude and frequency of these waves as they develop along a body is important to improve the current understanding of the formation and

propagation of this phenomena. Knowledge of the location and frequency of these waves allows for the correlation of numerical predictions from computational fluid dynamics (CFD) solvers and data collected from wind tunnel testing. Measuring the frequency of these waves non-intrusively is a significant contribution of this research [6]. Non-intrusive measurement allows for significant flexibility in where along the model data is collected and at how many points. As an example, using schlieren imaging data and the deflectometry diagnostic developed in the present work, the location of where data is collected can quickly be changed between wind tunnel runs based on the images collected using focused schlieren. Using a non-intrusive diagnostic such as focused schlieren and deflectometry diagnostic will open new avenues of research by adding a new capability for collecting this data.

Diagnostics fall into two categories, intrusive and non-intrusive. Measuring flow properties along the surface of a model in a wind tunnel is often done using intrusive methods. When investigating boundary layer properties it becomes more complicated to take measurements intrusively without altering the flow properties [9]. Intrusive measurement techniques such as pressure transducers, flow seeding, and hot-wire anemometry can be unsuitable for certain types of flows or experiments. Hypersonic wind tunnels present many challenges for flow seeding and hot-wire anemometry. Flow seeding becomes unfeasible as the flow Mach number increases due to the requisite particle size becoming extremely small in order to accurately follow the flow [10]. For hypersonic testing, hot-wire anemometry has two issues, first the wire can break in the high dynamic pressure and secondly there is a non-linear response due to large changes in enthalpy [11]. Pressure transducers, when

mounted flush to the surface, are minimally intrusive; however, the location of these transducers are fixed which reduces their flexibility. Non-intrusive diagnostic tools are advantageous because they are not physically limited to one point on the model and they do not interfere with the flow around the body.

Focused schlieren and deflectometry are non-intrusive flow diagnostic tools. The focused schlieren diagnostic is capable of spatially resolving regions of interest in the flow field along the optical axis. Deflectometry uses the schlieren image to measure the frequency of density fluctuations at a point in this region. The primary motivation for developing these diagnostics was to develop a non-intrusive, flexible diagnostic to image and measure density fluctuations in the hypersonic flows. The focus of this thesis was developing these diagnostics for examining boundary layer phenomena. These measurements are critical for understanding the physics of boundary layer transition [12].

1.2 Focused Schlieren and Deflectometry

Focused schlieren and deflectometry are diagnostic tools based on the schlieren principle where light refracted by density gradients is partially blocked and recorded. Schlieren imaging is a non-intrusive method of imaging density gradients over a body [13]. Conventional schlieren has two drawbacks. The first drawback is that this diagnostic has an infinite depth of field [14] because of the collimated light used to image the flow field. As a result, window aberrations, thermal gradients, and other disturbances will be imaged along with the flow of interest. The second

main drawback is that it is difficult to acquire quantitative data from conventional schlieren [15]. When quantitative data is calculated from conventional schlieren images, data from the flow of interest will be difficult to distinguish from other disturbances along the optical axis because the images along the optical axis are integrated. This limits the type of flows that can be examined to experiments involving simple flows such as jets [16–18].

Focused schlieren in conjunction with deflectometry rectifies these two drawbacks. The primary application of focused schlieren is flow visualization. The characteristic narrow depth-of-focus adds new capabilities to the commonly used schlieren technique. In situations where it is desirable to only visualize the flow in a specific plane, such as flow over a flap, focused schlieren provides this capability. This is useful in hypersonic wind tunnels such as Tunnel 9 which are capable of testing more than one model simultaneously. Focused schlieren allows for the selection of a region of interest to be imaged without imaging the shock waves created by other models or probes in the wind tunnel. Testing more than one model at a time decreases the amount of required runs. Since running a hypersonic wind tunnel is costly, having the ability to more efficiently utilize available resources is important.

Deflectometry is an important application of focused schlieren. This tool is coupled to the focused schlieren system to measure the frequency of density fluctuations at a point in the flow. These density fluctuations correspond to the fluctuations in light intensity in the schlieren image[16]. These fluctuations are measured by using an optical fiber to pass the light from the schlieren image to a photomultiplier tube and recorded using an oscilloscope. The important new capability this tool provides

is the ability to examine multiple regions in a hypersonic flow non-intrusively, while allowing for repositioning the measurement location in minutes. This is useful for measuring turbulence or boundary layer phenomena such as second-mode instability waves which was the application for this research.

1.3 Research Objectives

Previous work shows focused schlieren and deflectometry to be useful tools for investigating subsonic and supersonic airflows. These diagnostics are often used to investigate the internal structure of supersonic jets, transonic flow over flaps, and supersonic boundary layers. The few publications where focused schlieren has been used [12, 18–28] involve applications to well understood phenomena. Focused schlieren and deflectometry techniques have never been applied to hypersonic applications. An objective of this research was to apply focused schlieren and deflectometry to hypersonic boundary layer phenomena for the first time in order to develop a diagnostic for use in Tunnel 9's hypersonic wind tunnel.

The utility of this diagnostic for hypersonic applications was demonstrated during the Air Force Office of Scientific Research (AFOSR) sponsored transition cone test. Researchers from Sandia National Laboratory and Purdue University measured second-mode wave instabilities in the transition region of a 7° half angle sharp nosed cone at Tunnel 9. The objective of this research was to development a diagnostic capable of imaging and measuring the frequency of these waves. This diagnostic successfully accomplished this objective, thus demonstrating that deflectometry is

a suitable non-intrusive flow measurement technique for hypersonic boundary layer research. Measuring these waves non-intrusively can be difficult and having this capability adds new flexibility to current research techniques [6], which allows for future studies into the growth and propagation of second-mode instability waves.

In addition to imaging and measuring the frequency of second-mode instability waves. The other primary objective of this research is to simplify the construction of a focused schlieren diagnostic, which is more complicated than conventional schlieren set-ups. While the decision to use focused schlieren is application specific, by simplifying the set-up procedure for focused schlieren, this technique could become more widespread. Using updated techniques for creating different components, this diagnostic will be less time intensive to install and operate.

The research objectives are summarized as follows:

- Develop and install a focused schlieren system that is sufficiently sensitive, has a small depth of sharp focus, and has a field of view large enough to be practical for use in a hypersonic wind tunnel.

- Develop and install a deflectometry diagnostic that will be useful for acquiring quantitative flow data.

- Demonstrate the use of focused schlieren and deflectometry in hypersonic testing by successfully imaging and measuring second-mode instability waves.

- Improve on techniques used to design focused schlieren and deflectometry diagnostics.

1.4 Scope

The development of the focused schlieren and deflectometry diagnostic is the primary focus of this thesis. The fundamental optical principles behind schlieren imaging will be discussed from a practical implementation perspective. The optimization optical layout to optimize the depth of focus, depth of field, and sensitivity of the focused schlieren diagnostic will be discussed in depth. Additionally, a key focus of this thesis is the development of deflectometry. Improving the alignment process to simplify data collection will be described. In order for deflectometry to be a useful tool, the signal to noise ration must be maximized in order to measure the frequency of density fluctuations. Methods for improving the signal to noise ratio of the deflectometry diagnostic is an important aspect of this thesis.

Demonstrating the feasibility and potential of this diagnostic is an important part of the scope of this project. The potential was demonstrated by measuring the frequency of and imaging the second-mode instability waves in the hypersonic boundary layer of a sharp-nosed cone. It is important to note that the detailed physics behind the creation and propagation of these waves is beyond the scope of this thesis.

Chapter 2

Theoretical Considerations

The principles behind schlieren have been applied to research into fluid dynamics for several hundred years. Many advances in fluid dynamics were made possible due to discoveries made with this technique. Schlieren imaging takes advantage of the fact that light is refracted as it passes through a density gradient. Partially blocking this refracted light with a knife edge or a cutoff grid, in the case of focused schlieren, creates an image of the density gradients. Over time, this technique has evolved into the conventional schlieren systems used today. The first investigations into focused schlieren began in the 1950s and have slowly evolved to its present state.

2.1 Literature Review

Fish and Parnham [19] made first mention of focused schlieren in a testing report by in 1950. This report does not refer to it as focused schlieren, but as schlieren with multiple light sources which is descriptive of the underlying principle behind this technique. Instead of treating the focusing ability in the conventional sense, they refer to it as a method to average out unwanted disturbances. The authors experimented with different optical configurations in an attempt to determine which had the best sensitivity and depth-of-field. This technical report first described the

most practical way to create the cutoff grid, used to block refracted light in the same manner as the knife edge in conventional schlieren. This method involves placing a photographic plate at the exact location where the image of the source grid is in focus. The source grid is a series of slits placed in between the light source and the test section. The source grid is a series of slits that creates the effect of multiple light sources. The image of the source grid is then exposed onto the photographic plate and the negative is used for the cutoff grid. Despite these developments, their initial design was impractical for general usage due to its small field of view which can be attributed to two causes. The author's reported significant vignetting which reduced their already small field of view. Additionally, this was due to the fact that the field of view for a focusing schlieren system will always be smaller than the light collection optics. For the case of their experiment, their field of view was on the order of 2 inches. It was concluded that focused schlieren was impractical for wind tunnel testing and better suited for small three dimensional investigations. Fish and Parnham's major contribution was developing the basic optical layouts for different focused schlieren designs. These designs were later examined in greater depth in Boedeker's Master's thesis [20].

Boedeker's thesis in 1959 [20] was the first work to demonstrate that focused schlieren is feasible for wind tunnel testing. He introduced the usage of the Fresnel lens to improve the practicality of focused schlieren by increasing the field of view and the illumination of the schlieren image. His thesis went into great detail analyzing the sensitivity and focusing capabilities of three different optical set-ups. Boedeker analyzed the different focused schlieren systems developed by Fish and Parnham.

Each system had a unique optical layout. Boedeker derived a unique optical relation to compare the sensitivity of each system. A detailed description of each system can be seen in his Master's thesis, [20]. Boedeker chose his second system as it had the most potential for experimental work. The key feature of this set-up was that it possessed a field of view large enough to be practical for wind tunnel testing. The practical field of view is due to the Fresnel lens being used to collect the light and focus it through the region of interest. For focused schlieren, the field of view will always be smaller than the Fresnel lens. Fresnel lenses can be made to dimensions on the order of a meter for very low cost when compared to conventional glass lenses. His second set-up is the basis for all future work in focused schlieren. His work sparked the first practical implementation of focused schlieren.

Over the next several decades there was little interest in developing focused schlieren further. In the early 90's Weinstein [21] refined Boedeker's design to make it significantly more useful for experimental work by improving the sensitivity and simplifying the design process. Weinstein's results were first published at the 29th Aerospace Sciences conference and subsequently in a journal article [22]. His biggest contribution to the field of focused schlieren was to derive equations that quantified the diagnostic parameters, such as the sensitivity, depth of field, and the resolution. This allows for a methodical design approach. In addition, he described improved methods of developing a focused schlieren diagnostic, such as avoiding diffraction effects through careful design of the cutoff grid. Weinstein's system was tested with two crossed jets that were separated along the optical path. As one jet was moved further away from the plane of focus it became increasingly blurred [21],

demonstrating the ability to focus on a specific plane. The focused schlieren system was compared with a shadowgraph and conventional schlieren system. All three imaging diagnostics were used to image a Mach 2 jet into the air. The focused schlieren system was not as sensitive as the conventional schlieren; however, internal flow structures not apparent in the conventional schlieren image were observed. The focused schlieren system was able to show the internal shock structure of the center of the jet that neither the shadowgraph or the conventional schlieren were able to image. This shows that focused schlieren has a critical role to play in examining detailed flow structures that cannot be easily observed by traditional schlieren.

Two years after Weinstein presented his work on focused schlieren, Collicott [24] wrote a paper analyzing the principles behind focused schlieren from an analytical perspective as opposed to Weinstein's more empirical approach. Collicott viewed the focusing aspect of focused schlieren as a method of noise reduction. The author used Fourier optic analysis to analyze a schlieren system with multiple sources. Each slit, or source, was modeled by treating it as a unique incoherent imaging system, which means that the light propagation integrals can be separated [24]. This was used to calculate the intensity of the image. The goal of this analysis was to create an analytical model to estimate the change of illumination in a schlieren image due to density gradients at different points along the optical axis. An effective transparency approximation was used to model the density changes outside of the plane of interest. This approximate assigned different opacity values to a density gradient depending on the strength of the gradient. This simplifies the model because the alternative would be to calculate the mutual intensity of the density gradients at

each plane which would require non-linear solutions.

This analytical model was tested using a three slit schlieren system and a Mach 2.5 flow over a wedge. A holographic plate was placed in the light path to simulate background noise. This plate had minimal absorption and only introduced phase disturbances. As the plate was moved further from the region of interest, its visibility decreased. The decrease in intensity of the plate was similar to that predicted by the analysis [24]. This paper provides an excellent analytical explanation and a more rigorous explanation of how focused schlieren works.

Gartenberg and Weinstein [26] used focused schlieren to examine flow over a model of a space shuttle prototype in the NASA Langley Research Center's cryogenic transonic wind tunnel. The author's focused schlieren system is based upon the techniques developed by Weinstein [22]. Focused schlieren was chosen for its sensitivity, large field of view, low cost, and narrow region of sharp focus [26]. It can be considered to be low cost since focused schlieren does not image optical imperfections (pits and or scratches), assuming they are outside the region of sharp focus, which obviates the need for expensive windows. Additionally unwanted turbulence, such as thermal gradients, do not appear in the final image. The NASA Langley focused schlieren system had a sensitivity of 13.9 *arcsec* and a depth of sharp focus of 6 *mm*. Using a Nd:YAG laser as a light source allowed the authors to capture freeze frame images of the flow structure over the test article. One advantage of focused schlieren is that only flow over the region of interest will be imaged. This was demonstrated in Gartenberg's wind tunnel experiments. The model of the space shuttle prototype had extensions on both wings to support the model. Imaging the

flow over these extensions can obscure the flow of interest, demonstrating the need for focused schlieren. The resulting schlieren images did not image the flow around the extensions, demonstrating the usefulness of focused schlieren. Additionally, the imaging system functioned as desired across the cryogenic tunnel's range of Mach numbers, pressures, and temperatures. It was sufficiently sensitive to image wake flows at Mach numbers as low as 0.4 and to image the boundary layer separation along the top of the model. With conventional schlieren this separation would most likely be overwhelmed by other flow features present along the optical path.

Particle Image Velocimetry (PIV) is an interesting application of schlieren. Conventional PIV involves seeding flows with small particles which are illuminated using lasers and imaged by high speed cameras. The cameras record pairs of images which are separated by a small time step which allows for software to calculate the distance each particle travels. Using this information, a velocity field can be calculated. PIV can be complicated by the fact that it requires particles that are small enough and light enough so that they closely follow the streamlines. When it comes to high speed flows, especially hypersonic flows, seeding becomes impractical due to the extremely small particles required, on the order of micrometers.

Research was done by Jonassen, Settles, and Tronosky [29] into using conventional schlieren for PIV. The advantage of using schlieren is that it is non-intrusive and that seeding can be complicated. Schlieren PIV works by recording images in quick succession so that the motion of flow turbulence can be frozen. The turbulent structures in the schlieren image are used to measure the flow progression by the PIV software. The researchers first examined a helium jet. They used schlieren PIV and

traditional PIV with seeding. The results were very similar showing that schlieren PIV is just as accurate. However, it was necessary to perform an Abel transform in order to get similar results. This was necessary to take into account the optical integration in the schlieren image. A focused schlieren PIV system would not have this problem. This method was also applied to a Mach 3 turbulent boundary layer in the Penn wind tunnel. After applying an Abel transform, schlieren PIV reasonably matched the traditional PIV results. The authors showed that for two dimensional cases and turbulent flows, schlieren PIV gives valid results. However, the authors acknowledge that by using a focused schlieren system, schlieren PIV would be more practical. Focused schlieren is advantageous because the PIV software would process the turbulent motion in the same plane as opposed to all turbulent motion along the optical axis. This would result in more accurate results and obviate the need for an Abel transform.

Work by McIntyre [16] describes the development of an optical deflectometer and its application to conventional schlieren. Optical deflectometry is non-intrusive and has a theoretically unlimited frequency response. It is well suited to replace diagnostics such as Laser Doppler Velocimetry and hot-wire anemometry. The seeding issues of Laser Doppler Velocimetry and the fragile wires required for hot-wire anemometry are reasons why deflectometry can be advantageous. Deflectometry is coupled to a schlieren system and uses photomultiplier tubes to measure the frequency of light fluctuations which are proportional to the fluctuations in density.

For this experiment a deflectometry diagnostic was integrated into a conventional schlieren system to examine a CO_2 jet. Two optical fibers were placed in

the schlieren image plane. These cables were connected to two Hamamatsu R928 photomultiplier tubes. A 1000 Ω terminator was used to provide adequate voltage drop and a flat frequency response to about 500 kHz. The signal was amplified by a Stanford systems SR640 amplifier/filter box and recorded with a 12 bit 10 Mhz Nicolet 430 oscilloscope.

Deflectometry is only capable of measuring deflections large enough that the schlieren system can detect. Therefore sensitivity is the same as the parent schlieren system. The deflectometer was found to work best when the schlieren was near full cutoff which resulted in a better signal to noise ratio. As the cutoff increases the signal decreases but the spectrum remains the same. The sample rates were a little over twice the low pass filter to avoid aliasing. The probes were placed in the centerline of the mixing layer. In order to test the coherence of flow turbulence, the horizontal separation of the fiber optics was varied in the test. The resulting data was windowed and a Fast Fourier Transform was performed on each window. Peaks in the data were an indicator of coherence in the structure. These results were compared with a Kulite pressure transducer and the results were very similar.

Alvi, Settles, and Weinstein [23] wrote a paper applying McIntyre's development of deflectometry in reference [16] to focused schlieren. Focused schlieren is a natural evolution of this diagnostic from its use with conventional schlieren. Deflectometry measures the frequencies at a point in the focused schlieren image, in a specific plane as opposed to measuring all fluctuations along the optical axis. This significantly improves the applicability of this diagnostic by allowing the operator to select the measurement location.

The frequency of Kelvin-Helmholtz vortices were measured in order to verify the diagnostic. The diagnostic that was designed by Alvi et al. was based on the focused schlieren diagnostic developed by Weinstein [22] and the deflectometry system designed by McIntyre [16]. To measure the frequency of the vortices, the fiber optic cables were placed in the centerline of the jet. Testing the focusing ability of the diagnostic paper was a major focus of this paper. In order to compare off design performance, the sensors were moved progressively away from the best focus region. As predicted, the system was extremely sensitive to changing the location along the optical axis of the deflectometry fibers, demonstrating the focusing ability. The signal becomes undistinguishable from background noise once the fiber optic is greater than 2 mm from the jet center line.

Garg and Settles [12] applied focused schlieren and deflectometry to investigating the turbulent boundary layer present along a supersonic wind tunnel's walls. This diagnostic was chosen since it is less complex than flow seeding and provides virtually unlimited frequency response, however this provides only local velocity measurements in contrast to the velocity field provided by PIV techniques. This technique is especially suited to high speed flows because hot wire anemometers are fragile and particle seeding becomes less practical as the flow speed increases. Accurate velocity calculations cannot be made if the signal is from light deflections integrated across the optical path. To get meaningful data in a turbulent flow, the background noise from flow outside the region of interest must be reduced to measure information at a specific point. Focused schlieren is well suited to resolving this issue.

The authors' focused schlieren diagnostic on the developments of Weinstein [22]. For this experiment, sensitivity is important in order to image boundary layer turbulence. Adequate sensitivity is dependent on the extinction ratio of the focused schlieren system, which is the ratio between the brightness of the image when there is no cutoff and when there is full cutoff. The authors improved upon Weinstein's focused schlieren apparatus by increasing the extinction ratio to $15:1$ from $6:1$. The authors had to compromise the sensitivity in favor of the depth of focus. A small (on the order of 2 mm) depth of sharp focus was necessary for accurately measuring the velocity of the boundary layer. The depth of sharp focus is dependent on the diffractive response which is dependent on the grid line spacing. The closer the spacing, the more the image is dominated by diffraction effects and therefore has less sensitivity. However, the depth of sharp focus decreases as the number of grid lines increases. This depth of sharp focus can also be referred to as the minimal integration limit, which is the distance at which the object will produce an N-fold decrease in image intensity. It is important to have the size of the integration limit close to the dimensions of the object of interest.

In order to verify the velocities calculated using deflectometry, the results were compared with velocity information measured using hot-wire anemometry. Both diagnostics had similar results which is expected due to the Reynolds analogy, which states that density, velocity, and mass flux variations are linearly related. Stream wise velocity correlations were performed by making deflectometry measurements separated by a known distance, x. The time between turbulent structures convection downstream was measured by correlating the data sets from each sensor. Using

the spacing distance, and the time between the two measurements, the velocity was calculated. It was found that these structures are fairly long lived and thus the sensors could separated by a distance as large as twice the thickness of the boundary layer. This technique was able to accurately measure the velocity profile in the boundary layer and matched the hot-wire measurements. An additional experiment was performed by spacing the deflectometry sensors vertically. The vertical sensors, received data before the horizontal sensors, implying that the boundary layer turbulence was not uniform in the horizontal direction. This paper is another example of how effective and flexible focused schlieren and deflectometry can be.

Deflectometry can also be used for acoustic research as shown by the radiated jet noise study by Petitjean et al [31]. Conventional schlieren, deflectometry, and microphones were used to analyze circular and beveled nozzles. The tests were performed with jets with a Mach number of 0.6, 0.9, and 1.5. Deflectometry was used to examine the turbulent mixing which is a major factor in the creation of jet noise. Jet noise is created by two components, large-scale turbulent structures and fine scale turbulent structures. The paper states that beveled nozzles produce less noise but the reason for this is not well understood. Their goal was to use deflectometry to enhance the understanding of the flow structures to better describe this reduction in noise. Conventional schlieren was used in conjunction with the deflectometry instruments. The authors acknowledged that the lack of focusing was a drawback to their experiment. Their deflectometry set up was based on an experiment by Doty [32], which was based upon work by McIntyre [16]. The authors used multiple photomultiplier tubes to calculate the velocity ratio between the jet

velocity and convection velocity. This value matched tabulated values, which again demonstrates the usefulness of deflectometry. Deflectometry was able to provide quantitative data on the flow structures in the jets. However, the authors were not successful in determining a reliable way to correlate the flow structure with noise production.

2.2 Theory

2.2.1 Conventional Schlieren

The first practical conventional schlieren diagnostic, which had a large field of view and was sufficiently sensitive, was developed by August Toepler in the 1850s as part of his doctoral studies at the Agricultural College of Poppelsdorf [33]. This schlieren system was sensitive enough to distinguish between air thermals that have a temperature difference of 1 °C. Toepler's technique was instrumental in many early discoveries in fluid dynamics. Over time improvements have been made to this original technique but the underlying design remains the same.

The fundamental principle that schlieren imaging is based upon is that when light passing through a transparent medium encounters a density gradient, it is refracted. The relationship between the refractive index n, and density ρ is:

$$n - 1 = k\rho \tag{2.1}$$

where k is the Gladstone-Dale coefficient which is approximately 0.23 cm^3/g and

n is 1.000292 for air [33]. This equation implies that sensitive optics are required since a two-fold change of density for air only results in a 3% change in the index of refraction. The relationship between the angle of deflection, ϵ_y and the change in refraction ($\frac{\partial n}{\partial y}$) and density $\frac{\partial \rho}{\partial y}$ is as follows:

$$\epsilon_y = \frac{L}{n_0}\frac{\partial n}{\partial y} = \frac{L}{n_0}k\frac{\partial \rho}{\partial y} \tag{2.2}$$

This equation came from Settles' book *Schlieren and Shadowgraph Techniques* [33]. The angle of deflection varies linearly with the change in density where n_0 is the index of refraction of the surrounding medium and L is defined in figure 2.1. As light passes through a density gradient, it is refracted. By partially blocking the refracted light, an image of the density gradient can be created.

The simplest schlieren system consists of a light source, source slit, two lenses or mirrors, a knife edge, and a viewing screen or camera. Light is emitted from the light source and passes through the source slit,which approximates a point source, and is collimated by the first lens or mirror. The collimated light passes through a test area. Any light that passes through a density gradient is refracted slightly by an angle ϵ. The light is then re-focused by the second lens or mirror. A knife edge is placed at the focal point and any light that has been refracted will be partially blocked by the knife edge. The amount of light blocked is dependent on the vertical placement of the knife edge, this placement controls the sensitivity. A diagram of conventional schlieren can be seen in figure 2.1 below. When the resulting light is imaged, the refracted light will show up as either darker or brighter regions in the

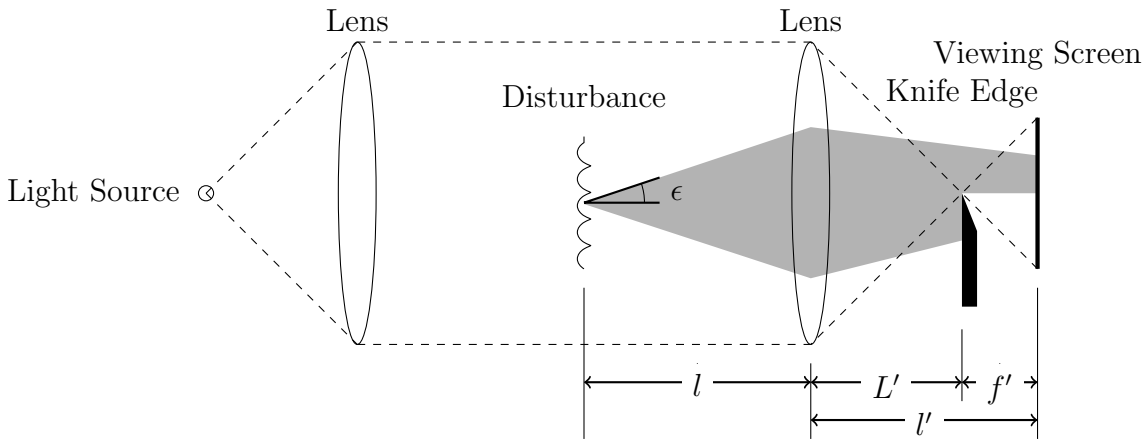

Figure 2.1: Conventional schlieren schematic

image, depending on the direction of the refraction. This image will therefore show the density gradients that correspond to the flow of interest. An alternative way to think of this, as described in Boedeker's 1959 Master's thesis [20], is that the knife-edge creates a light reservoir. As the height of the knife edge is raised, more light is blocked, decreasing the light reservoir. Smaller refractions of light which correspond to weaker density gradients, will be more visible when the knife-edge is higher. When the height is decreased more light is let through, increasing the illumination or light reservoir. The density gradients present in flow perturbations add or subtract from the light reservoir.

The main drawback to conventional schlieren systems is that it has an infinite depth of field. Every disturbance between the imaging optics is visible in the schlieren image. The same density gradient will produce the same change in light intensity regardless of where it is along the optical path. As a result, turbulence along wind tunnel walls or flow around instrumentation in the tunnel will be visible

along with the flow in the region of interest. In addition, any aberrations (scratches, dirt, etc.) in the wind tunnel windows will be visible in the final schlieren image. The significance of this issue depends on the test being run and the desired results. In situations such as deflectometry where total integration along the optical path is detrimental [23], focusing is needed. To overcome this drawback, focused schlieren has been developed and refined over the past 50 years.

2.2.2 Focused Schlieren

If multiple schlieren systems are used to examine slightly different regions in a flow, by merging the resulting images, the image of disturbances outside of a region of interest can be diminished in the final schlieren image. In order to simulate multiple schlieren systems, multiple light sources are needed [19], which are simulated by using a series of slits in front of the light source. This grid is referred to as the source grid. In conventional schlieren, the light passing through the source slit is a single band of light. The more bands of light, the greater the focusing ability. The basic focused schlieren system was developed and improved by Boedeker [20], Weinstein [21], and Settles [23].

Instead of a collimating mirror or lens present in conventional schlieren, focused schlieren has a Fresnel lens to collect and focus light from the light source. A Fresnel lens is used because as shown by Fish [19] and Boedeker [20], the field of view is always smaller than the lens used. The price of lenses increases dramatically as their size increases which renders traditional lenses impractical for large scale

experiments. Fresnel lenses are relatively cheap and can be made in sizes that allow for a substantially more practical system. In front of the Fresnel lens is a source grid that consists of equally spaced horizontal slits, each slit simulates a light source. The light passes through the region of interest and is imaged onto a cutoff grid which is the photographic negative of the source grid and the equivalent of multiple knife-edges. Behind the cutoff grid is the imaging plane. The image plane is where the image of the density gradients, present in the region of interest, is focused.

In order to focus, light is focused by the Fresnel lens through the source grid. Each slit simulates a separate light source, the bundles of light then pass through the object of interest creating an image for each band of light. If one has a view screen that can be adjusted along the optical axis, as the screen is moved towards the plane of focus, the objects will slowly begin to merge into one image. When the separate images align, the object is in focus. A diagram of this can be seen in figure 2.2. The object is represented by the pentagon in this simplified schematic. This schematic has been simplified by only showing the case where there are two slits, which will create only two separate images. All disturbances outside of the region of interest will be increasingly blurred the further their distance from this plane. This can be seen in figure 2.3, where the object is out of the plane of interest. As a result, the final image shown in the project has two offset images of the object, which is no longer in sharp focus. As the number of slits increases, the number of images of the density gradient or object will increase. If the number of slits are on the order of 20 or more, this diagnostic will have significant focusing capability. The plane of interest is not fixed for this diagnostic, to examine other regions it is simply a

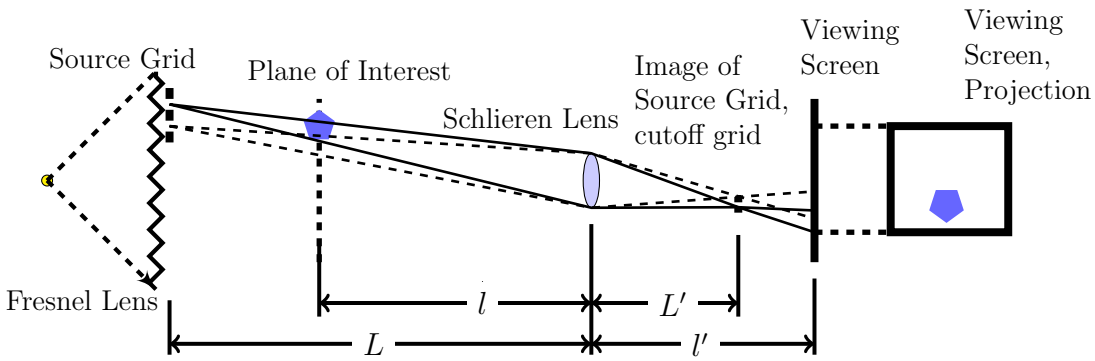

Figure 2.2: Focused schlieren theory, object in focus.

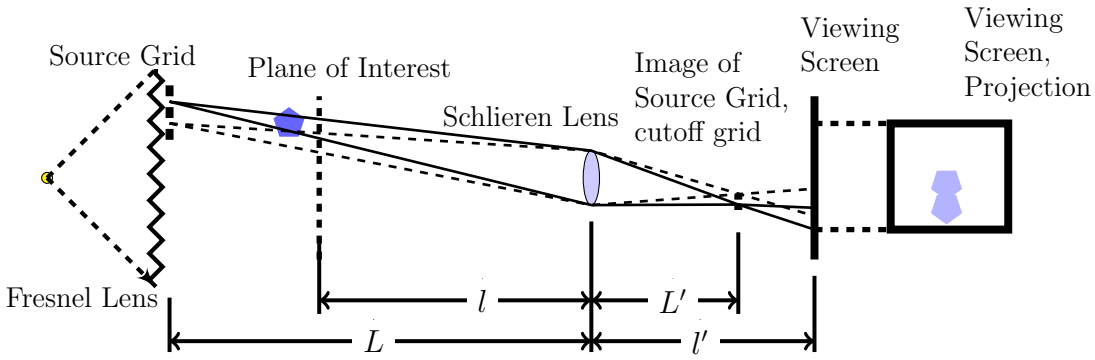

Figure 2.3: Focused schlieren theory, object out of focus.

matter of adjusting the image plane along the optical axis until the desired object is in focus.

Each light ray emitted from the source grid passes through multiple disturbances, which slightly refracts the light passing through the disturbance. These images will combine at a specific point on the optical axis, resulting in the final image. As light rays are added to the system, the resulting deflections are averaged together. Disturbances present in both light rays will be present, if there is a disturbance present in one ray but not another, the resulting image will have the disturbances intensity reduced. As light sources are added, this increases the

number of rays, which improves the focusing ability. Perturbations can never be completely eliminated from the final image, [19] but will reach a point where they surpass the ability of the optics to image and can be considered invisible.

Boedeker derived equation 2.4 in his Master's thesis [20]. This equation determines the smallest detectable angle of refracted light that the schlieren system can detect. This corresponds to the smallest detectable density gradient. S is the distance from the disturbance to the knife edge or cutoff grid. The value of S depends on the placement of lenses in the system and can be derived from the thin lens formula, equation 2.3 where f is the focal length of the lens, l is the object distance to the lens, and l' is the object's image distance from the lens.

$$\frac{1}{f} = \frac{1}{l} + \frac{1}{l'} \tag{2.3}$$

Using equation 2.3, a relationship between the location of the knife edge and the placement of the optics was determined for each of Boedeker's focused schlieren systems. The maximum sensitivity of a system is inherently dependent on the optical layout. Once the optical layout is set, the only variable that effects the amount of cutoff is the height of the knife edge a and the change in illumination α of the schlieren image. The definition of α can be seen in equation 2.5 where E is the image illumination. The value S is the distance from the region of interest to the cutoff grid. S is determined using the thin lens equation above, the geometry

of the focused schlieren system, and the optical properties of the lenses.

$$\epsilon_m = \frac{a\alpha}{S} \tag{2.4}$$

$$\alpha = \frac{\Delta E}{E} \tag{2.5}$$

Once S was calculated, Boedeker derived the equation for sensitivity [20]. This equation can be seen in equation 2.6 is as follows:

$$\epsilon_{mII} = \frac{(L-f)a\alpha}{f(L-l)} \tag{2.6}$$

The terms in this equation can be seen in figure 2.4. The notation has been modified from the original thesis to be consistent with this thesis. The performance of this system depends on the arrangement of the optics. The focusing ability improves as $\frac{l}{f}$ approaches one where f is the focal length of the schlieren lens and l is the distance from the region of interest to the schlieren lens. However this results in a smaller field of view and decreases the sensitivity. As the focal length increases, the system becomes more sensitive. Determining design trade-offs is an important part of designing a focused schlieren system. It is important to know which parameters depth of focus, sensitivity, or field of view are most important for one's experiment. The downside of focused schlieren is that its more complicated than conventional schlieren. Exact alignment of optical components such as the cutoff grid is critical to a functional focused schlieren diagnostic. Creating components, such as the source grid and cutoff grid, is a complex procedure. Any resulting defects can have

significant consequences to the functionality of this tool.

Due to the reasons stated previously, Weinstein [21] based his focused schlieren system on arrangement two as defined above. One significant contribution made by him is the definition of design criteria to help design a system to meet a set of desired specifications, such as the depth-of-focus. The definition of minimal sensitivity is similar to that of Fish and Parnham [19]. This definition, from Weinstein's paper [21], is as follows:

$$\epsilon_m = \frac{0.1aL}{L'(L-l)} rad = \frac{20626aL}{L'(L-l)} arcsec \tag{2.7}$$

The ratio between the change in illumination due to a disturbance and the initial illumination (α) was defined as 10%. This value was chosen because at the time 10 % was the smallest discernible change in illumination that could be imaged. The parameters in the above equation can be seen in figure 2.4 and 2.5. This differs from Boedeker's definition of sensitivity, equation 2.6, because Boedeker defines sensitivity as the smallest deflection detectable, while Weinstein defines it as the amount of deflection required to be visible when the system is cut off entirely. Weinstein's paper also differs from Boedeker by stating that sensitivity of a schlieren system cannot be arbitrarily increased by changing to focal length of the schlieren lens. There is a limit where diffraction effects overwhelm the refractions due to small disturbances. The accepted value [21] for maximum sensitivity (smallest detectable refraction) for both conventional and focused schlieren is $\epsilon_m = 4\ arcsec$. The ideal design of a focused schlieren system can be seen in figure 2.4. Figure 2.5 shows the geometric parameters of the cutoff grid. The black lines in this figure represent the

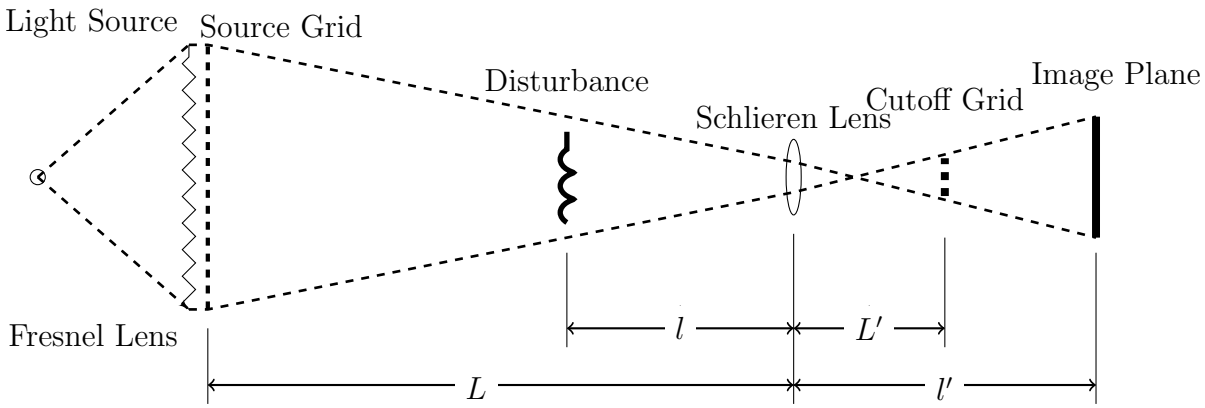

Figure 2.4: Focused schlieren schematic

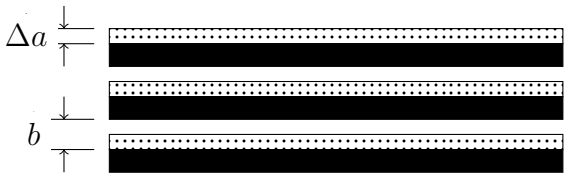

Figure 2.5: Cutoff grid dimensions, Shaded Region, Δa is the height of the light above the cutoff grid line, b is the spacing of the cutoff grid lines. $\Delta a = b$ when the schlieren system is not cutoff

opaque grid lines while the shaded regions indicate the amount of light allowed to pass over the grid lines.

Weinstein states that there are two definitions of depth-of-focus. His first definition of the depth-of-focus is the distance at which a density gradient will result in an image that is sufficiently blurry that it exceeds the resolution of the optical system. In other words, there is a certain point along the optical axis where a density gradient will not be imaged. The other definition is where the decrease in resolution of a density gradient's schlieren image due to being out of focus exceeds

a specific threshold. Any gradient outside of this region may still be visible but it won't be sharply imaged. Weinstein refers to the first definition as the depth of unsharp focus and the second the depth of sharp focus. The resolution of a focused schlieren diagnostic, from Weinstein [21], is defined as the following equation and can be derived from equations given in reference [30] where m is the magnification of the image, b is the spacing of the cutoff grid lines, and λ is the wavelength of light emitted from the light source.

$$w = \frac{2(l' - L')\lambda}{mb} \tag{2.8}$$

The depth of focus is related to the angle created by the effective aperture and the flow field. For focused schlieren, the effective aperture is the schlieren lens. Depth of sharp focus is defined by the following equation 2.2.2 where A is the aperture of the schlieren lens.

$$DS = \frac{2wl}{A} \tag{2.9}$$

Disturbances will be in sharp focus if they are within the region defined in the equation for the depth of unsharp focus as shown in equation 2.2.2.

$$DU = 4R = \frac{4l}{A} \tag{2.10}$$

These disturbances will be increasingly blurred the further they are located from the region of interest, any density gradient outside of the region of unsharp focus

will not be visible in the schlieren image. Using Weinstein's set-up as an example in order to get a general idea of how the size of these two regions compare, the region of sharp focus was on the order of 2 mm [21], while region of unsharp focus was significantly larger, 36 mm. These properties are dependent on the exact geometric layout of the focused schlieren system's optical components.

The cutoff grid is the most critical aspect of designing a focused schlieren system. Weinstein describes three important criteria. The cutoff grid must be designed so that the focused schlieren system is sensitive, diffraction effects cannot overwhelm the image, and the resulting schlieren image will be free of aberrations such as grid lines. To ensure that the schlieren images are aberration free, Weinstein developed a design criteria [21]. This equation can be seen in equation 2.2.2, where ϕ is the number of images blended together to form the final focused schlieren image.

$$\phi = \frac{An(l' - L')}{2l'} \tag{2.11}$$

Empirically, Weinstein found that ϕ needs to be greater than 5 to ensure that the individual schlieren images created by the source grid will be blended well and diffraction effects will not be noticeable.

The optical components must be mounted rigidly for the focused schlieren diagnostic to be functional. Any slight misalignment will result in poor sensitivity and focus. It is important to use fine adjustments on the optical components, especially the cutoff grid in order to achieve proper alignment [22]. The cutoff grid is the most critical component when it comes to alignment issues. If aligned

properly, the schlieren image's illumination will change uniformly when the cutoff grid is adjusted. If the grid is not properly aligned, broad lines will appear in the image. To eliminate these lines, adjust the grid gradually along the optical axis in the direction that causes these lines to increase in size. Once the cutoff grid is aligned properly, these lines will blend together and result in a perfectly uniform schlieren image.

Collicott [24] derived equation 2.2.2 using Fourier optics to more rigorously describe focused schlieren.

$$I_p(x) = \sum_{i=-N}^{N} sinc^2 \left[\frac{b}{2\lambda f_2} \left(x - \frac{i\theta mla_2}{f} \right) \right] \tag{2.12}$$

Where f_2 is the focal length of the schlieren lens and f is the focal length of the Fresnel lens. The position of the disturbance on the optical axis, measured from the image plane, is represented by x, θ is the angle of the light leaving the source grid. The intensity is highest at the plane of interest and decreases as x increases. A key finding is that density disturbances can never be eliminated but they will be significantly reduced as their distance from the plane of interest increases. A useful application of this equation is determining how significant of an effect an undesirable flow feature will be in the final image.

Focused schlieren adds the ability to spatially resolve density gradients along the optical axis. Unlike conventional schlieren, specific regions in a flow can be examined without density gradients outside the field of view being imaged. For example, some possible applications where focused schlieren imaging is better suited

than conventional schlieren, are examining the flow over a fin or particular feature on a model, examining internal flow structures, or the boundary layer. Additionally, different diagnostic tools including schlieren PIV [29] and deflectometry [12], can be integrated into a focused schlieren diagnostic to provide quantitative information on the flow.

2.2.3 Deflectometry

Deflectometry is an important application of focused schlieren and its application is a fundamental part of this thesis. Deflectometry uses photomultiplier tubes to measure changes in light intensity at a point in the schlieren image. As previously state, these fluctuations of light intensity correspond to changes in density. Deflectometry measures the frequency of fluctuations of disturbances, or it can be used to make local velocity measurements by correlating the frequencies from two closely spaced optical fibers. The primary focus of this thesis is making frequency measurements in the hypersonic boundary layer using deflectometry.

Deflectometry is best used in conjunction with focused schlieren imaging due to its inherent narrow region of sharp focus. Data from the deflectometry system is only useful if the measurement location in the flow is known. Conventional schlieren is poorly suited [16] because all disturbances in the image plane are measured by the deflectometry diagnostic. Having no focusing ability results in all disturbances in the field of view being measured, which makes it impossible to distinguish between the frequencies in the region of interest and the frequencies due to disturbances along

the optical axis. Focused schlieren only images disturbances in a narrow region. This allows for precise frequency measurements.

When designing the focused schlieren diagnostic, an important parameter is the integration limit. The integration limit is the range along the optical axis where a disturbance will be detectable in the focused schlieren system. A key design objective is to minimize unwanted disturbances that fall within the region of interest. This can be achieved by designing the system to reduce the size of the integration limit. In order to do this equation2.2.3, the equation for the integration limit, can be used to modify the layout of the focused schlieren optics. This equation is dependent on the geometrical configuration of the focused schlieren system, its geometric parameters are defined in figure 2.4, is referenced from Garg and Settles' paper [12].

$$L_{min} = \frac{4\lambda(L + l')}{\alpha m b} \tag{2.13}$$

This equation estimates the distance required to reduce the image intensity of an out-of-plane disturbance. It is important to be aware of the integration limit so that the region of flow that results in the data is well known.

Deflectometry is only as sensitive as the schlieren system it is used with. However, this diagnostic can measure light fluctuations more effectively than a camera due to the dynamic range of the photomultiplier tube. Density fluctuations correspond to the pressure fluctuations based on the relationship between the two parameters given by the equation of state, making this diagnostic well suited for measuring pressure fluctuations. Unlike pressure transducers, photomultiplier tubes

have almost an unlimited frequency response and are only limited by the rate of data acquisition.

The theory behind focused schlieren and deflectometry utilize the principle that light transmitting through a transparent medium is refracted upon encountering a density gradient. Focused schlieren functions by simulating multiple schlieren systems in order to only image density gradients in a user specified plane of interest. Deflectometry is built upon this focused schlieren diagnostic, by placing an optical fiber in the schlieren image that is connected to a PMT, the frequency of density fluctuations can be measured at a specific point. Designing a focused schlieren set-up that has adequate sensitivity and field of view requires meticulous work. This process involves significant experimentation to get a system that is practical for wind tunnel testing. The following chapter expands on the theory behind focused schlieren and deflectometry by going into greater detail the design process and set-up at the Tunnel 9 hypersonic wind tunnel.

Chapter 3

Diagnostics Development

Building upon the theory that was described earlier, this chapter will focus on the practical concerns of developing a sharp focusing schlieren and deflectometry diagnostic. The goal of this development was to build a diagnostic for use in the Tunnel 9 hypersonic wind tunnel to measure and image the second-mode instability waves in the hypersonic boundary layer. By imaging and measuring these waves, focused schlieren and deflectometry will be successfully demonstrated to be a useful addition to wind tunnel testing. To achieve this, a meticulous development process was pursued. The methodology consisted of expanding an initially basic set-up by adding complexity overtime. The increase of complexity of the set-up grew in conjunction with beginning to examine flows that were increasingly more representative of what would be seen in the hypersonic wind tunnel.

3.1 Focusing Schlieren

The development of the focused schlieren diagnostic began in the optical diagnostic laboratory at AEDC White Oak. This laboratory was ideal for initial development due to the wide array of optical equipment available for experimentation. This equipment includes optical stable tables, optical rails, mounts, and lens holders, a vast array of lenses, and numerous light sources. The initial focused schlieren

system was set-up on an optical table, which provided a vibration isolated platform that allowed for quick set-up and modifications. Access to a variety of optical mounting equipment allowed for extensive experimentation with the arrangement of optical components in order to optimize the diagnostic. As an example, a selection large aperture lenses, approximately 5 *in*, were available. The lenses used are uncommon and would be expensive to buy new. This allowed for experimenting with different focal lengths and aperture sizes to develop a focused schlieren system capable of sufficient sensitivity and field of view for use in the hypersonic wind tunnel. Additionally, several light sources were available for experimentation. These sources include: continuous halogen bulbs, pulsed xenon arc lamps, and an Oxford Lasers copper vapor laser. This allowed for experimenting with three distinct light sources to determine how the diagnostic's behavior changed with each light source. Ordinarily, Zemax®, a commercial optical design software package, would be used to model the system, but the design information for lenses was not available making this unfeasible.

The first iteration was modeled after Weinstein's system [21]. This system consisted of a wooden box containing a continuous halogen light bulb. Four feet in front of the bulb was a 11" square Fresnel lens with a 24" focal length. In front of this was a piece of overhead slide transparency with a source grid printed on it. This source grid consisted of 0.25 *in* thick black lines that were separated by 0.08 *in*. The Fresnel lens focused the light through the source grid, the image of the source grid was focused onto the cutoff grid by a double convex singlet lens. This lens produced significant barrel distortion. Located behind the source grid was a

piece of ground glass used for visualizing the image. The shadow of the threads of a 8-32 screw was used for testing the focusing capability. The screw was placed in between the imaging lens and source grid to mark the plane of sharp focus. This system was tested by using a candle and a can of aerosol duster. The diagnostic was used to image the thermals from the camera and the spray of the duster. This initial system performed poorly and density gradients were barely visible. The following subsections will describe how each component was improved.

3.1.1 Light Source and Source Grid

The source grid provides the focusing ability of focused schlieren by simulating multiple light sources as previously discussed. This grid consists of parallel lines that alternate between opaque and clear. Opaque lines are an absolute requirement, for the source grid, otherwise light will pass through and reduce to the sensitivity and focusing ability of the system. This is one reason why the first system performed poorly.

The initial source grid was made by printing black lines on an overhead transparency using a laser printer. The black lines that were created were not sufficiently opaque. To remedy this, a photograph was taken of the illuminated source grid and processed to create opaque black lines which did not permit light transmission. This technique was well suited for the initial system, which only had a 12 inch wide grid. This method is not well suited for large grids, necessary for a large field of view, due to the difficulty of enlarging a photograph to on the order of 3 feet.

After various prototype source grids, the ideal method to create large source grids that was decided upon, was to use vinyl tape adhered to scratch resistant Lexan®. Placing the tape at precise intervals can not be done reliably by hand. To solve this problem, a local print shop was used to print a large grid out of black vinyl, using the same technique used to create car decals. The printed grid was then adhered to the Lexan® plate. This method allows for source grids of any size to be constructed with evenly spaced slits.

Each slit in the source grid simulates an independent light source. For each slit to approximate a light source, the source grid requires diffuse light. Otherwise, the final image will have grid lines present. To remedy this, a 30° diffuser was used. Three light sources were used in the focused schlieren and deflectometry diagnostic. A 300 W continuous halogen lamp was used for deflectometry. Deflectometry requires a continuous source when measuring frequency data. A 5 mJ per pulse copper vapor laser was used to image the second-mode instability waves. The laser pulsed at 10 kHz with each pulse having a duration of 25 nanoseconds. This was critical to imaging the waves because this short pulse freezes the motion of the waves. A pulsed xenon arc lamp was used for exposing film to make the cutoff grid. This was chosen because the lamp could pulse a set number of pulses allowing for control over the exposure of the film.

The depth of focus and the sensitivity to density gradients depends on the number of grid lines used in the focused schlieren system. As the number of grid lines increases, the width of the slits will decrease. However, these lines cannot be too thin otherwise diffraction will occur at the cutoff grid which will decrease

sensitivity. Initially, the source grid was designed with 0.25 *in* thick black lines separated by 0.08 *in*. However, following discussions with Prof. Settles, it was determined that using black lines that were spaced at the same distance as their thickness produces an image that has a more uniformly illuminated background. The final source grid used in the Tunnel 9 system consists of 0.125 *in* thick black lines separated by 0.125 *inches*.

3.1.2 Cutoff Grid

The cutoff grid is the most important component in the focusing schlieren system. The cutoff grid is the equivalent of a knife edge in conventional schlieren. Since a focused schlieren system can be thought of as multiple conventional schlieren systems with each slit in the source grid acting as a light source, there needs to be a knife edge for each slit. As stated previously, the knife-edge is the critical component for creating schlieren images. The knife-edge and cutoff grid is responsible for partially blocking the light refracted by density gradients. The cutoff grid must be perfectly aligned, with the image of the source grid, which can be seen in figure 3.1. The grid lines must be opaque in order to create a very sensitive schlieren system with an excellent depth of field, and a uniformly lit and aberration free image. Unfortunately, it is the most difficult component to create.

The most effective method to make the cutoff grid is by creating a photographic negative of the source-grid. This technique began with Boedeker [20] and was used by Weinstein [21] as well. The advantage of using the photographic negative is that

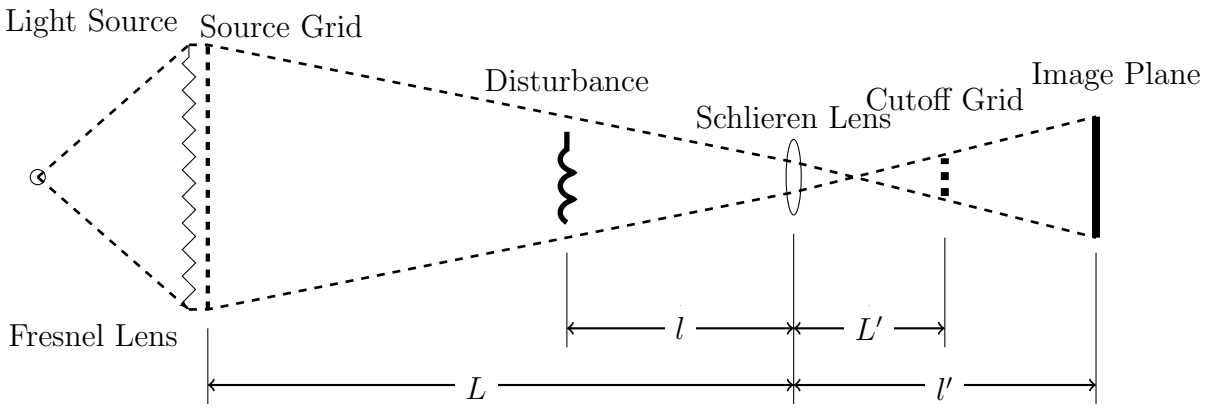

Figure 3.1: Focused schlieren schematic

it accounts for all optical aberrations and the resulting grid is much more accurate than attempting to make the cutoff grid from an alternative method. To make a cutoff grid, the source grid's image is focused onto a piece of film by the imaging lens. This film is then exposed and developed. The photographic negative is then placed exactly where the source-grid's image is in focus. Making the cutoff grid requires patience and fine control over the light source and positioning of the film. High contrast black and white film, Arista II Ortholithographic film was found to be well suited, should be used for best results. This film resists being exposed by background light which causes the clear slits to become cloudy. In order for the cutoff grid to be a useable size, 4" x 5" film was used. It is important to ensure that the film is flat and firmly mounted. To do this, the backing of a vintage 4" x 5" camera was mounted to a rail. This backing held standard 4" x 5" film holders which allow for quick swapping of unexposed film. To ensure that the cutoff grid is properly focused, a piece of exposed film was used to examine the projected image

of the source grid. A handheld focusing aid in conjunction with fine adjustment in multiple directions was used to verify that the image was sharp and well defined. It is important to verify that the film holder is not rotated before exposing the film. Corners that are out of focus will be detrimental to the final schlieren system.

Once the image is in focus, the film can be exposed. It is important to eliminate all background light. Stray light will ruin the cutoff grid by washing out the image. There are two ways to expose the film. The first method is to use a continuous light source and an electronically controlled shutter. The alternative, is to use a pulsed light source. The light source can be pulsed multiple times to expose the film for different amounts. Both methods were attempted and it was found that using the pulsed xenon arc lamp and controlling the number of light pulses was the most accurate method to control the exposure time. Due to the complexities of determining the required exposure time with a pulsed light source, the ideal method is to expose several pieces of film for different numbers of pulses or lengths of time and then choose the best grid. The best grid will have opaque dark lines with very sharp edges, and clear (not cloudy) slits between the dark lines. Cloudy slits will reduce the amount of available illumination. In order to have maximum sensitivity and produce a clear image, it is imperative that the dark lines be opaque. Otherwise, light will pass through the grid lines and less refracted light will be blocked which will wash out the images of the density gradients thus ruining sensitivity. The use of a lithographic type film is necessary in order to achieve this. Figure 3.2 is representative of an ideal cutoff grid. Lines are opaque, sharp, and the lines do not bleed into the clear region.

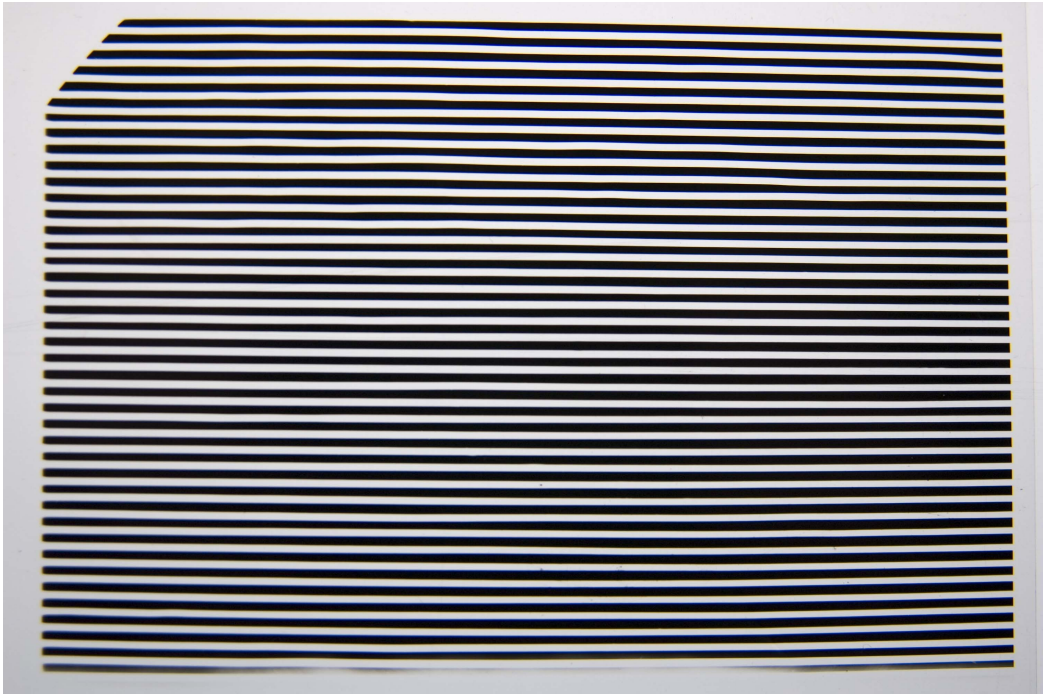

Figure 3.2: Example cutoff grid, spacing approximately 0.4 mm.

A high quality imaging lens is critical in making a functional cutoff grid. The first iteration of the focused schlieren system used a double convex singlet lens. The resulting image had significant barrel distortion. The source grid made from this lens resulted in a focused schlieren system that had almost zero sensitivity. This lens was replaced with a compound lens from a 70 mm camera. The images from this lens were perfect reproductions of the source-grid with no distortion present. The first attempts at exposing film resulted in over exposed cutoff grids. Through experimentation with exposure times and number of light pulses, the results improved but oftentimes the grids were still cloudy. Another issue was that the background light would overwhelm the image before the grid lines could be adequately exposed. The resulting lines were not thick enough which resulted in the system not being

able to achieve an adequate amount of sensitivity. The type of film that was initially used did not have a sufficiently high contrast to expose the lines before the clear regions in the slits became cloudy. This problem was discussed with Settles and a higher contrast lithographic film, Arista II Ortholithographic film, was recommended. This film was extremely resistant to background light and resulted in very sharp lines that were opaque and thick. Over the course of this project over 100 grids were made.

The final step is to place the cutoff grid in the focusing schlieren system. The grid, as shown in figure 3.1, must be placed in the plane where the image of the source grid is in focus. The mounting system must have fine adjustment in the vertical, horizontal, and forward directions. It is also important to be able to rotate the grid so that it can be positioned correctly. When a grid is improperly placed, the schlieren system will not be as sensitive to density gradients, dark bands of lines will be visible, and there will be dark and bright regions. When properly adjusted, the image will be uniform with no visible banding. The suggested steps to follow to quickly adjust the location of the cutoff grid are as follows:

1. Place the cutoff grid as close as possible to where the source grid's image is in focus.

2. Using the hand held focus aid, ensure that the cutoff grid lines match up with the source grid lines.

3. Verify that the schlieren image to determine if there are bands of lines visible.

4. Adjust the cutoff grid so that any visible lines in the image become parallel.

5. If lines are still present, adjust the cutoff grid towards the imaging lens so that the lines become larger.

6. When the lines are no longer visible the image should be uniformly lit and therefore the grid is in the proper location.

7. Adjust the grid's position in the vertical direction to get the desired amount of cutoff.

3.1.3 Recording Schlieren Images

Recording the schlieren image while preserving the focused schlieren's depth of focus is complicated. One complication is adequately capturing the focused schlieren image. The image plane is located just behind the cutoff grid and the light expands from the cutoff grid through the image plane. This results in an image that is larger than the aperture of most camera lenses. Placing a piece of ground glass in the image plane is the simplest way to view the schlieren images. This is not very useful because a digital image is necessary to store the data for later analysis. A Redlake high-speed camera was used to record the schlieren images that was projected onto the ground glass. After this initial attempt, this approach was abandoned because the graininess of the glass overwhelmed the schlieren images, eliminating the ability to discern fine details. The best option is to use a relay lens to focus the image into the camera. A large aperture (5 *in* diameter) lens with a focal length of 12" was placed at the image plane behind the cutoff grid. This lens focused the schlieren image into the Redlake camera's Nikor macro lens. This approach requires a significant

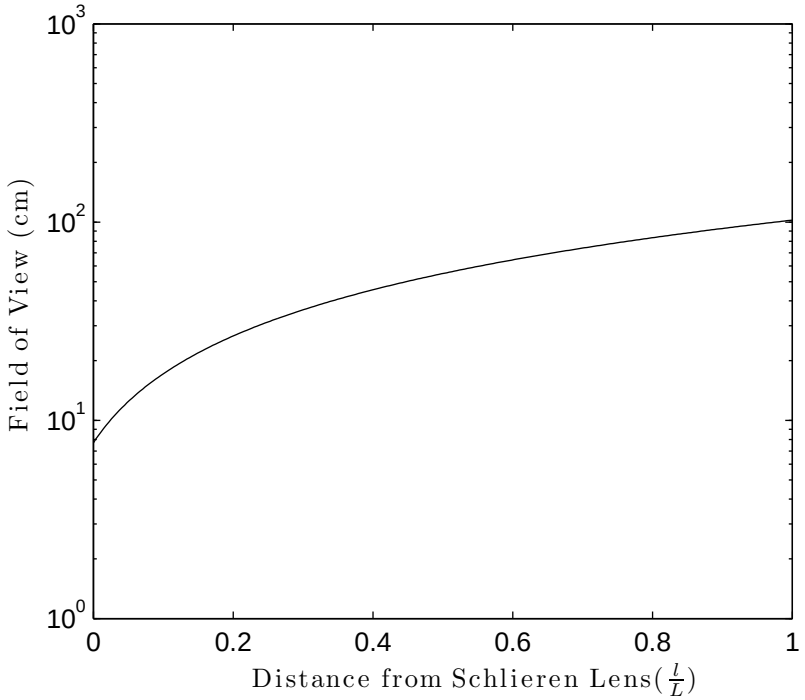

Figure 3.3: Change in field of view as model approaches the source grid ($l = L$) from the schlieren lens ($l = 0$), refer to figure 3.9.

amount of adjustments to place the relay lens and camera in a way that will permit sharply focused images to be recorded.

3.1.4 Design Trade-offs

Designing a focused schlieren system is fraught with compromise. Before beginning the design process it is important to determine the most important parameters. If the main goal is to examine a large model in its entirety, the system should be optimized for a large field of view. This means the model will need to be placed near the Fresnel lens, refer to figure 3.3. These figures were based on the equations described in Chapter 2. The geometric parameters used for the plots were based on the final set-up in Tunnel 9, described in the next section. The distance l'

from the schlieren lens is normalized by L, the distance from the Fresnel lens to the schlieren lens. However, the closer the region of interest is to the Fresnel lens, the worse the sensitivity of the system but the depth of focus will be better, which can be seen in figures 3.4 and 3.5. For examining phenomena with small densities,

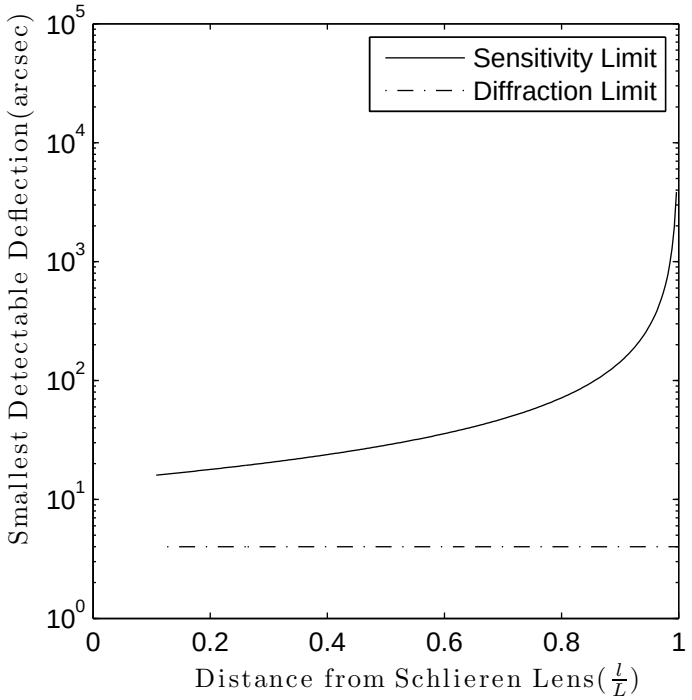

Figure 3.4: Change in sensitivity limit as model approaches the source grid ($l = L$) from the schlieren lens ($l = 0$). Smaller detectable deflections are equivalent to higher sensitivity.

a higher sensitivity schlieren system is necessary, which means the model needs to be closer to the schlieren lens. Additionally, the source grid design is critical to the parameters. The more grid lines, the more sensitive the schlieren system which can be seen in figure 3.6 and is based on equation 2.6. Unfortunately this increases the depth of focus which is shown in figure 3.7.

Since the design data for each lens was unavailable, rendering the usage of the optical engineering program Zemax untenable, experimentation was critical to

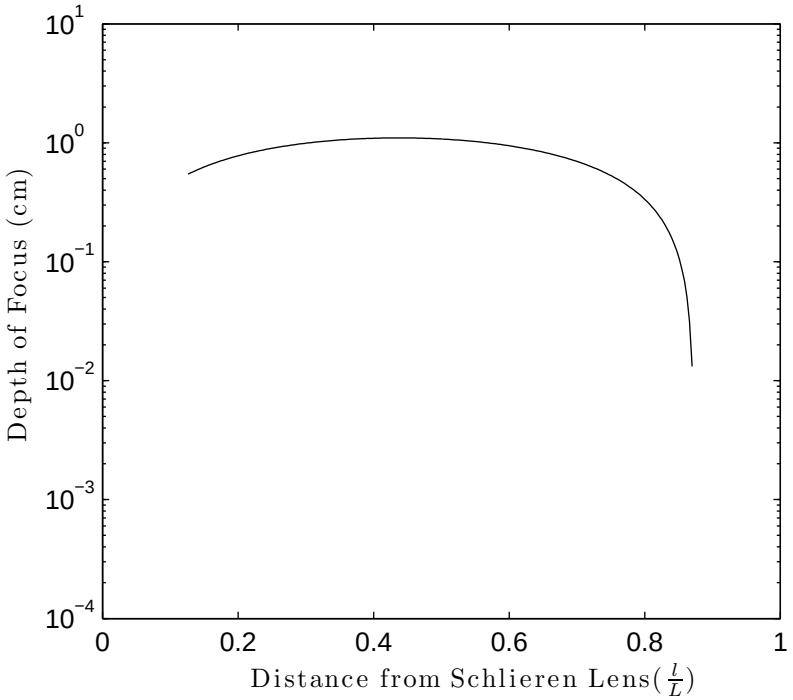

Figure 3.5: Change in depth of field as model approaches the source grid ($l = L$) from the schlieren lens ($l = 0$).

optimizing the placement of optics for each new application. When developing the final set-up for Tunnel 9's hypersonic wind tunnel, there were significant constraints placed on the design. The placement of the model was a fixed distance from the test section wall. Along side the test section, two optical benches were mounted on rails that allowed for the benches to be moved along the length of the test section. However, these benches did not allow for adjustments in height nor could they be moved closer or further to the test section. The focused schlieren optical equipment was mounted inside of these optical benches. This meant that there was only a small margin for adjusting the placement of the optics. This limited the optimization of the focused schlieren parameters. For this experiment, imaging and measuring second-mode instability waves in the boundary layer, sensitivity was

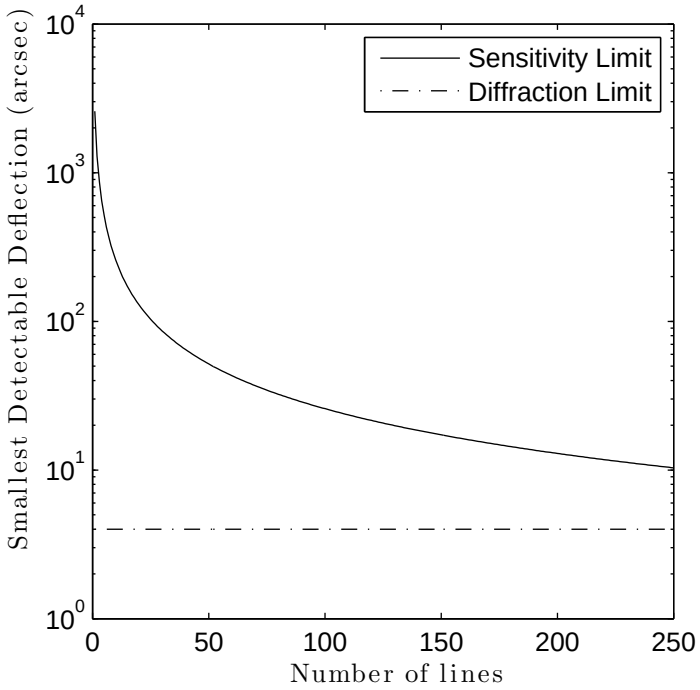

Figure 3.6: Change in sensitivity limit with increase of grid lines, Smaller detectable deflections is equivalent to higher sensitivity.

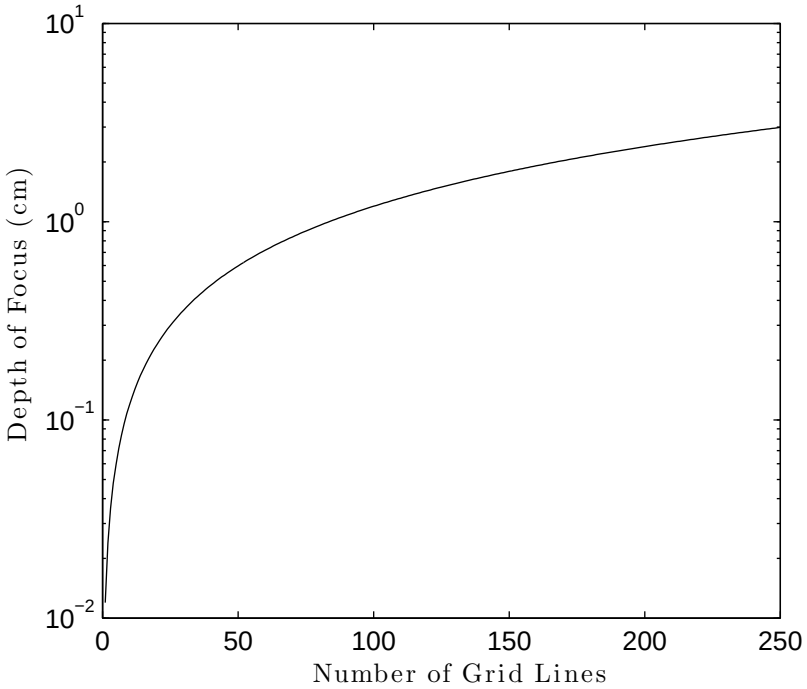

Figure 3.7: Change in depth of field with increase of grid lines.

the critical parameter. Because of the large test section diameter, 5 ft, the depth of sharp focus was not as critical. Using the methodology discussed here and the equations in Chapter 2, it was determined that the receiving optics of the focused schlieren system needed to be as close as possible to the model. As shown in figure 3.4, the closer the model is to the schlieren lens, the higher the sensitivity. This set-up will be discussed in more detail in the subsequent section.

There is no optimal geometric layout where sensitivity, depth of field, and field of view can are all maximized. Due to this reality, it is critical to determine a compromise between the system characteristics to successfully achieve the desired experimental results. Using the equations in Chapter 2, approximations to the system characteristics can be calculated. By adjusting the different locations of the optics, as discussed in this section, the focused schlieren diagnostic can be optimized.

3.1.5 Final Set-up

Two focused schlieren systems were developed. The first was built in the optics lab and moved to the calibration lab's Mach 3 test section. The lessons learned from the experience of building and optimizing the sensitivity of the first system were applied to the creation of the larger focusing schlieren system in Tunnel 9. The majority of optical components used in the calibration lab set-up were reused for the final, large scale set-up in Tunnel 9. The Tunnel 9 system is four times larger than the calibration laboratory set-up. Since the experiment requirements are for a larger system, a larger Fresnel lens and source grid were used. These components

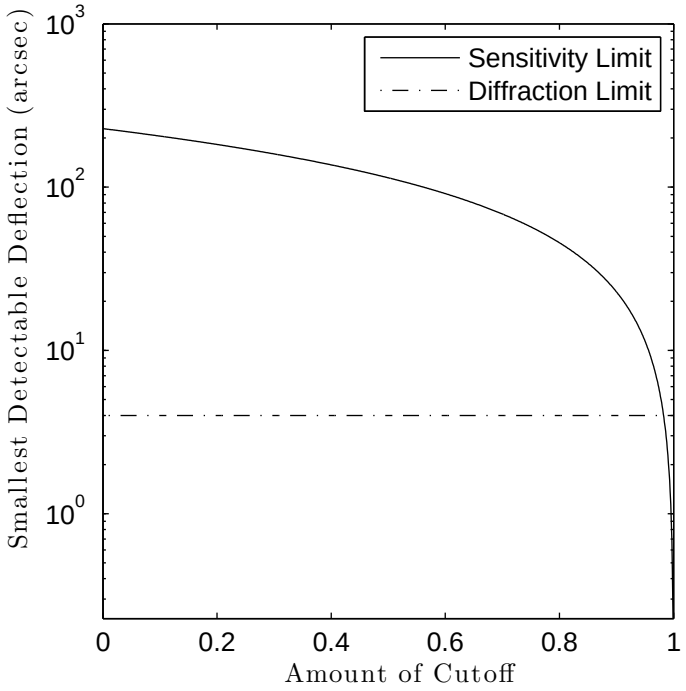

Figure 3.8: Calibration laboratory focused schlieren sensitivity curve, full cutoff = 1.

can be seen in table 3.2. Additionally, the position of the components along the optical axis were changed to optimize the focused schlieren system's properties. As previously mentioned, the alignment of the components is critical for optimizing sensitivity and the depth of sharp focus.

The sensitivity, depth of sharp focus, depth of unsharp focus, image size, and the resolution of the system were calculated using equations derived in Weinstein's paper [21] and from the spacing of the optics in the calibration laboratory. The design characteristics of the initial design can be seen in table 3.1. The range of sensitivity of the calibration laboratory, depending on the height of the cutoff grid, can be seen in figure 3.8. Using these parameters and results from the calibration laboratory, discussed in Chapter 4, the Tunnel 9 focused schlieren system was

Table 3.1: Design parameters, calibration Lab

$w\ (cm)$	$DS\ (cm)$	$DU\ (cm)$	$Field\ of\ view\ (cm)$	ϕ
0.03	0.5	33	11	6

Table 3.2: Focused schlieren diagnostic components

Component	Description	Specifications
Light Sources	Oxford Laser LS 20-50	Copper Vapor laser, 5 mJ per pulse @ 10 kHz, 25 $nsec$ pulse width
Diffuser	Edmund Optics, NT54-501	Holographic 30°
Fresnel Lens (L_F)	Edmund Optics NT66-212	40.5"x 54.0",f_{LF} = 47.2" (119.9 cm) nominal
Source Grid	Custom source grid adhered to Lexan® sheet	Equally spaced grid: 0.125" lines
Schlieren Lens (L_S)	Spherical Convex Lens	f-no. 3.5, f_{LS} = 10.6" (27 cm) nominal
Cutoff Grid	Photographic negative of source grid	Created on Arista II Ortho lithographic film
Relay Lens (L_R)	Kodak Aero Ektar	f-no. 2.5, f_{LR} = 12" (30.5 cm) nominal
Camera	Redlake MotionXtra HG-XR	1504 x 1128 resolution @ 1000 fps

designed in order to successfully fulfill the goals of the experiment.

The conventional schlieren benches used in Tunnel 9 were retrofitted to be used as a focused schlieren diagnostic. The idea behind this modification was to allow for switching between conventional and focused schlieren per the test requirements. This placement was advantageous because the optical benches were rigid, blocked background light, and helped isolate the optics from vibrations. The primary disadvantage was that it placed a restriction on where the optics could be placed along the optical axis. For example, the Fresnel lens and source grid could only fit on

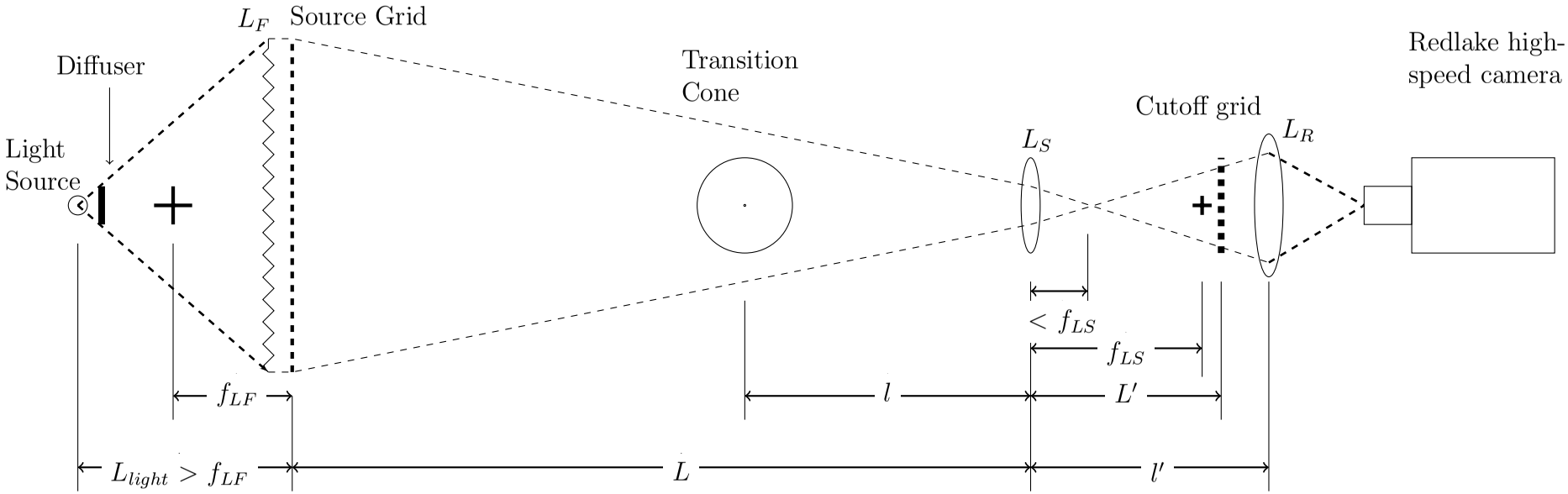

Figure 3.9: Detailed component layout, dimensions are nominal

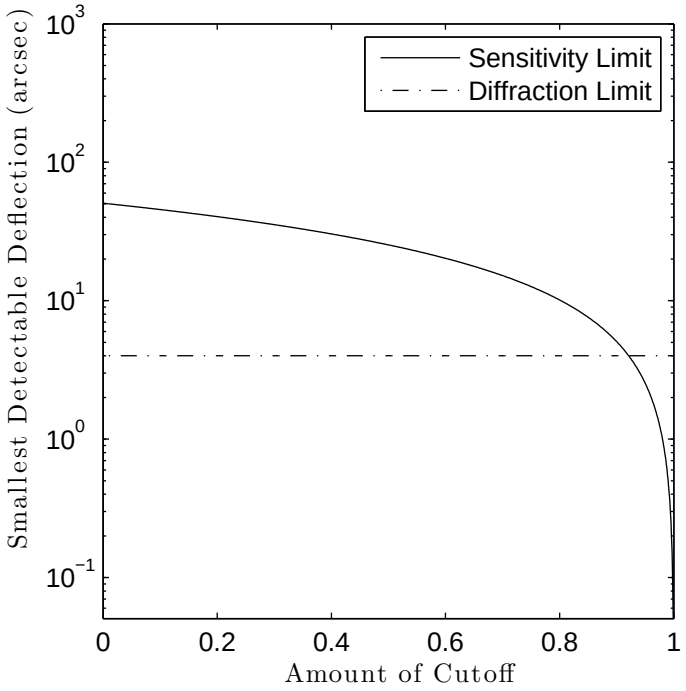

Figure 3.10: Tunnel 9 focused schlieren sensitivity curve, full cutoff = 1.

the front of the optical bench which fixed the l parameter and therefore fixed l'. These restrictions limited the maximum possible sensitivity and depth of focus of the system.

Klinger® rails were clamped to the internal support beams in the optical benches to allow for relatively quick adjustment and replacement of optics. Optical mounts, rails, and posts were mounted to these rails, which provided excellent rigidity. The Fresnel lens and source grid were mounted to the front of one of the schlieren benches using T-slotted aluminum extrusions. These allowed for the lens and source grid to be adjusted vertically in order to center the field-of-view on the desired model. This allows for easy removal and replacement while maintaining rigidly mounted components. The final spacing for the Tunnel 9 set up can be seen

Table 3.3: Component spacing of Tunnel 9 focused schlieren set-up

$A\ (cm)$	$l\ (cm)$	$L\ (cm)$	$l'\ (cm)$	$L'\ (cm)$	R	$(n)\ \frac{gridlines}{cm}$	m	$b\ (cm)$
7.7	117	269	35	30	15	12.0	.30	0.04

Table 3.4: Design parameters of Tunnel 9 focused schlieren set-up

$w\ (cm)$	$DS\ (cm)$	$DU\ (cm)$	$Field\ of\ view\ (cm)$	ϕ
0.04	1	60	25	7

in table 3.3 and the design parameters can be seen in table 3.4. In figure 3.10, the variation of sensitivity with the cutoff level can be seen. It is important to note, the higher the amount of cutoff, the more illumination is required to capture the schlieren image with a camera. For this reason, the cutoff was approximately 50 % in this set-up. When comparing the two systems, it shown that the Tunnel 9 system is over four times as sensitive while providing a larger field of view. Sensitivity is extremely important due to the low densities that were be examined, on the order of 0.01 $\frac{kg}{m^3}$.

The copper vapor laser was located next to the optical bench and a 1 mm diameter fused silica fiber optic cable delivered the laser beam to inside the bench where it was mounted 5 ft behind the lens. Mounted on one side of the fiber optic cable was a xenon flash lamp, used for exposing the film, and on the other was a 300 W halogen bulb used for deflectometry. The mounting system allowed for any of the three light sources to be used by sliding the mount to the left or right. The final dimensions of the focused schlieren diagnostic are shown in table 3.3. An image of the final set-up of the focusing schlieren diagnostic in Tunnel 9 can be seen in figure 3.11.

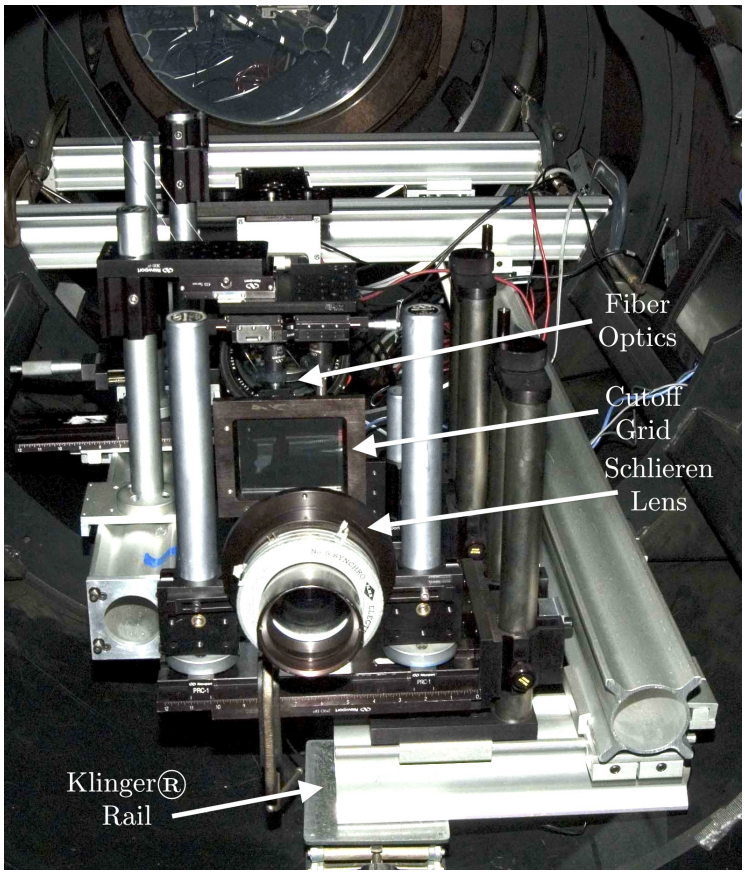

Figure 3.11: Tunnel 9 focused schlieren components layout.

Schlieren images were recorded using the same technique for both the calibration laboratory and the Tunnel 9 focused schlieren systems. All imaging was performed using a copper vapor laster as a light source. For both set-ups, a Stanford Systems pulse generator was used to pulse the laser at 10 kHz. The copper vapor laser is an ideal schlieren light source because it produces very bright, 5 mJ, low-coherence light pulses that have a duration of 25 $nsec$. The 25 $nsec$ pulses are short enough to freeze the motion of the second-mode instability waves in the boundary layer. The low-coherence light is important to eliminating laser speckle in the schlieren image. A separate pulse generator receives a pulse from the laser, which indicates when the laser fires. This pulse generator uses this signal to synchronize the camera, running at 1 kHz, with the 10 kHz laser. After every tenth laser pulse, a pulse is sent to the Redlake high-speed camera. This pulse triggers the camera so that the shutter is open during the laser pulse. The only difference between the calibration laboratory and the Tunnel 9 systems is that the Tunnel 9 set-up has an additional trigger line, to trigger the camera when the wind tunnel starts. Also, the Tunnel 9 set-up has an IRIG line (for timing) connected to the camera to identify the exact time each frame was recorded during the tunnel run.

3.1.6 Design Summary

Focused schlieren has many advantages over conventional schlieren as shown in table 3.5. As this table shows, the optimal use of this diagnostic is to investigate flow phenomena present in a narrow region of the flow field. This is important

for imaging boundary layer phenomena on a model because other density gradients along the optical axis could overwhelm this information. Also, this permits for two or more test articles to be present in the test section, while only imaging the flow around one model. Additionally, focused schlieren can result in monetary savings while operating a wind tunnel. Not only can multiple models be tested, reducing the number of wind tunnel runs, but aberration free windows are no longer a necessity. Pits and scratches do not show up in the final schlieren image if focused schlieren is used. It is important to note that focused schlieren is not ideal for every experiment. Conventional schlieren has a larger field of view because light is collimated across the test section as opposed to be focused. Focused schlieren cannot equal the same amount of sensitivity for a similarly sized conventional schlieren system. With these differences in mind, each schlieren system has its own applications that it is uniquely suited for.

During the development of this diagnostic, several improvements to focused schlieren systems were developed. These improvements on work by Weinstein and Settles allow for a simpler focusing schlieren set-up process. These improvements are as follows.

- Using a holographic diffuser with a 30° diffusing angle increases the illumination of the focused schlieren system
- To make a large source grid, the grid lines can be printed as a vinyl decal which is adhered to a sheet of Lexan®
- Using a pulsed light source to expose the film for making the cutoff grid allows

Table 3.5: Comparison of focusing schlieren and conventional schlieren

	Focused Schlieren	Conventional schlieren
Advantages	• Narrow depth of field • Focusing ability permits testing multiple models simultaneously which results in cost reduction •Window imperfections are not present in schlieren images, expensive polished windows not required • Narrow depth of field allows for other non-intrusive measurements i.e. deflectometry	• Large field of view • Simple set-up • Widely used and well understood technique which means wide base of knowledge to build upon • Theoretical higher sensitivity
Disadvantages	• For an equivalent lens, field of view is smaller than that of conventional schlieren • Complicated set-up • Optimizing one parameter results in degradation of other parameters	• No spatial resolution due to flow disturbances being integrated along optical path • Non-intrusive measurements with deflectometry not feasible • Investigations in to flow phenomena such as second-mode instability waves hampered by flow outside of the region of interest being present in the schlieren image

for greater control to create high quality negatives of the source grid

- Previous focused schlieren systems used Kodalith film, which is no longer in production, the use of Arista II Ortholithographic film is critical to creating high contrast opaque cutoff grids

3.2 Deflectometry Development

Deflectometry is a non-intrusive diagnostic tool for measuring the frequency of density fluctuations. This tool is coupled to a focused schlieren system and adds the ability to collect quantitative information. The development of a focused schlieren system that is sensitive with a useful depth of sharp focus is critical to deflectometry. The photomultiplier tubes used can only detect what the focused schlieren system is sensitive enough to image. This deflectometry implementation was based upon research by McIntyre [16].

To implement the deflectometry tool, one end of a fiber optic cable is mounted in the image plane of the focused schlieren diagnostic. The other end is then connected to an adjustable voltage photomultiplier tube. The output signal is loaded with a 1000 Ω resistor to improve the frequency response and amplitude of the signal. The signal requires a load because the oscilloscope supports either a 50 Ω or 1 $M\Omega$ impedance on the input. An impedance of 1 $M\Omega$ limits the frequency range measured while the 50 Ω impedance does not limit the frequency range but results in a significant voltage drop with the resulting signal being less than a mV. Using a 1000 Ω resistor balances these two issues, resulting in a signal of several mV and a frequency bandwidth of a few MHz. The photomultiplier tube is a low impedance device and therefore when a resistor is placed in parallel, there is a linear drop of signal. For this set-up, the signal was filtered and amplified using a Stanford Research Systems filter-amplifier box. A band-pass filter was applied to filter out frequencies below 10 kHz and the signal was digitized using a Tektronix oscilloscope. A more

Table 3.6: Components used in the deflectometry diagnostic

Component	Description	Specifications
Light Sources	Continuous Halogen Bulb	Halogen, 300 W
Fiber Optic Cable	Manufactured by Polymicro	200 μ fused silica with SMA connectors
Photomultiplier tube	Hamatsu R928	Spectral response: λ=185 - 900 nm
Preamplifier	Stanford Research Systems SR560	Gain: 1 - 50000, High-pass cutoff 10 kHz Low-pass cutoff 1 MHz
Oscilloscope	Tektronix TDS5104B	1 GHz Bandwidth, 5 GS/s Sample Rate, 16 M Record Length.

detailed description of the components can be seen in table 3.6. The layout of these components in relation to the schlieren components can be seen in figure 3.12. In this figure, one can see how the deflectometry diagnostic integrates into the focused schlieren system. The primary difference is that the fiber optic cable is placed in the image plane instead of there being components to record the image.

Experimentation is critical to developing a set-up that is sufficiently sensitive enough to measure the density fluctuations of interest. Each component has a plethora of possible adjustments such as the amount of voltage on the photomultiplier tube or gain on the amplifier. Additionally, determining the correct amount of cutoff and alignment of the fiber optic cable has a significant effect on what the system can measure. These adjustments can have either positive or adverse effects on the signal to noise ratio and response of the deflectometry system.

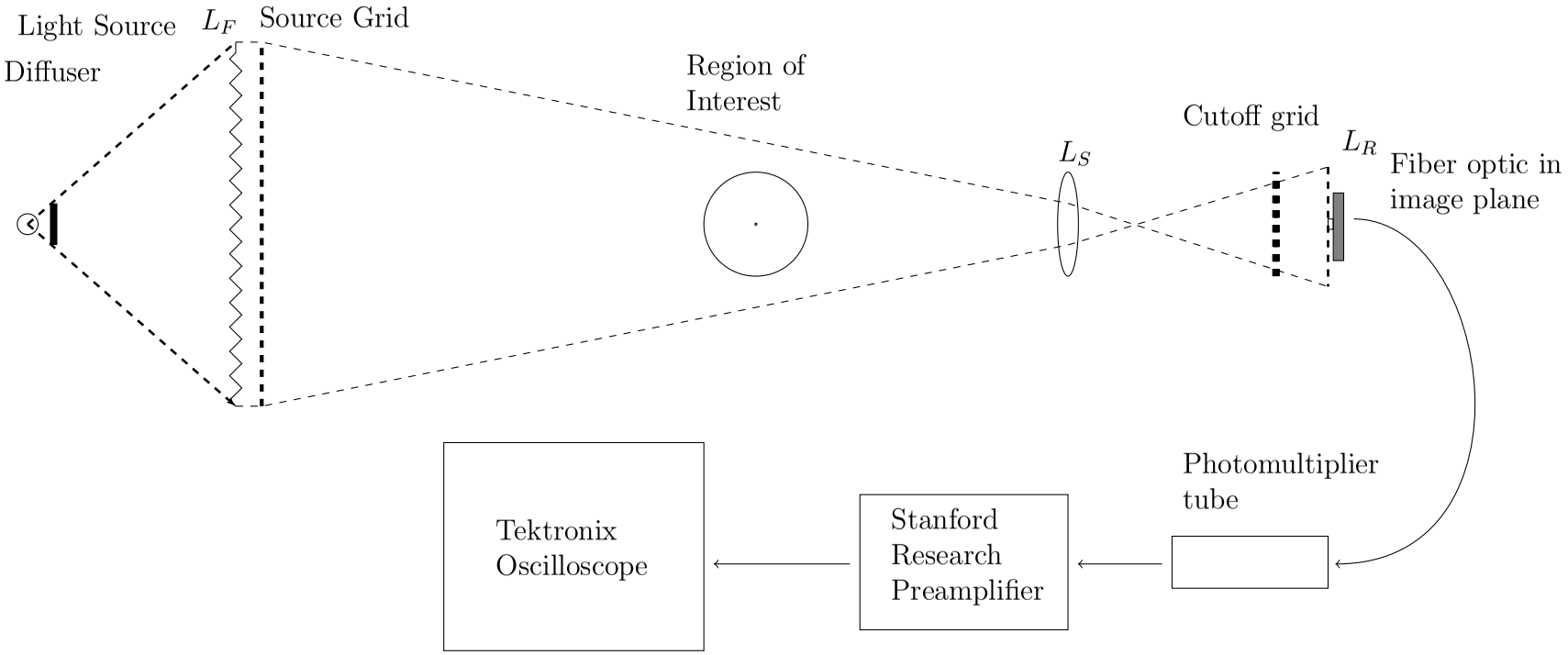

Figure 3.12: Deflectometry component layout

3.2.1 Deflectometry Optimization

The increased sensitivity of the photomultiplier tubes compared to a high-speed camera means that the configuration of the focused schlieren system is different for deflectometry than for imaging. For imaging, it is desired to have well illuminated images which can saturate the photomultiplier tube in a deflectometry set-up. This means that the image needs to be almost entirely cutoff. When the diagnostic is entirely cutoff, the cutoff grid lines block all incoming light which reduces the signal significantly. The advantage of being just above full cutoff results in the most sensitivity with the least amount of noise. Noise, in this context, refers to the amount of background light which results in increased signal from the multiplier tube. The light source is the other primary difference between the two configurations. Critically, a continuous light source must be used as there is no associated limit on the range of detectable frequencies. The copper vapor laser is a pulsed light source operating at 10 kHz which limits which frequencies could be measured. The second-mode rope waves in hypersonic boundary layers have a frequency on the order of several hundred kHz.

To reduce the illumination and maximize the sensitivity, experimentation is necessary to determine what level of cutoff results in the most sensitivity. This was determined through experimentation. Proper alignment of the cutoff grid is critical to having a sensitive deflectometry system. As an example, during the course of experimentation in the calibration laboratory, it was discovered that the cutoff grid was tilted forward and was not perpendicular to the optical axis. This resulted in

reduced sensitivity and was a significant factor in not being able to measure the frequencies of interest. Once the tilt was eliminated, the signal to noise ratio was boosted significantly and the desired frequencies were measured. The details of this experiment will be discussed in Chapter 4.

The Tunnel 9 main tunnel set-up uses a more rigid mounting system to obviate the usage of shims. If the alignment of the cutoff grid is off, the image will not be uniformly illuminated. This can be verified with a piece of white card stock. Using the card stock, it was discovered that it was not possible to achieve full cutoff. The reason was that the type of film used did not allow for adequate exposure of the grid lines which meant they were not sufficiently wide. The light projected on to the cutoff grid lines went around the lines which reduced sensitivity since it was not blocking enough of the light refracted by density gradients. This is due to the cutoff grid not being a true negative of the source grid. While examining this issue another source of reduced sensitivity was found. It was discovered that the opaque lines were not sufficiently opaque resulting in light passing through the lines. If the refracted light is not blocked then it is impossible to achieve maximum sensitivity. After switching to the higher contrast Arista II Ortho-lithographic film, this issue was resolved, allowing for longer exposure to create a more accurate negative of the source grid without degrading the transparency between these lines. As a precaution, two identical cutoff grids were overlapped to increase the opacity of the grid. This was only necessary in the calibration laboratory. A caveat to this technique is that if the grids are not aligned with each other properly, the sensitivity of the system will be degraded. This can be verified by checking the illumination with

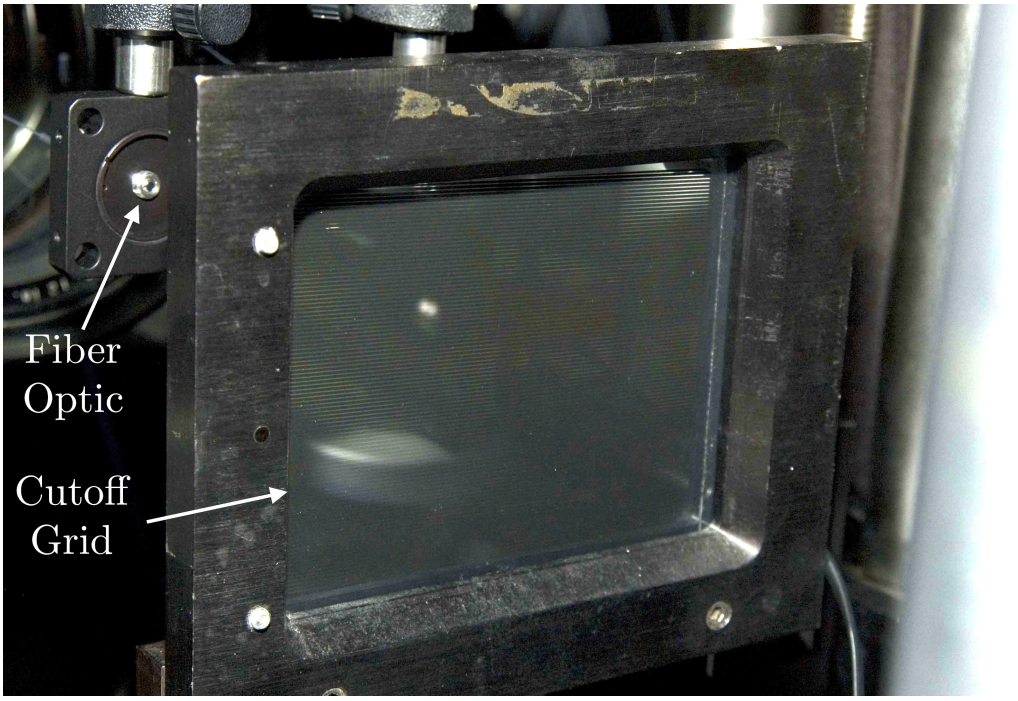

Figure 3.13: Tunnel 9 fiber optic cable located in image plane behind cutoff grid.

white card stock.

With the cutoff grid optimized, the next step was to investigate the correct placement of the end of the fiber optic cable. The fiber optic cable input needs to be placed exactly in the image plane. An example can be seen in figure 3.13 for the Tunnel 9 set-up. As discussed previously, the focused schlieren diagnostic has a depth of sharp focus of approximately 1 cm for the Tunnel 9 set-up and 2 mm for the calibration laboratory set-up. If the fiber optic is not in the plane of focus, the signal will drop off dramatically the further away it is in accordance to equation 2.2.2. To verify the position of the plane of focus, a piece of white card stock was pressed against the fiber optic cable mount so that it was in plane with the fiber tip. The mount was then adjusted along an optical rail to the correct spot.

Determining the ideal plane of focus must be done by gradual adjustment of the fiber's tip while monitoring the signal that results from spraying a can of compressed air in the region of interest. The signal will be highest when the fiber is in the plane of best focus.

Unacceptable noise levels due to background light were an issue during development in the calibration lab. A major source of noise is background light. Light from the room and from the schlieren image that isn't being examined are the two main sources. Ideally, the only light entering the fiber optic would be the light from the point of interest. Since this is not possible, steps were taken to reduce unwanted light. To reduce the light from the room, the room lights were switched off and a large piece of black material was placed over the receiving end of the schlieren and deflectometry system to block out stray light. Another measure undertaken was to place a tube with an iris on the end over the tip of the fiber optic cable. A tube of 1 in in length was used since a longer tube could prevent the image of interest from being projected onto the fiber if it was slightly tilted. To ensure the fiber was aligned with the image, the fiber using a piece of white card stock was adjusted until it was in the correct position. Once in place, the tube was attached with the iris fully open. After it was verified that the image was projected onto the fiber, the iris' aperture was reduced by 75 %. This significantly improved the signal to noise ratio. To verify that the fiber was not blocked, a can of air duster was sprayed which would result in the deflectometry signal to change dramatically due to the sudden presence of density gradients.

3.2.2 Signal Processing

Maximizing the signal to noise ratio is critical to improving the efficacy of deflectometry. As discussed previously, the noise due to stray light was minimized, which leaves several additional sources of noise. These other sources include the photomultiplier tube, amplifier, and oscilloscope. These components have adjustable settings for example, the amount of voltage applied to the device or the gain applied to the signal. Increasing the voltage or the gain increases the signal, however depending on the device, there will be a point where the noise level increases resulting in a drop in the signal to noise ratio. Extensive experimentation was necessary to optimize these settings to maximize the signal to noise ratio. Each component was optimized before moving to the next.

In order to quantify the improvements, an experiment was devised. This experiment placed a hollow pipe in a Mach 3 flow in the calibration laboratory wind tunnel. Since the pipe was hollow, it has a characteristic frequency due to the pipe organ effect [34], which will be discussed in the next chapter. A pressure transducer was located in the back of the pipe to measure the frequency. This frequency was compared with the deflectometry data which was measuring the fluctuations at the entrance to the tube. With this initial baseline, changes in the signal to noise ratio were made quantifiable.

The first component optimized in this fashion was the Hamamatsu R928 photomultiplier tube. The tube was powered by a DC power supply and has a linear response from 200 to 1000 VDC. The voltage was initially set at 800 VDC for

the baseline data. The voltage was then adjusted in 100 volt increments from 200 VDC to 1000 VDC. Data was collected at each point and it was determined that the maximum signal to noise ratio was when the voltage was 600 VDC. This is a similar finding to experiments done by McIntyre [16]. Below this value, the signal was too weak and above it, noise was more predominant. An additional reason for limiting this voltage is that the photomultiplier tube can saturate during the run. When this happens, it can take several seconds for the tube to recover which means that no useful signal can be recorded during this time. Another source of noise is the dark current, which is inherent to photomultiplier tubes. At warmer temperatures, dark current can register temperature fluctuations as photons which increases the amount of noise. To mitigate this noise source, the photomultiplier tube was packed in dry ice to lower the temperature to approximately -70 $^\circ$ C which increases the signal to noise ratio by almost 3 orders of magnitude.

The Stanford Research Systems SR560 preamplifier has a built in band-pass filter and the capability of applying a gain of up to$50,000$. The bandpass filter has a range from 0.03 Hz to 1 Mhz. The signal entering the box was loaded with a 1000 Ω resistor to moderate the voltage drop. After several test runs it was determined that in order to boost the signal to noise ratio it was necessary to keep the gain as low as possible on the amplifier. In order to compensate for this, the Tektronix oscilloscope was used to boost the signal. The bandpass filter was very effective in reducing the amount of noise as long as the amplifier's gain was kept to a minimum.

Once the equipment has been optimized, data processing techniques can be used to reduce the amount of noise by averaging the noise together. Using MAT-

LAB, a code was developed to perform a fast Fourier transform with a Blackman windowing scheme to average out the noise. To avoid aliasing, the data was sampled at a rate several times faster than the frequency of the low pass filter. The averaging of the data in the frequency domain is a very effective way to reduce the amount of noise. The code used for post-processing can be found in Appendix A.

In conclusion, the highest signal to noise ratio is achieved by apply 600 VDC to the photomultiplier tube, reducing the gain on the pre-amplifier while using the bandpass filter, boosting the gain with the oscilloscope, and using a FFT routine that is capable of averaging the results. Dry-ice was a critical improvement to previous deflectometry designs. The dry-ice cooled the photomultiplier tubes which boosted the signal to noise ratio by reducing the amount of noise due to dark current. Figure 3.14 shows the photomultiplier tube's response before any of the previously discussed improvements were implemented. Based up on the peak of the signal and the average of the noise amplitude, the signal to noise ratio is approximately 3. Figure 3.15 shows the results of these improvements, run 82 has a signal to noise ratio of approximately 8. This is a substantial improvement. The details of this test can be seen in Chapter 4.

3.2.3 Design Summary

Deflectometry is a non-intrusive diagnostic that measures the frequency of density fluctuations at a point in a flow. As shown in table 3.7, there are many diagnostics used to measure flow turbulence including diagnostics such as, hot-wire

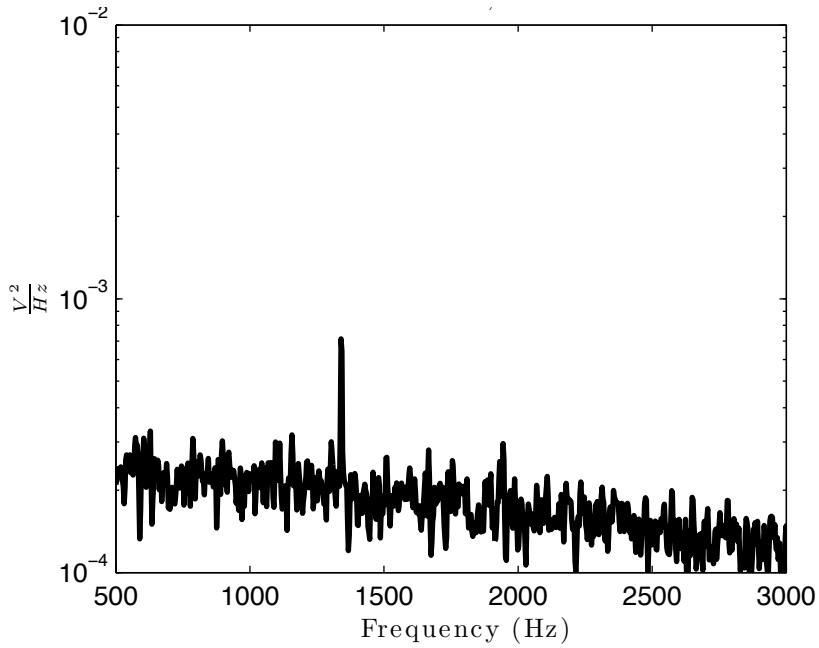

Figure 3.14: Run 37, signal before improvements to deflectometry diagnostic, L = 2.25".

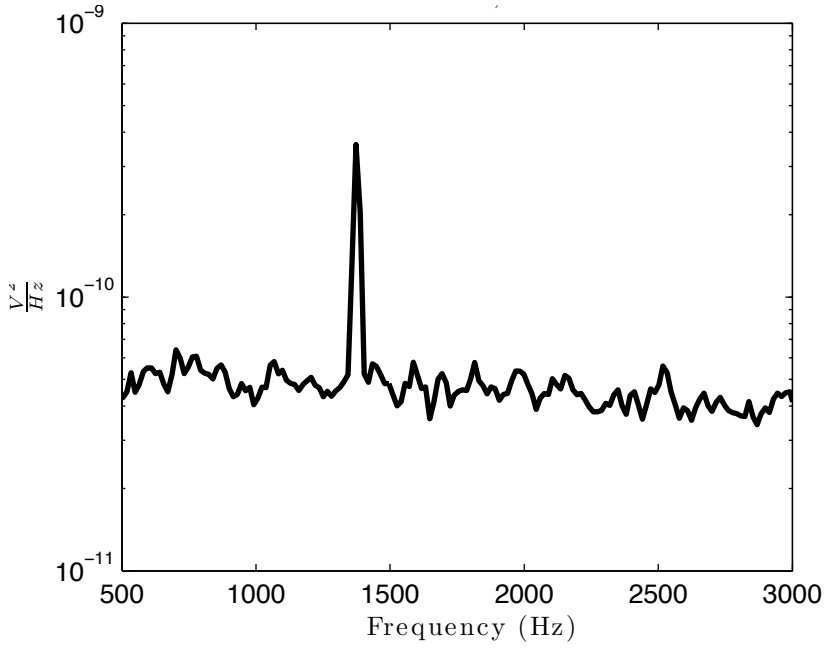

Figure 3.15: Run 82, signal after improvements to deflectometry diagnostic, L = 2.25".

anemometry, laser differential interferometry, and pressure transducers. Deflectometry extends the usefulness of focused schlieren by making quantitative measurements from the schlieren image. Other diagnostics can accomplish the same measurements but deflectometry allows for more points to be measured simultaneously with a virtually unlimited frequency response [16] and a relatively simple operation. Laser differential interferometry (LDI) has a lot in common with deflectometry (both are based on schlieren principles [36, 37]). However deflectometry requires fewer components and allows for greater flexibility. Deflectometry can easily be repositioned between runs by adjusting the location of the optical fiber in the image plane. This adjustment can be done in a matter of minutes and greatly expands the capabilities of this diagnostic tool

Several improvements on previous work done by McIntyre [16] and other deflectometry diagnostics were developed. These are as follows:

- Cooling the photomultiplier tubes with dry-ice results in substantial gains in the signal to noise ratio
- Placing tubes and irises over the inlets to the fiber optic cables reduces noise by reducing the amount of stray light
- Positioning fibers is extremely difficult. This process is simplified by using the amplitude of the photomultiplier tube's response to determine their location with respect to the model surface

Table 3.7: Comparison of diagnostics used to measure fluctuations in a flow

	Advantages	Limitations
Deflectometry	• Frequency response is only limited by data acquisition • Measurement position quickly changed by repositioning fiber optic • Small fiber optics allow for multiple simultaneous measurements in a flow field • Accurate frequency measurements • Non-intrusive measurement	• Limited by the sensitivity of the parent focused schlieren system • Fiduciary mark is necessary for determining exact position in schlieren image
Hot-wire anemometry	• High frequency response • Excellent spatial resolution	• Fragile wire makes high speed flow measurements difficult • Intrusive measurement
LDI	• Non-intrusive measurement • Sensitive	• Multiple simultaneous measurements not feasible [6] • Complicated optical set-up
Pressure Transducers	• High signal to noise ratio	• Inflexible, transducers must be physically mounted in the model

Chapter 4

Experimental Demonstration of Diagnostics

Demonstrating the potential and utility of the non-intrusive focused schlieren and deflectometry diagnostics is a key aspect of this research. Once these diagnostics were refined, the next step was to perform experiments that demonstrated their potential. The calibration laboratory's Mach 3 wind tunnel was used to image supersonic flow over different fundamental geometries. In order to demonstrate the deflectometry diagnostic, characteristic frequencies of different sized hollow pipes were measured. This work culminated in the transition cone test in the hypervelocity wind tunnel 9. The results from this test demonstrate the potential of this diagnostic. The goal behind this test was to image and measure the frequency of second-mode instability waves that occur in the transition region of a hypersonic boundary layer.

4.1 Calibration Laboratory

Testing focused schlieren and deflectometry in Tunnel 9's calibration laboratory was a critical part of the development process. This facility was an important stepping-off point before implementing these diagnostic tools in the Tunnel 9 hypersonic wind tunnel.

The calibration laboratory features a vacuum vessel with an attached Mach 3

nozzle The test section has a height of 6 in, a width of 4 in, and a length of 6 in. To operate the wind tunnel, the vacuum vessel is evacuated to near vacuum and a butterfly valve, located between the nozzle and the vacuum vessel, is opened. Air is pulled through the converging-diverging nozzle generating a Mach 3.1 flow with a duration of 10 seconds. The vacuum pumps and valves were controlled by a desktop computer running a custom Labview program. On both sides of the test section were tables, which were used for mounting the schlieren and deflectometry diagnostic equipment. This allowed for imaging supersonic flows over a variety of basic geometries, such as a sphere and wedge, and for testing the deflectometry system. This laboratory was critical in developing a sensitive schlieren and deflectometry diagnostic. The lessons learned in this laboratory were critical to the successful testing in Tunnel 9. The final layout of the focused schlieren diagnostic in the calibration laboratory can be seen in figure 4.1.

4.1.1 Focused Schlieren

The focused schlieren's measurement capabilities were tested by imaging Mach 3 flow over a sphere and a wedge. One of the first investigations was to examine the focusing ability of the diagnostic. This was done by spraying a can of aerosol duster in the focal plane, figure 4.2 and out of the focal plane, figure 4.3. The spray can was 12 cm away from the focal plane in figure 4.3. The images of the flow over these models that was taken in the calibration laboratory were of excellent quality. Images were sharp, sensitive, and aberration free. The results can be seen in figures

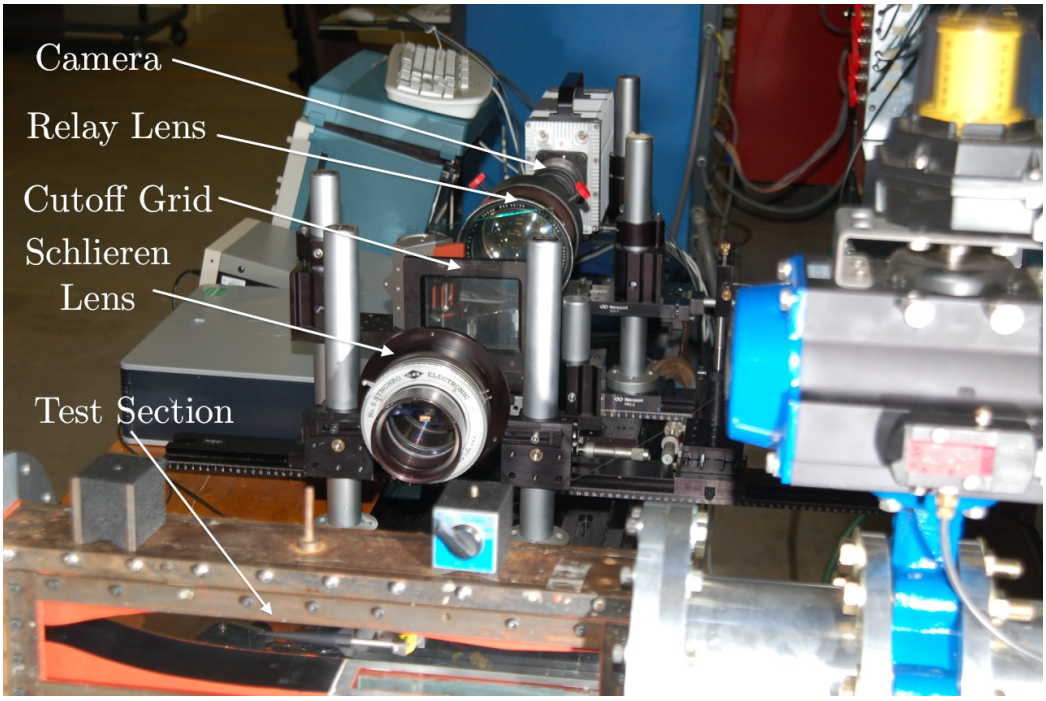

Figure 4.1: Layout of focused schlieren diagnostic in the calibration laboratory.

4.4 and 4.5. Both images were recorded using a Redlake high speed camera at 1000 fps. A copper vapor laser was used for the light source. Figures 4.4 and 4.5 demonstrate the narrow region of sharp focusing. Despite using scratched windows in the calibration laboratory wind tunnel, none of these aberrations are present in these images. Additionally, density gradients due to the boundary layer along the wall and thermal gradients outside the test section are not visible. These images demonstrate the sensitivity of the focused schlieren system. As an example, in figure 4.4, the point where the flow separates from the sphere is clearly visible. In figure 4.5, the boundary layer can be seen on the top surface.

In these images, banding due to the source grid is visible, which is due to two factors. First, in order for the schlieren image to be adequately illuminated,

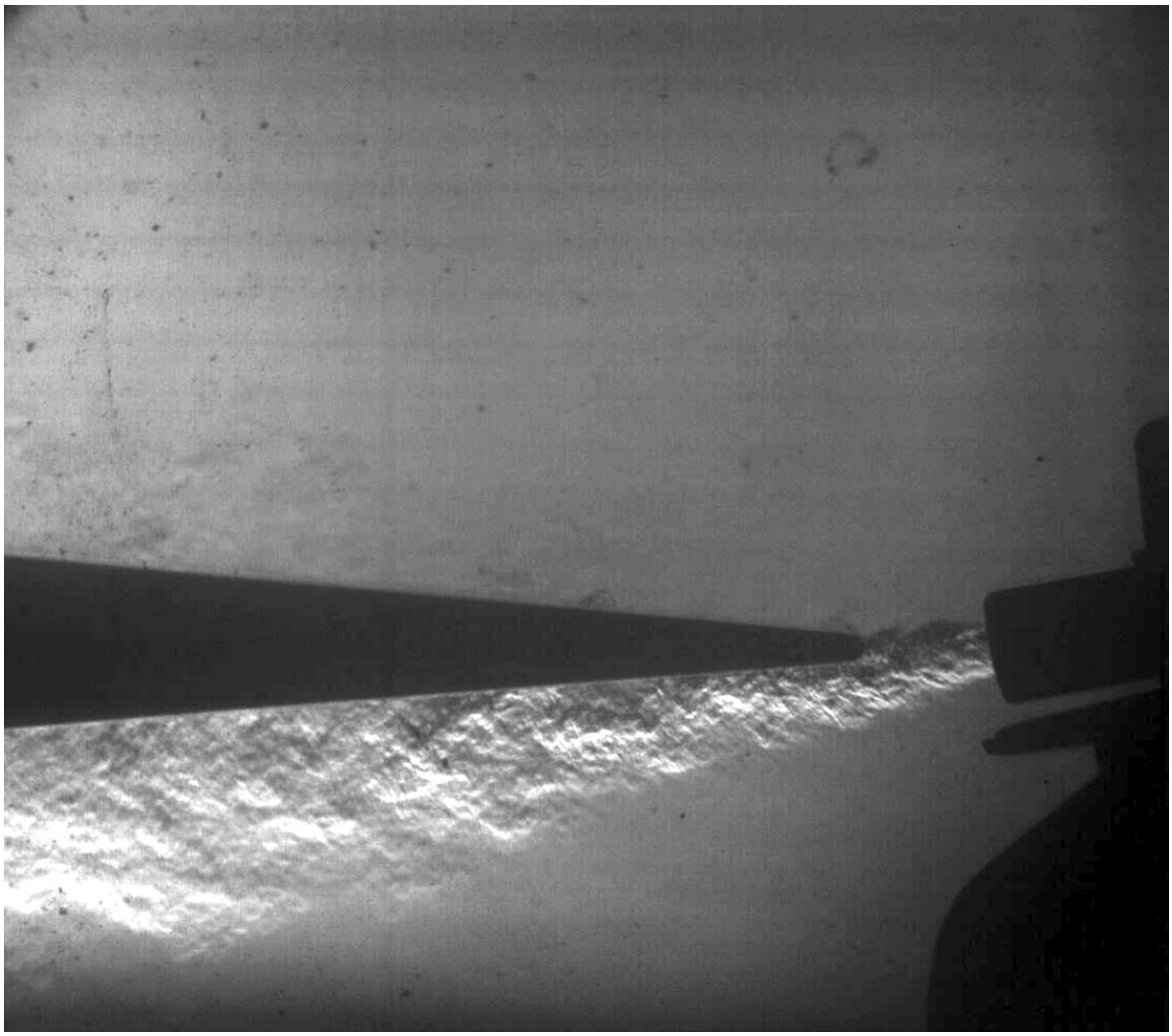

Figure 4.2: Image of jet in focal plane using copper vapor laser.

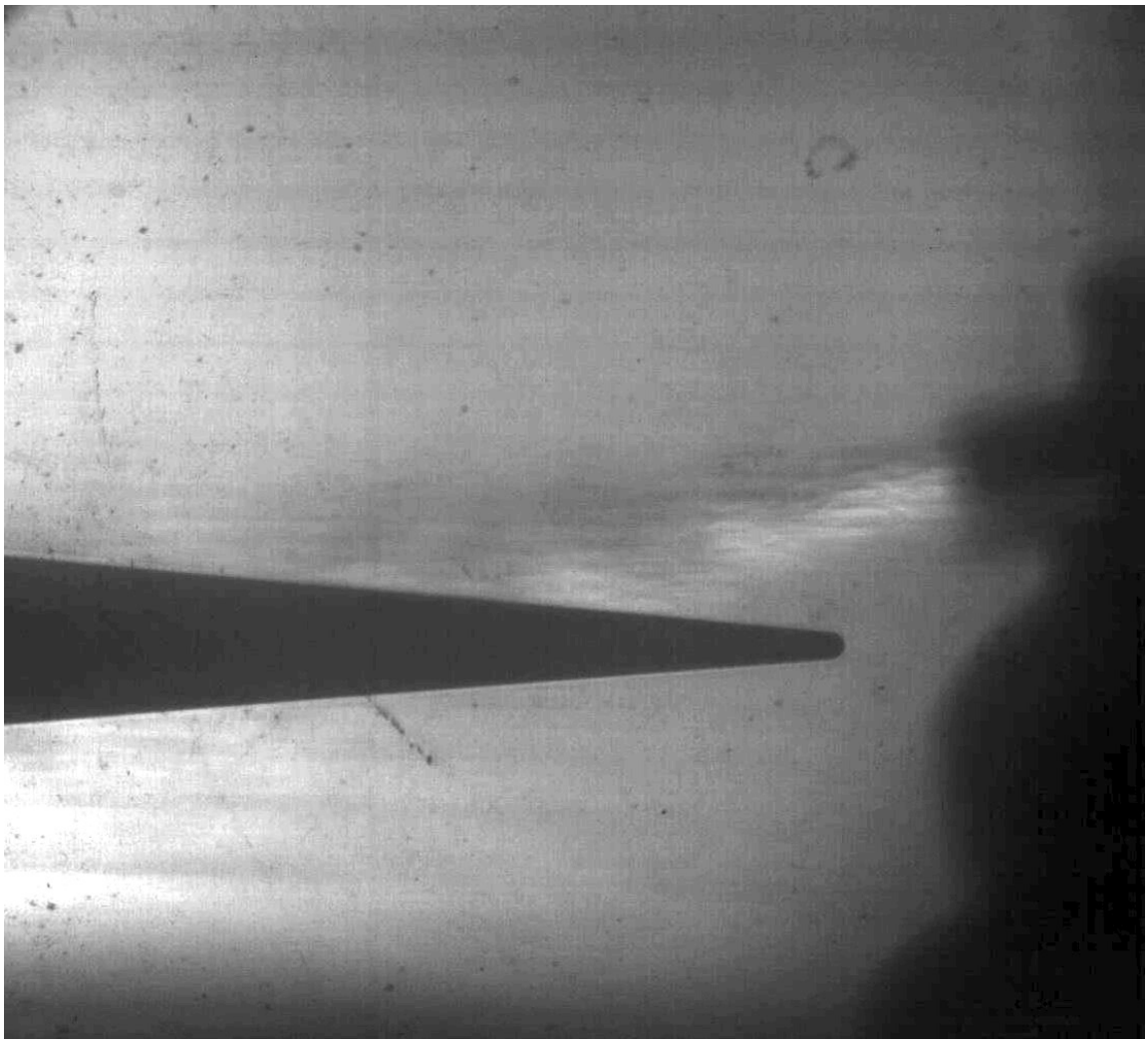

Figure 4.3: Image of jet out of focal plane using copper vapor laser.

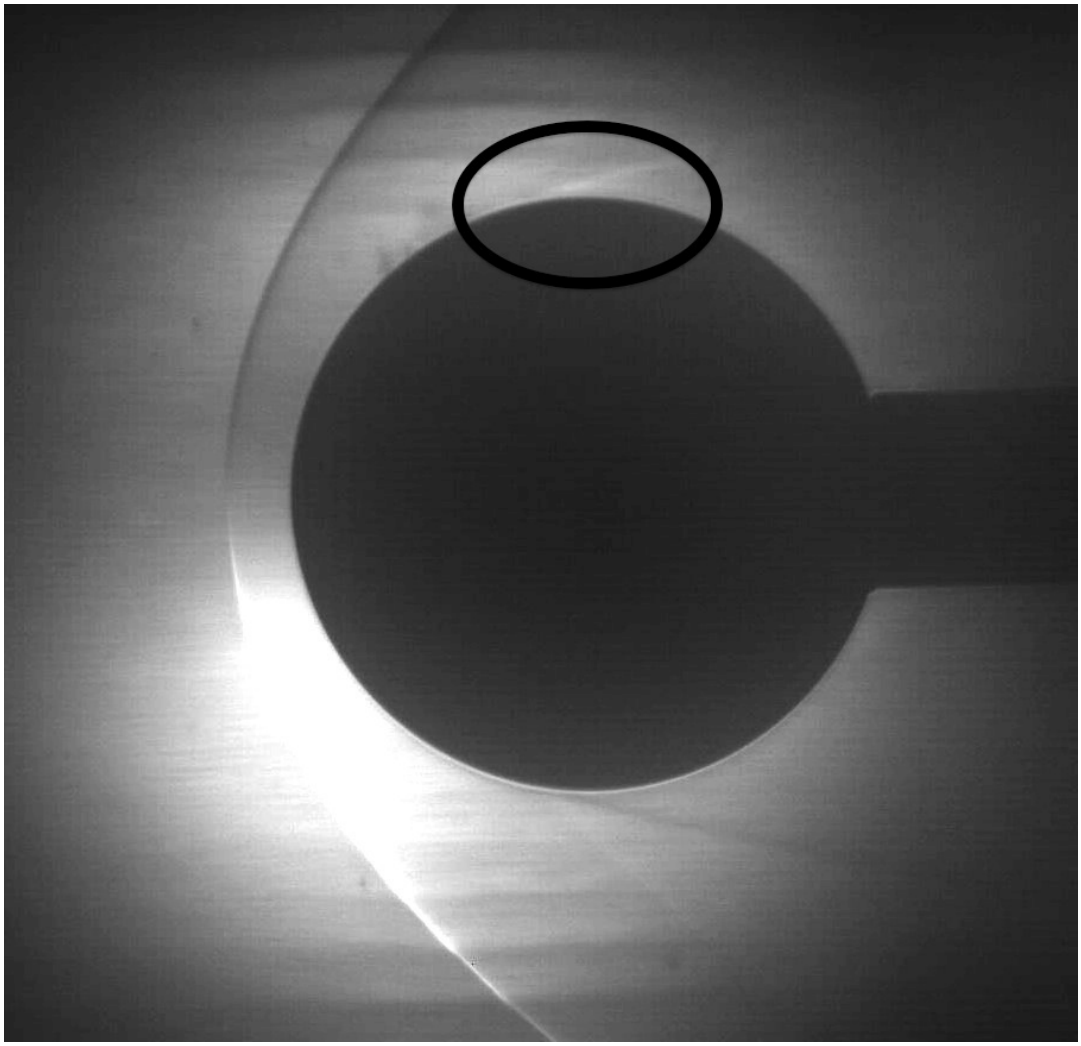

Figure 4.4: Sphere in the Mach 3 calibration laboratory test section, note flow separation.

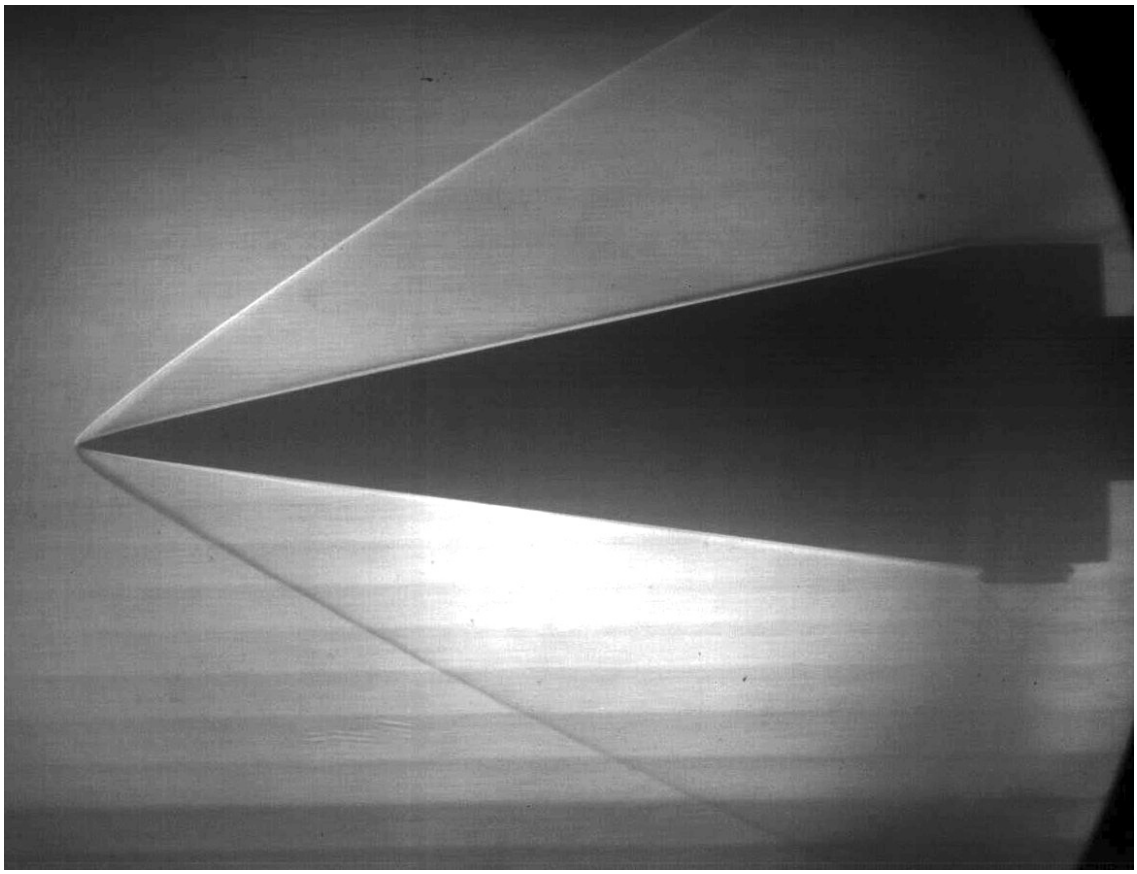

Figure 4.5: Wedge in a Mach 3 flow, in the calibration laboratory.

a camera is used instead of ground glass. The lens on the camera, despite using a macro lens, can still image the grid lines since its depth of field is wider than the image plane of the object of interest. The other contributing factor is that the image of the source grid did not match perfectly with the cutoff grid lines. Attempts were made at eliminating this banding. The Tunnel 9 set-up improved this slightly by making the source grid lines equally spaced. However this is a purely aesthetic issue and does not effect the quality of data The lessons learned from this experiment were critical to the deployment of this diagnostic in the Tunnel 9 hypersonic wind tunnel. As the example images have shown, this diagnostic was demonstrated to be ready for large scale deployment.

4.1.2 Deflectometry

The calibration laboratory's Mach 3 wind tunnel was a critical test bed for the development and improvement of the deflectometry diagnostic system. Deflectometry's ability to measure frequencies of density fluctuations non-intrusively allows for many possible experimental applications. The calibration laboratory was critical for refining the deflectometry tool. To properly design this system, experimentation is necessary since the system is dependent on the optics used and their alignment. It is critical to be able to quickly repeat tests in order to improve the diagnostic, this is why the calibration laboratory, with its 15 minute turn around time, played a significant role in this development process.

In order to develop this diagnostic, it was necessary to devise an experiment

that allowed for measured frequencies to be compared to frequencies that can be predicted and measured by other means. To achieve this, organ pipe theory [34] was used to devise an experiment. This theory states that a characteristic frequency is inherent to a hollow pipe placed parallel to a flow. This frequency, as shown by equation4.1 from Kim's paper [34], varies with length, where f is the characteristic frequency, R_{air} is the gas constant, T_o is the total temperature, and L^* is the effective length.

$$f = \frac{\sqrt{\gamma R_{air} T_o}}{4L^*} \tag{4.1}$$

In equation 4.1 the corrected length term, L^*, includes the gap between the shock wave and the tip of the pipe. The gap was approximated to have the same dimensions as the pipe diameter, which was 0.25 in. To verify the deflectometry measurements, a Kulite pressure transducer was placed at the base of the pipe to measure the frequency of the pressure fluctuations. Kulite gages have a maximum frequency response of 20 kHz. For the deflectometry measurements, a tip of a fiber optic cable was placed in the focused schlieren image, at the image of the entrance of the pipe. The pressure and density fluctuations are coupled so the pressure transducer and deflectometry diagnostic measured the same frequencies. Tubes of different lengths were used to test and optimize the deflectometry system. The lengths and the frequencies of the different pipes tested can be seen in table 4.1. The measured frequencies matched the predicted values very well, which can be seen in the Power Spectral Density (PSD) plots of the deflectometry and pressure data. Figures 4.7, 4.9, 4.11, 4.13 show the dominant characteristic frequency as

measured by the deflectometry diagnostic. These plots match very well when compared to the PSD plots of the Kulite pressure transducer, in figures 4.6, 4.8, 4.10, 4.12. These two diagnostics measured the exact same frequencies. These excellent results demonstrate the potential of this diagnostic for wind tunnel testing. This diagnostic is non-intrusive and provides extremely accurate frequency information. This capability combined with the flexibility of being able to quickly reposition the measurement locations, makes it well suited to a range of different experiments.

Despite the potential of this diagnostic, there are some disadvantages of deflectometry. As the plots show, the primary disadvantage is that the signal to noise ratio is not as strong as that of the Kulite pressure transducers. The primary factor, as discussed in Chapter 3, the deflectometry system introduces noise into the measurement. This noise only affects the amplitude of the signal and not the frequency. It is important to note that the deflectometry diagnostic did not measure data at the same point in the flow as the pressure transducer. Due to optical access requirements, the deflectometry measured the frequency at the tip of the pipe while the pressure transducer measured the frequency at the base of the pipe. With future development, the signal to noise ratio can be improved through refinement of the optics.

4.2 Transition Cone Experiment at Tunnel 9

For the transition cone experiment, focused schlieren and deflectometry were used to image and measure the frequency of second-mode transition waves on a 7°

Table 4.1: Pipe lengths tested in Mach 3 nozzle

L (in)	Predicted (Hz)	Pressure Gage (Hz)	Deflectometry (Hz)	Figures
1.125	2462	2380	2380	4.6 and 4.7
1.500	1934	1933	1933	4.8 and 4.9
2.250	1354	1340	1340	4.10 and 4.11
3.000	1042	1040	1040	4.12 and 4.13

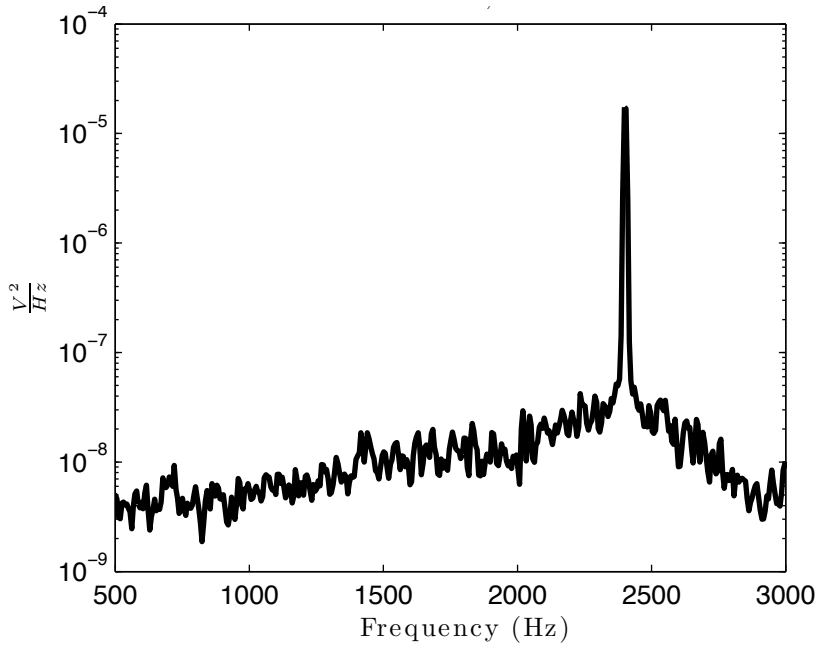

Figure 4.6: PSD plot of run 51, L = 1.125" Pressure transducer frequency measurement.

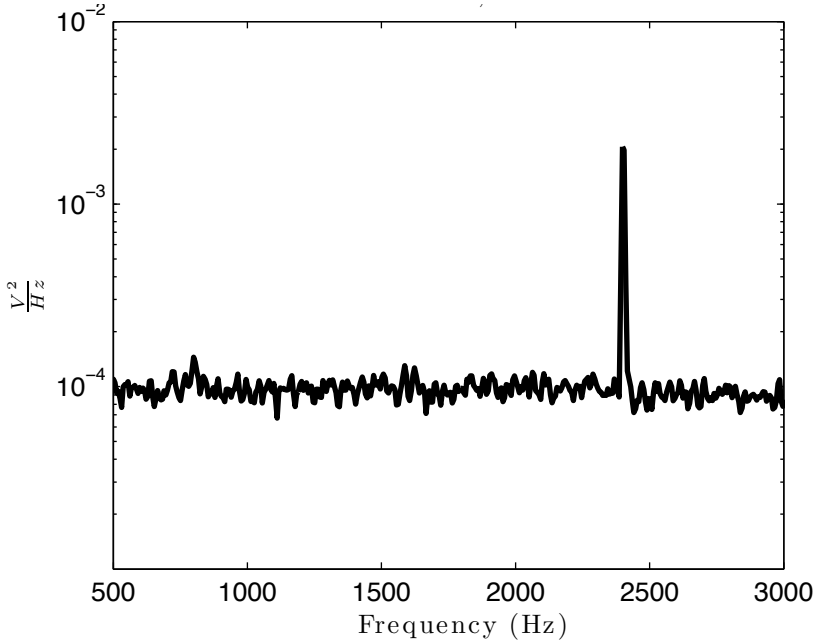

Figure 4.7: PSD plot of run 51, L = 1.125" Deflectometry frequency measurement.

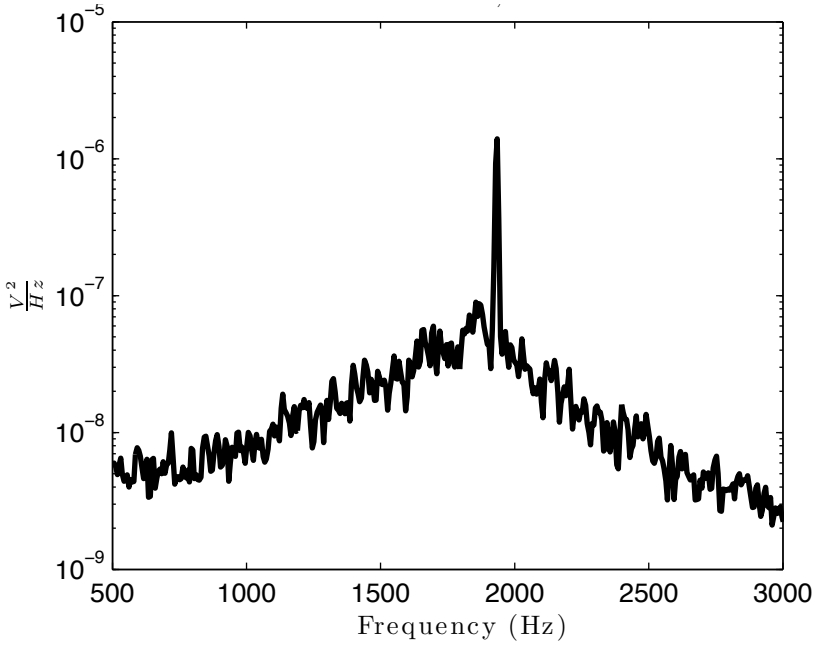

Figure 4.8: PSD plot of run 50, L = 1.5" Pressure transducer frequency measurement.

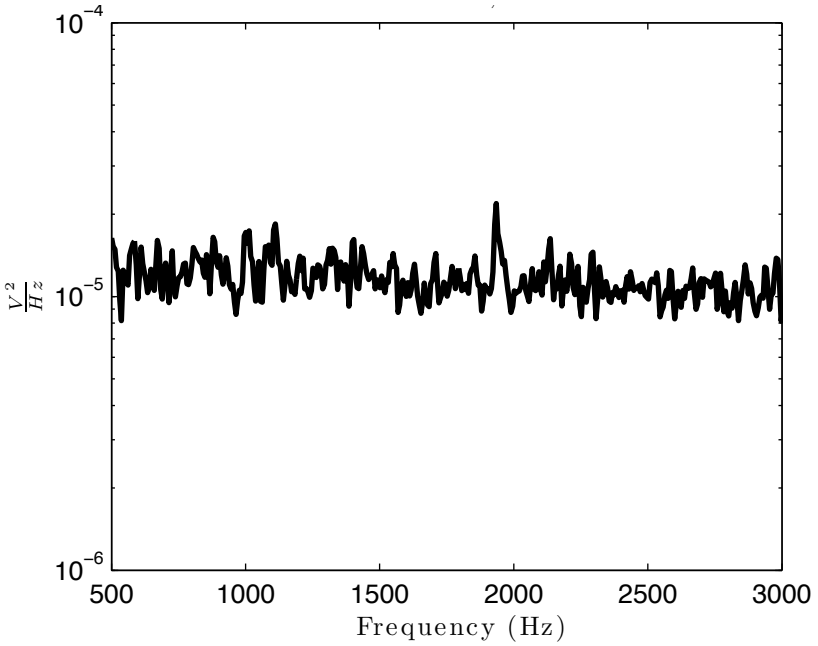

Figure 4.9: PSD plot of run 50, L = 1.5" Deflectometry frequency measurement.

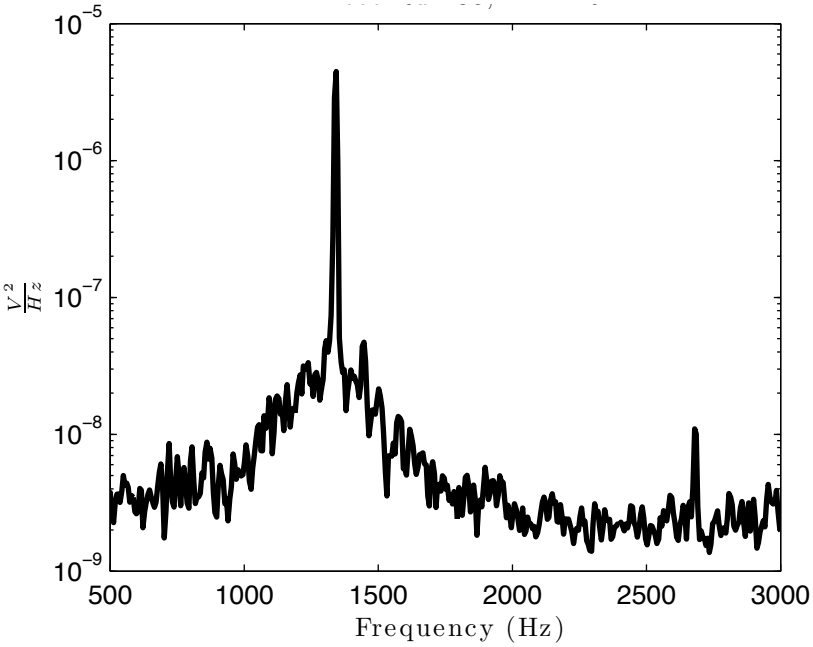

Figure 4.10: PSD plot of run 38, L = 2.25" Pressure transducer frequency measurement.

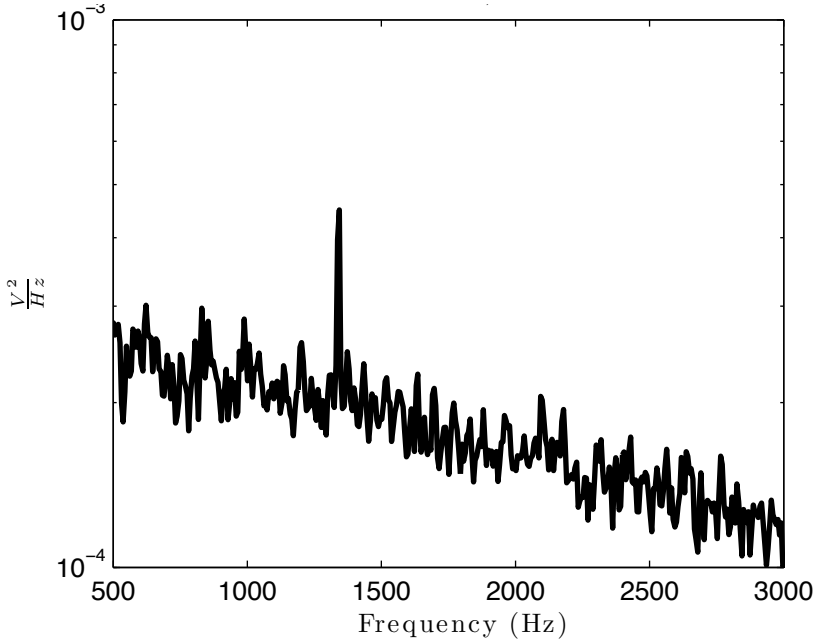

Figure 4.11: PSD plot of run 38, L = 2.25" Deflectometry frequency measurement.

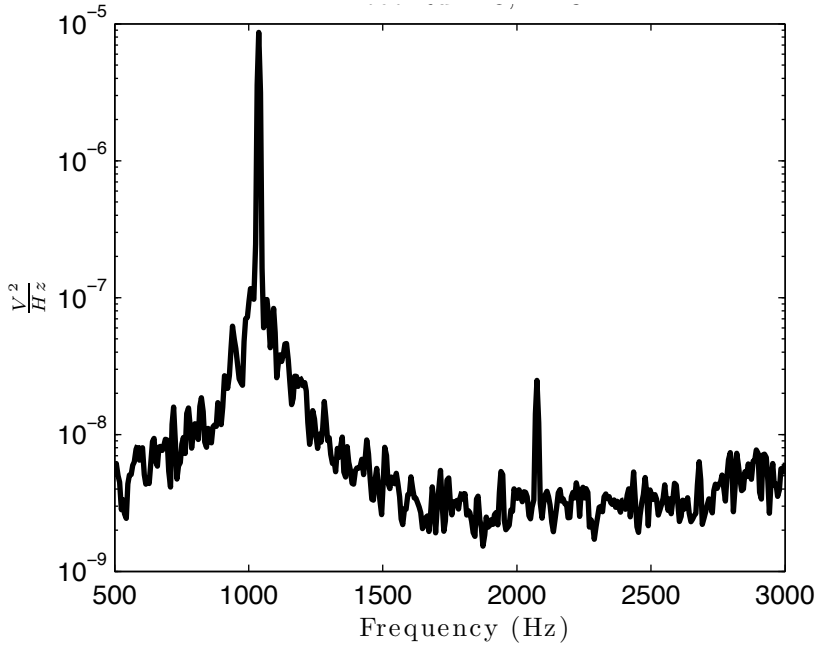

Figure 4.12: PSD plot of run 48, L = 3" Pressure transducer frequency measurement.

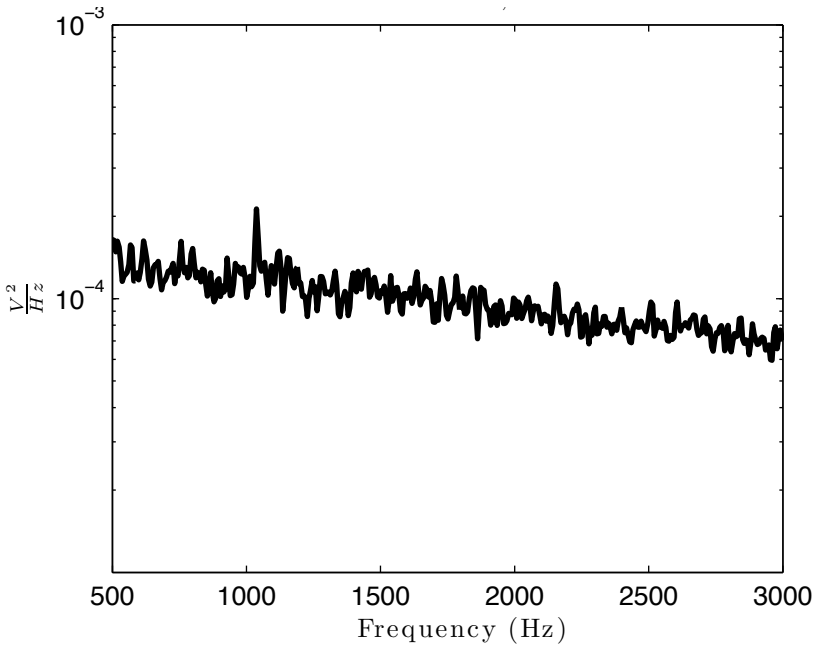

Figure 4.13: PSD plot of run 48, L = 3" Deflectometry frequency measurement.

half-angle sharp nosed cone. This cone is part of an AFOSR sponsored project run by researchers from Purdue University and Sandia National Laboratory. The goal of this research is to investigate the physics associated with second-mode instability waves in the hypersonic boundary layer of this cone. Second-mode instability waves are present just before the point of transition from laminar to turbulent in the boundary layer. These waves can be thought of as trapped acoustic waves in the boundary layer. The formation and amplification of these instabilities can be attributed to the rate of wall cooling, tunnel noise, surface roughness and nose bluntness [6]. Researchers at Purdue University were particularly interested in the effect acoustic waves generated by turbulence along wind tunnel walls, has on second-mode wave formation. To do this, researchers tested this cone at hypersonic wind tunnels throughout the country, including hypersonic wind tunnels at Purdue Univer-

sity, Sandia National Laboratory, Boeing/AFOSR Quiet Wind tunnel, and NASA Langley, under similar conditions. With this data, the goal is to validate CFD solvers to improve boundary layer transition prediction [7] as well as provide data for CFD solvers. These second-mode waves were measured using PCB132A31 pressure transducers. The location of these transducers can be seen in figure 4.14, and are numbered 1, 2, and 3 beginning at the tip of the model. The focused schlieren diagnostic was used to image these second-mode waves, while deflectometry was used to measure their frequency at these points. This test was performed in the Tunnel 9 hypersonic wind tunnel.

Tunnel 9 is a hypersonic wind tunnel capable of operating at Mach numbers of 7, 8 , 10, and 14. It is capable of operating at supply pressures and temperatures as high as 21,000 $psia$ (144.8 MPa) and 3500 $^{\circ}R$ (1944 $^{\circ}K$). Tunnel 9 is a blowdown facility that uses nitrogen as its working fluid. The test cell has a diameter of 5 ft (1.5 m) and a nozzle length of 40 ft (12.2 m). The large test cell allows for the testing of large-scale models to more accurately replicate high speed aerodynamic effects. This size also allows for testing more than one model at a time, as demonstrated in the transition cone test. On both sides of the test cell are 5 ft (1.5 m) diameter tubes, 14 ft (4.3 m) in length. These tubes can be tilted upwards and moved in a lateral direction. These tubes contain the conventional schlieren (z-type) system used by Tunnel 9. The focused schlieren and deflectometry equipment were placed inside of these schlieren benches. Rigid Klinger® rails were clamped to the internal support beams inside these benches to support the focused schlieren equipment, this can be seen in figure 3.11. This allows for adjustment and quick removal of focused

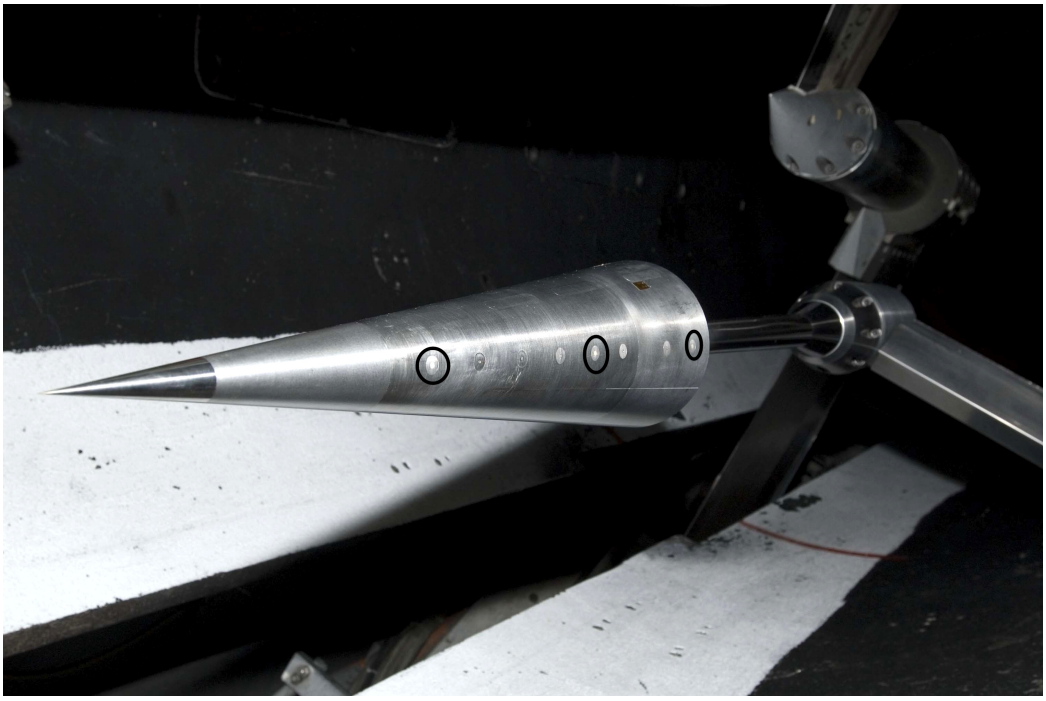

Figure 4.14: Image of Sandia transition cone, 20" in length, PCB gages marked by black ovals.

schlieren optics without interfering with the placement of the conventional schlieren optics.

4.2.1 Focused Schlieren

Focused schlieren was implemented in the Tunnel 9 hypersonic wind tunnel in order to image second-mode instability waves. This is the first time, based on a detailed literature review, that this schlieren technique has been used to examine hypersonic flow phenomena. This diagnostic was used across a range of Reynolds numbers as shown in table 4.2 which demonstrates the potential of this diagnostic. The focused schlieren's field of view was located between $x = 8\ in$ and $x = 16\ in$

Table 4.2: Tunnel 9 nominal test conditions

Run #	Mach #	Re #/ft	ρ_{inf} $(\frac{lbm}{ft^3})$	t (s)	Focus. Schlieren	Deflectometry
3317	10	1.0E6	6.10E-4	3.00	Yes	No
3318	10	4.0E6	1.91E-3	0.80	Yes	No
3320	10	2.0E6	1.0E-4	1.5	Yes	No
3321	10	0.57E6	9.43E-6	5.00	No	Yes
3322	10	0.57E6	9.43E-6	5.00	No	Yes
3323	10	2.0E6	1.0E-4	1.50	No	Yes
3324	10	2.0E6	1.0E-4	1.50	No	Yes
3325	10	10E6	5.26E-3	0.55	Yes	No
3327	10	10E6	5.26E-3	0.55	No	Yes
3328	10	10E6	5.26E-3	0.55	No	Yes
3329	10	2.0E6	1.0E-4	1.50	No	Yes

from the tip of the sharp cone with the exception of the $10x10^6$ $Re\#/ft$ flow where it was located between $x = 0$ in and $x = 8$ in. These regions were where second-mode waves were expected based upon the calculations made by the STABL solver by the Air Force Research Laboratory. These waves were visible on runs 3317 and 3320 which have Reynolds numbers per unit length of $1x10^6$ $Re\#/ft$ and $2x10^6$ $Re\#/ft$.

Figures 4.15 and 4.16 shows the flow over the transition cone for the $1.0x10^6$ $Re\#/ft$ case. Even though the density is low, the second-mode waves are clearly visible in figure 4.16. For the images taken for the unit Reynolds number of $2.0x10^6$ $Re\#/ft$, second-mode instability waves are much more clearly visible, as shown in figure 4.17.Figure 4.18 shows an enlarged image of these waves. Figures 4.19 and 4.20 are images of the second-mode waves 0.033 s later. Second-mode waves are not steady, their locations shifts and are not present in every frame that was imaged.

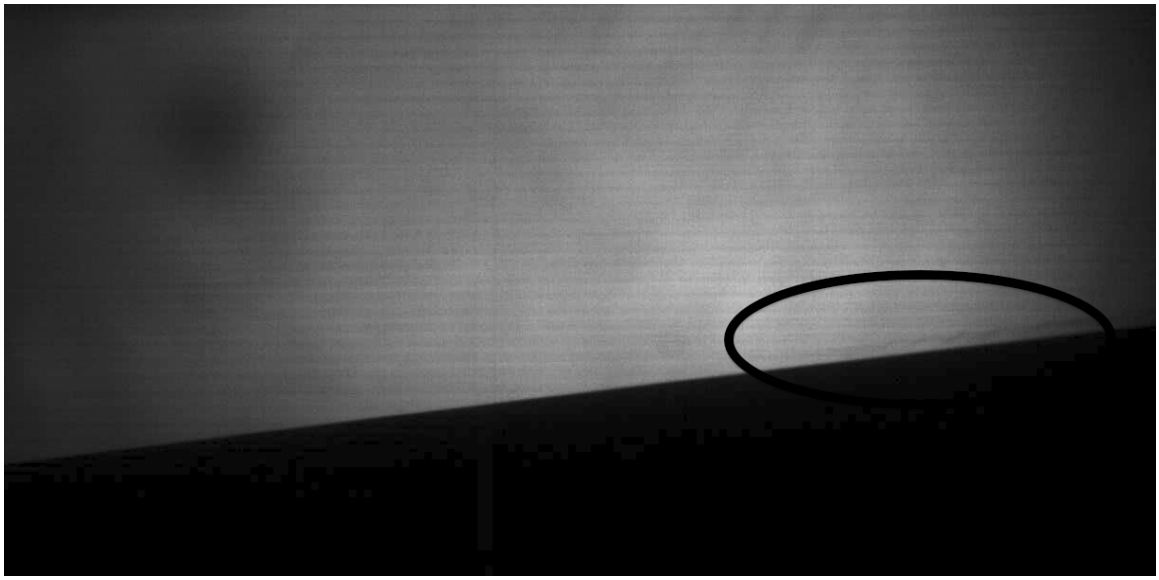

Figure 4.15: Run 3317, frame 2661 focused schlieren view of transition cone.

This is why the 25 *nsec* pulse duration is critical to capturing an image of these waves. Figure 4.21 demonstrates the amount of useful flow data this diagnostic is capable of capturing. This image shows the laminar boundary layer towards the tip of the cone followed by second-mode waves in the middle of the cone before they break down just before transition to turbulence in the right most side of the image.

These images were enhanced by background subtracting each frame and applying a 3 x 3 filter in Matlab . The background image was created by taking an average of 100 frames. Despite the presence of multiple test articles in the test section as shown in figure 4.22, the shocks and other disturbances emanating from these items were not visible. This is a testament to the utility of having a narrow region of sharp focus. These excellent results demonstrate the capability and utility of focused schlieren in a hypersonic wind tunnel.

Despite the successes of this diagnostic, some inadequacies were discovered.

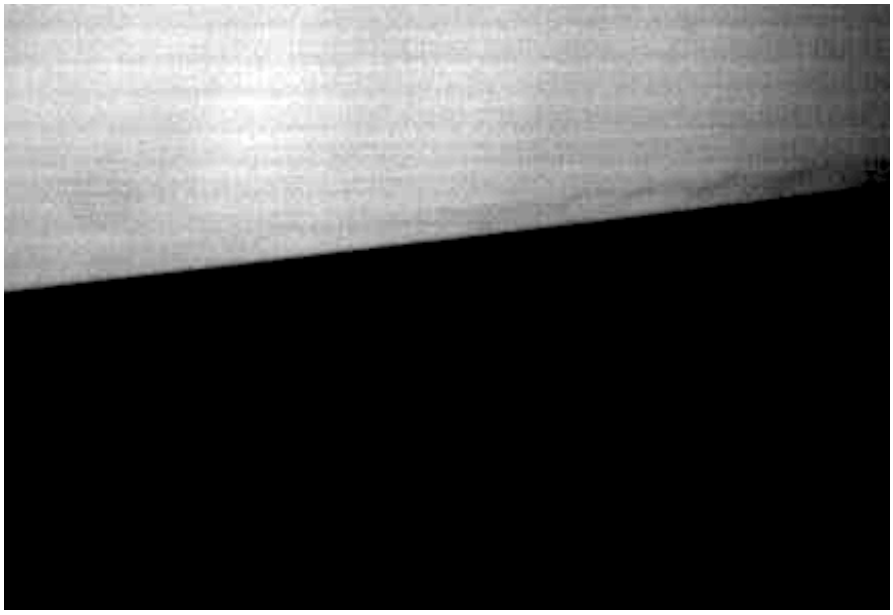

Figure 4.16: Run 3317, frame 2661 zoomed into region of second-mode instability waves.

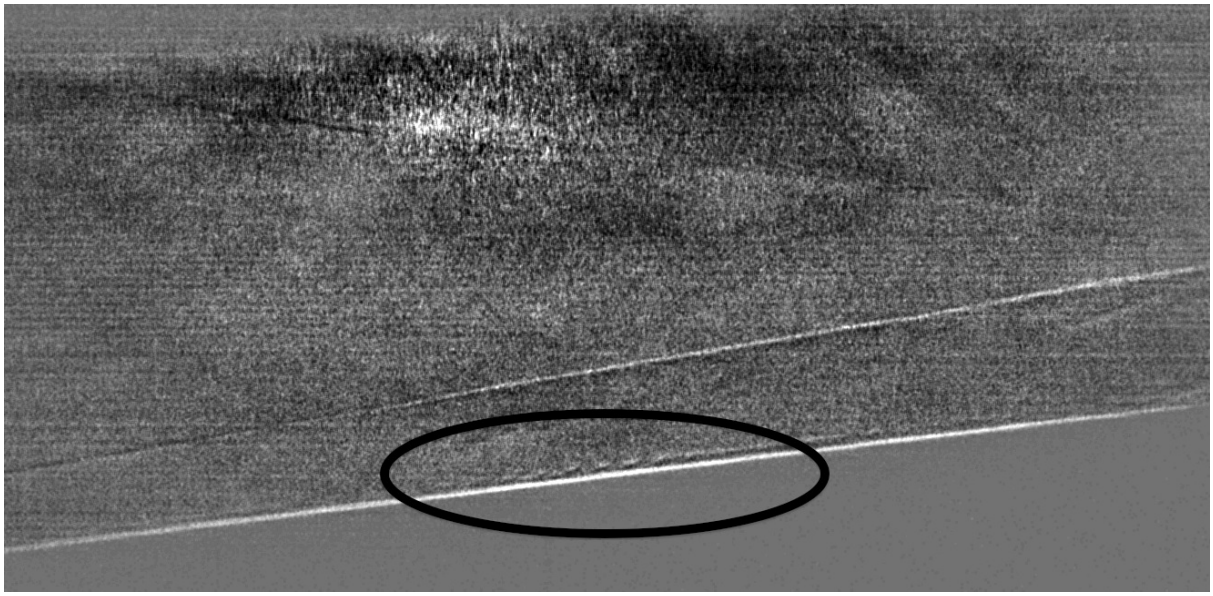

Figure 4.17: Run 3320, frame 1757, t=1.757 s focused schlieren view of transition cone.

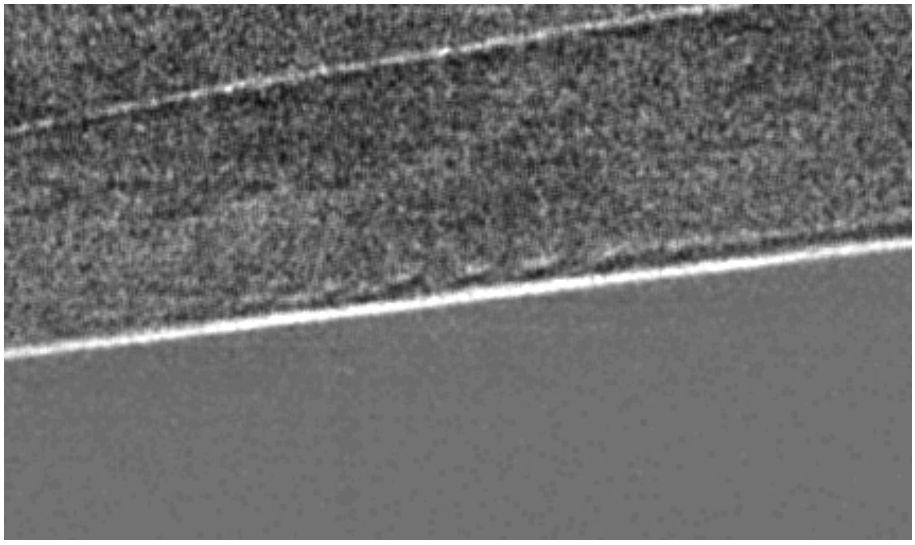

Figure 4.18: Run 3320, frame 1757 zoomed into region of second-mode instability waves.

Focused schlieren was unable to image the density gradients for Reynolds numbers of $0.57x10^6$ $Re\#/ft$. For this run, the density gradients were not strong enough for the diagnostic to image. However, transition was not expected to occur on the cone due to the low Reynolds number, which means second-mode waves would not have been present. The sensitivity of this diagnostic could be improved by optimizing the optical layout and components. The constraints on the optical layout due to the focused schlieren's placement in the schlieren benches is partially responsible for the reduced sensitivity. The focused schlieren system was placed inside of these benches to allow for quick removal and redeployment with minimal realignment. This was to reduce time spent aligning the system each time the tunnel was opened for inspection and model adjustment. The optical benches prevented the source grid and Fresnel lens from be adjusted in a significant amount along the optical axis. This also limited

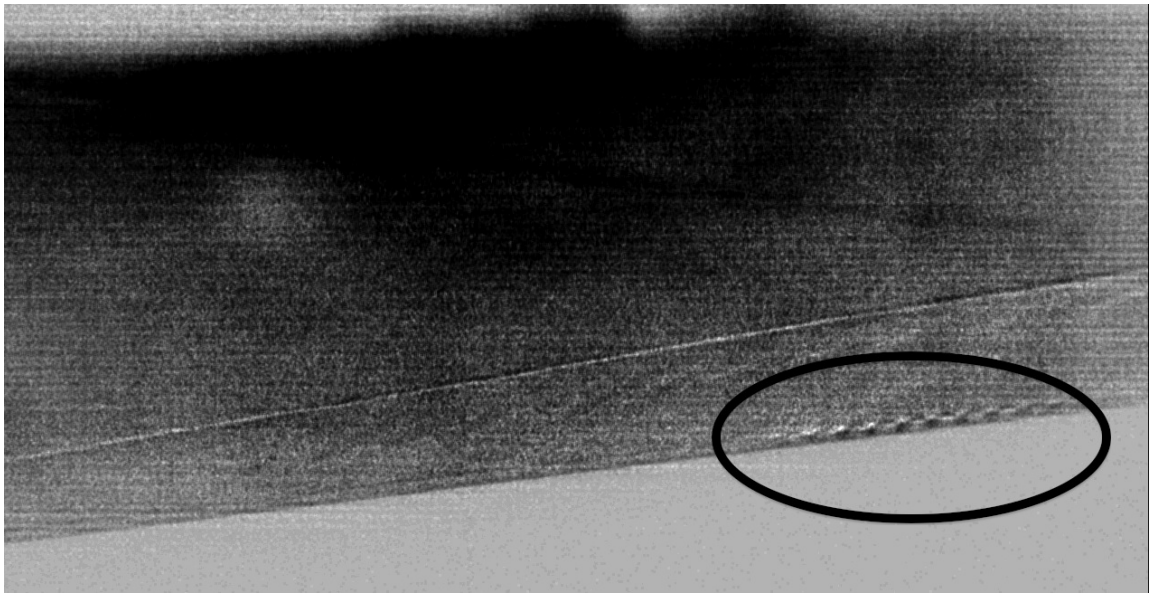

Figure 4.19: Run 3320, frame 1790, t=1.790 s focused schlieren view of transition cone.

the placement of the imaging lens along the optical axis. As discussed in Chapter 2, these dimensions play a critical role in the sensitivity of the diagnostic. Another important factor is that in order to clearly record the focused schlieren images, the Redlake high-speed camera requires a significant amount of light. This is in conflict with an increased amount of cutoff which increases sensitivity. As the amount of cutoff increases, the amount of illumination decreases which means it is important to balance the over all sensitivity of the diagnostic with the ability to record images of sufficient quality. Another issue in this experiment was that in order to avoid interference with the temperature sensitive paint diagnostic, half of the light from the source grid was blocked off. The light from the focused schlieren system caused reflections which were recorded by the temperature sensitive paint diagnostic which would affect the TSP diagnostic's data. This light would also excite the temperature

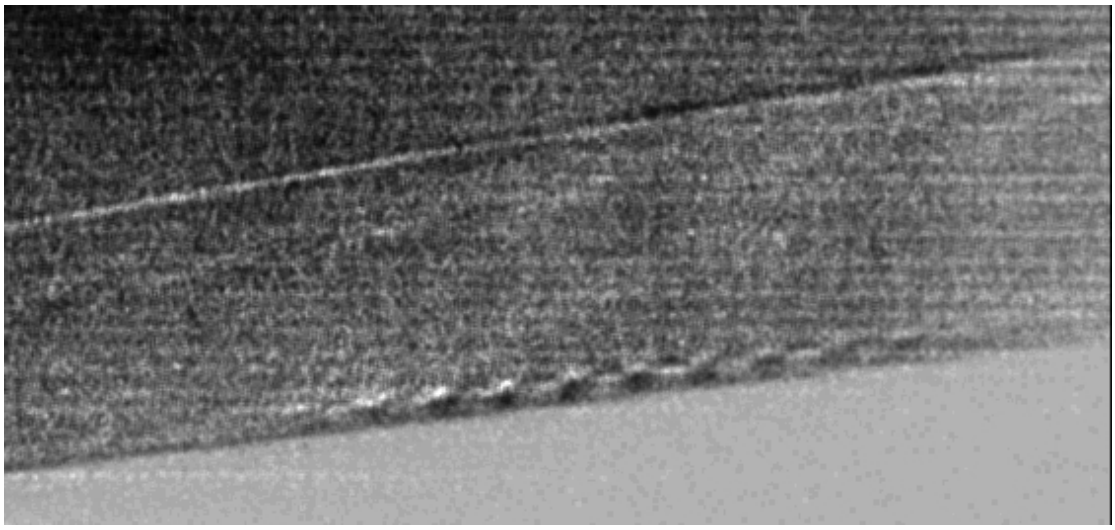

Figure 4.20: Run 3320, frame 1790 zoomed into region of second-mode instability waves.

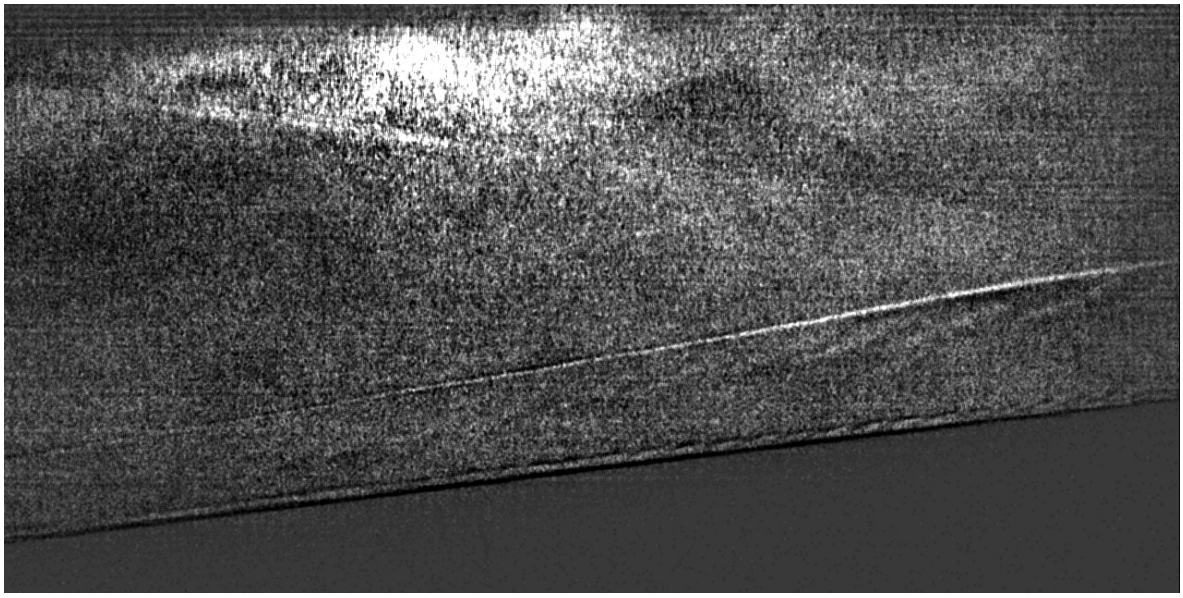

Figure 4.21: Run 3320, frame 1734, t=1.734 s focused schlieren view of transition cone.

Figure 4.22: Layout of test articles in Tunnel 9 test section.

sensitive paint and prematurely wear out the paint. Despite these drawbacks, the results were very good.

4.2.2 Deflectometry

Deflectometry is a non-intrusive diagnostic that was used to measure the frequency of second-mode instability waves in the transition cone's boundary layer. The frequencies measured using deflectometry were compared to PCB pressure transducers mounted on the model's surface. The primary advantage that deflectometry has over pressure transducers is that deflectometry affords greater flexibility. This tool allows the user to quickly reposition the sensors between runs or add additional sensors to investigate flow over a model of interest. A relevant example

would be that the growth of the second-mode waves could be examined over a large region of the boundary layer. This technique has never been successfully applied to measuring these instability waves. According to T. Roedinger et. al. [6], "A non-intrusive technique for simultaneous measurements of instabilities using stream wise arrays..." would be extremely useful for research into these second-mode rope waves. This experiment has shown the feasibility of this diagnostic by successfully measuring second-mode instability waves in the hypersonic boundary layer.

The most challenging aspect of the deflectometry system is ensuring that the fiber optic tips are aligned to measure the flow in the boundary layer. The boundary layer thickness in the image plane is on the same order as that of the 200 μ diameter fibers. These fibers, based upon the magnification ratio, have a field of view of approximately 1 mm or 0.04 in. To ensure that the fiber was located in the boundary layer, the fibers were positioned so that the shadow of the model was blocking them. With the 300 W light source on and the photomultiplier tube outputs connected to the oscilloscope, the fibers were raised towards the edge of the image of the model. The point where the signal from the photomultipliers started to increase, due to the light present above the model's surface, marks the boundary layer.

Deflectometry was used on the $10x10^6$ $Re\#/ft$, $2x10^6$ $Re\#/ft$, and $0.5x10^6$ $Re\#/ft$ runs. Second-mode waves were measured on the $2x10^6$ $Re\#/ft$ runs. Second-mode waves were not expected on the $0.5x10^6$ $Re\#/ft$ run due to the laminar boundary layer present over the majority of the model. If these waves were present, they would have been towards the base of the model in a region not accessible by the fibers used by deflectometry. No data was collected for run 3325,

the $10x10^6$ $Re\#/ft$ unit Reynolds number case, due to the square window being replaced by a round window with a smaller viewing area. The boundary layer was expected to be mostly turbulent for this case and the second-mode waves were expected to be present near the tip, if at all, which was not optically accessible. For the $2x10^6$ $Re\#/ft$ cases, second-mode waves were measured at different points along the surface of the cone. These results matched very closely to the PCB gage measurements and the computational predictions made using the STABL package. The first measurements were made on run 3323, figure 4.23, the fiber optic was located 0.7 in upstream from the number 2 PCB pressure gage or 13.5 in from the tip of the model. The frequency measured was 277 kHz which matches reasonably well to STABL predictions. As the second-mode waves appear further upstream towards the nose of the cone, their characteristic frequency increases. PCB gage 2, which is further downstream, measured a frequency of 250 kHz which is inline with the expected values. For run 3324, figure 4.24, the fiber optic was aligned with the second pressure transducer. The oscilloscope was saturated on this run but the deflectometry diagnostic measured the frequency of the second-mode wave because the photomultiplier tube was still responding. Run 3329 resulted in the best signal to noise ratio, figure 4.26. The fiber optic was aligned with the third PCB gage, 19.3 in downstream from the tip for this run. As figures 4.23, 4.24, 4.25, 4.26, and 4.27 below show, the implementation of the deflectometry diagnostic was extremely successful. The standard deviation for the deflectometry measurements was calculated to be about 10 kHz. This is larger than any difference of the measured frequencies using deflectometry or the pressure transducers. As mentioned previously, the main

drawback to deflectometry is the reduced signal to noise ratio which is evident when the PSD plots of the PCB measurements in figures 4.25 and 4.27 are compared to the PSD plots of the deflectometry data in figures 4.24 and 4.25. The results of this experiment are summarized in table 4.3. The deflectometry diagnostic proved to be

Table 4.3: Transition cone deflectometry results

Run	Position (in)	PCB Gage (kHz)	Deflectometry (kHz)
3323	13.5	-	277
3324	14.2	250	254
3329	19.3	216	211

very well suited for measuring the frequency of second-mode waves. The measurements matched almost exactly with the pressure transducer measurements. These successful measurements are a proof of concept of this diagnostic and the potential of this tool opens the door to more interesting experiments that fully utilize the flexibility of this deflectometry tool. Using deflectometry, it is straight forward to quickly examine additional points in the flow or adjust the location of what is currently being measured. This flexibility, and non-intrusive nature, provides a significant advantage over fixed gages on the surface of a test article.

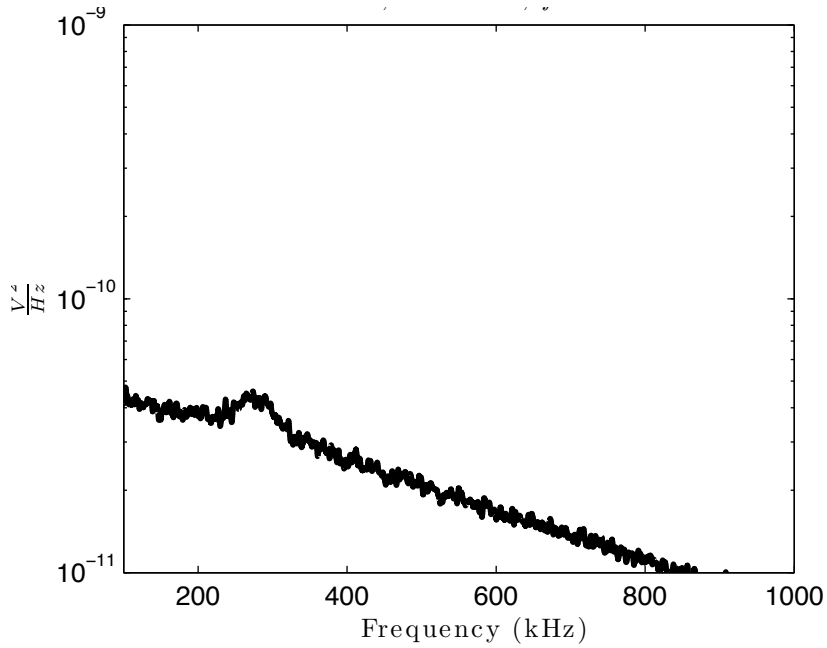

Figure 4.23: Run 3323, x = 13.5" from tip, PSD plot of deflectometry frequency measurement, $f = 277\ kHz$.

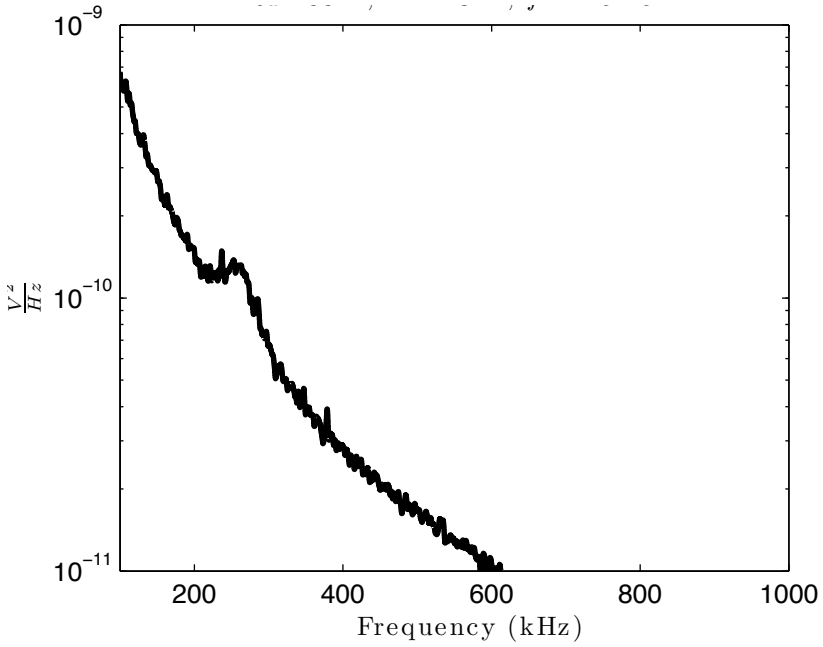

Figure 4.24: Run 3324, x = 14.2" from tip, aligned with PCB gage 2, PSD plot of deflectometry frequency measurement, $f = 254\ kHz$.

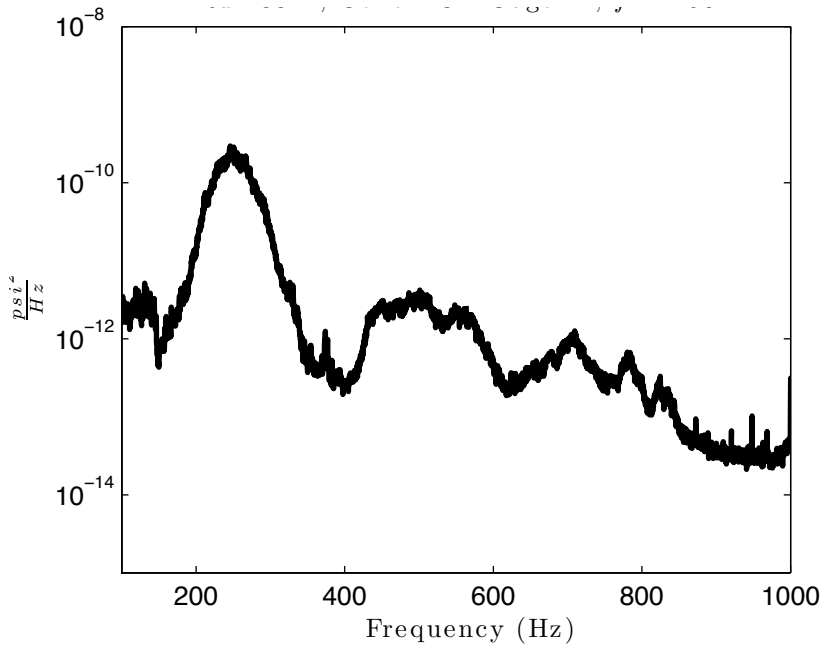

Figure 4.25: Run 3324, PSD plot of PCB Gage 2 frequency measurement, $f = 250\ kHz$.

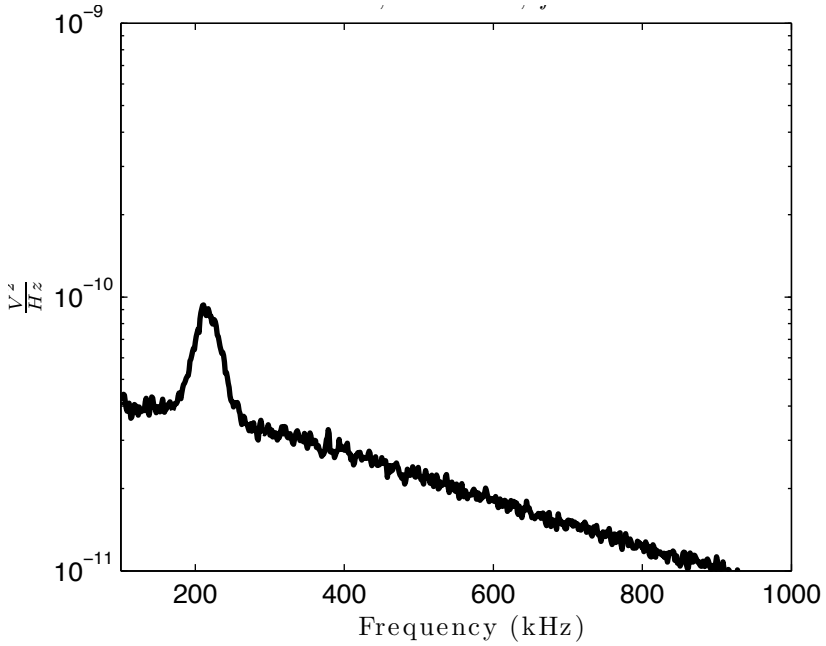

Figure 4.26: Run 3329, x = 19.3", aligned with PCB gage 3, PSD plot of deflectometry frequency measurement, $f = 211\ kHz$.

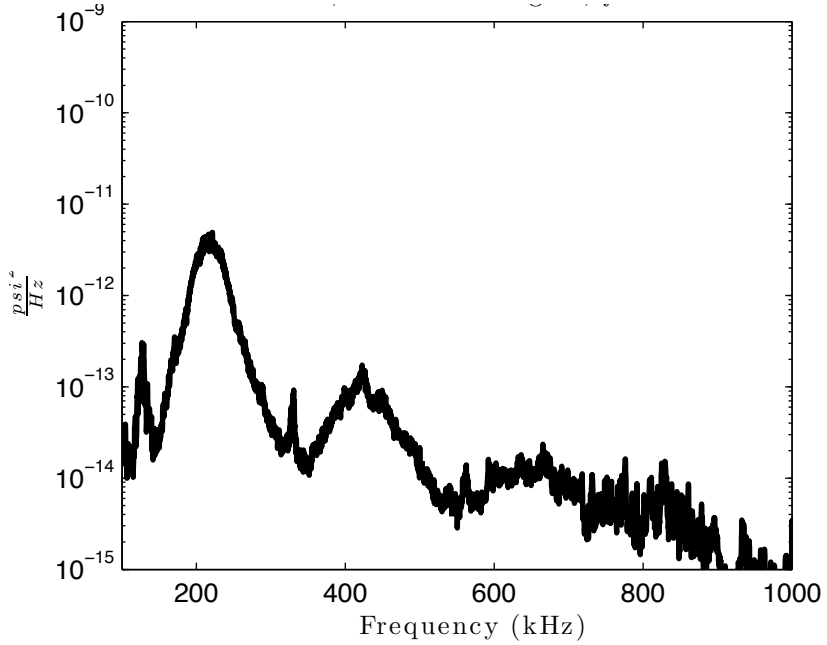

Figure 4.27: Run 3329, PSD plot of PCB Gage 3 frequency measurement, $f = 216\ kHz$.

Chapter 5

Summary and Conclusions

Focused schlieren and deflectometry have never been demonstrated in hypersonic windtunnel testing. This diagnostic is a non-intrusive, optical method of imaging density gradients and measuring the frequency of density fluctuations in a narrow region of flow. The focused schlieren and deflectometry system that was developed for the Tunnel 9 hypersonic wind tunnel has a large field of view (25 cm), a narrow region of sharp focus (1 cm), and is sensitive enough to measure boundary layer phenomena such as second-mode waves with free-stream densities as low as 0.01 $\frac{kg}{m^3}$. This research tool was demonstrated to have significant potential to expand upon conventional applications of schlieren.

Focused schlieren improves upon the conventional schlieren diagnostic in use at Tunnel 9 by reducing the depth of sharp focus, the region where density gradients are in focus. Tunnel 9's conventional schlieren system has a depth of focus on the order of 2 m, the spatial resolution of the focused schlieren diagnostic that was built in Tunnel 9 is 1 cm. This dramatic decrease in the depth of sharp focus opens new possibilities for hypersonic flow visualization. This narrow depth of sharp focus allows for flow in specific planes to be imaged without unwanted flow such as thermal gradients, shocks emanating from probes, and the boundary layer along the wind tunnel wall being imaged. As shown in this research, this narrow region of sharp

focus allows for phenomena, such as second-mode instability waves, to be imaged, in the hypersonic boundary layer.

Deflectometry improves the temporal resolution of the data that can be acquired from schlieren images from being on the order of the camera frame rate to being capable of measuring density fluctuations up to 450 MHz, the limit of the photomultiplier tube. This new tool for Tunnel 9 is a significant contribution to the facility's flow measurement capabilities. Deflectometry is designed to measure the frequency of density fluctuations in boundary layer phenomena and adds a new capability for measuring second-mode waves. This tool is advantageous because it is extremely flexible. In order to increase the number of measurement locations, researchers only need to add photomultiplier tubes and fiber optic cables in the image plane. Mounting a fiber optic cable is much simpler than physically mounting a new gage in the surface of a model. Once installed, the fiber optics can quickly be repositioned to allow for different points in the flow to be examined for each run. In light of these technical contributions, focused schlieren and deflectometry have a lot of potential to aid in new research and development in wind tunnels.

5.1 Summary of Results

The unique capabilities of focused schlieren and deflectometry were demonstrated during the AFOSR sponsored sharp nosed transition cone experiment. The goals of this experiment were to image second-mode instability waves and measure their frequency in the hypersonic boundary layer. The goals of this research were

accomplished as shown in the previous chapters. These waves were imaged at two different unit Reynolds numbers and their frequencies were measured successfully at different points in the boundary layer.

5.1.1 Focused Schlieren Visualization

The initial development of the focused schlieren diagnostic in the Mach 3 calibration laboratory nozzle produced extremely sharp and sensitive images of the flow capable of imaging in detail flow over a wedge and sphere. Flow phenomena such as separation and the boundary layer were imaged with this diagnostic without imaging any aberrations present in the wind tunnel windows. The characteristics of the initial focused schlieren design can be seen in table 3.3. This set-up was critical to improving the diagnostic for implementation in Tunnel 9.

The Tunnel 9 large scale focused schlieren diagnostic was an evolution of the initial calibration laboratory design. A summary of the design characteristics of this diagnostic can be seen in table 3.5. The Tunnel 9 set-up improved significantly upon the previous diagnostic in the calibration laboratory. The field of view was increased, the image blending was improved, and the sensitivity is approximately a four-fold improvement upon the previous diagnostic. The depth of sharp focus increased slightly, however this is insignificant given the ten-fold increase in the optical axis of the Tunnel 9 focused schlieren system in comparison to the calibration laboratory.

Second-mode waves were successfully imaged in $1.0x10^6$ $Re\#/ft$ and $2.0x10^6$ $Re\#/ft$ Mach 10 flow. These waves are very difficult to image due to their high

frequencies. To overcome this, a copper vapor laser with 25 *nsec* duration pulses was used to capture still images of the fluid motion. Conventional schlieren is not well suited for imaging second-mode waves due to out of plane disturbances being imaged in addition to the waves. These disturbances would make it difficult to pick out these waves in the image. The narrow depth of field of the focused schlieren system developed for Tunnel 9 makes it uniquely suited to imaging these waves. The images of the second-mode waves highlight the flow information that can be acquired using this diagnostic. In several frames it was possible to see the laminar boundary layer followed by the second-mode waves which then broke down into turbulence.

The following are critical lessons learned in the course of developing the focused schlieren system.

- A diffuser is necessary to prevent grid lines from being predominant in the final image.
- The source grid must have opaque, equally spaced lines for maximum sensitivity.
- The cut-off grid must be focused properly using a high quality lens.
- The cut-off grid must be adequately exposed using a high contrast lithographic film for producing high contrast negatives with opaque grid lines.
- Improper alignment of the cut-off grid will result in unwanted patterns, poor sensitivity, and poor depth of field.

5.1.2 Deflectometry

Deflectometry is a non-intrusive diagnostic for measuring the frequency of density fluctuations. This diagnostic was tested and developed by measuring the characteristic frequency of different pipe lengths in a Mach 3 flow. The frequencies were predicted using pipe organ theory and were verified using a Kulite pressure transducer in the rear of the pipe cavity. The deflectometry results matched the predicted and Kulite gage results perfectly, as seen in table 4.1. This set-up in the calibration laboratory was critical to improving the signal to noise ratio of the deflectometry diagnostic.

The deflectometry diagnostic is a major contribution to hypersonic testing. This tool opens new avenues of experimentation. The potential was demonstrated by accurately measuring the frequency of second-mode instability waves. These measurements were verified using PCB pressure transducers mounted the model's surface. The deflectometry diagnostic non-intrusively measured these waves within 2% of the intrusive pressure transducers. The standard deviation was on the order of 10 kHz. This method is a significant addition to the methods used to measure second-mode waves [6]. Previous attempts to measure these waves non-intrusively using LDI proved difficult with mixed results. Deflectometry is much simpler to implement and more flexible than this technique. This allows for multiple measurements to be taken easily which will aid in the understanding of the formation and propagation of these waves. The benefits of being a non-intrusive diagnostic will be extremely useful to future research into this phenomena. The ease of set-up and

ability to quickly rearrange measurement locations is a critical feature of this tool.

The critical lessons learned from the development of deflectometry can be summarized as follows.

- Deflectometry is only as sensitive as the accompanying focused schlieren diagnostic.
- The ratio of the image's illumination without cut-off to the illumination of the image with full cut-off must be as high as possible to reduce signal to noise.
- A 1000 Ω preload on the preamp is required to avoid losing frequency resolution and to reduce the photomultiplier tube output to avoid saturation.
- Dry ice is critical for reducing noise on the photomultiplier tube.
- The effects of different gain settings must be understood in order to reduce the amount of noise present.

5.2 Technical Contributions

A non-intrusive focused schlieren and deflectometry diagnostic capable of measuring second-mode waves was developed for hypersonic wind tunnel applications. This diagnostic opens new avenues for research in hypersonic wind tunnel experiments. Advancing hypersonic technologies requires substantial research into hypersonic boundary layer phenomena. Knowledge of the transition location is critical to understanding the heating and lifting properties of hypersonic vehicles. Without reliable prediction techniques, sustained hypersonic travel will remain infeasible.

Being able to accurately predict where transition occurs and the underlying contributing factors to boundary layer phenomena is critical to the design of the next generation of hypersonic vehicles [7]. Improving the understanding of second-mode wave propagation and formation is a key part of this research. As this research has shown by successfully measuring second-mode waves, this diagnostic adds unique capabilities to hypersonic wind tunnel testing. These capabilities are an excellent tool for researching hypersonic flow phenomena and can play a key part of future aerospace developments. These contributions have two parts, the improvement of the focused schlieren technique and the application of deflectometry.

The focused schlieren diagnostic adds new capabilities to the Tunnel 9 hypersonic wind tunnel. This imaging diagnostic is capable of imaging flows in densities as low as 0.01 $\frac{kg}{m^3}$ (free stream) with a large field of view (25 cm), for a focused schlieren diagnostic. The narrow region of sharp focus inherent to focused schlieren, allows for phenomena to be imaged without out-of-plane disturbances appearing in the final image. As a result, multiple models can be tested simultaneously to reduce the number of necessary wind tunnel runs, which reduces cost. These disturbances include thermal gradients, noise emanating form the wind tunnel wall, shock waves due to probes or other models, and even pits in the wind tunnel windows. This diagnostic is an improvement over the previous conventional schlieren due to its focusing ability which allows for quantitative data from the schlieren image to be measured using deflectometry.

The high frequency response, spatial resolution, and sensitivity of deflectometry is a significant contribution to this field. Non-intrusive measurements of second-

mode waves opens many new experiments to better understand the development and propagation of these waves. Deflectometry's frequency response is primarily limited by the rate of capture by the oscilloscope. This allows for a significant array of phenomena to be investigated. The integration with focused schlieren allows for the deflectometry diagnostic to measure frequencies that are present in a 1 mm wide region parallel to the test object and less than 1 cm along the optical axis. This ability gives the researcher significant confidence in where the measurements are being made. A feature of deflectometry that makes it well suited for wind tunnel testing is that it can quickly be repositioned to examine any region of the flow. When applied to researching second-mode waves, fibers can quickly be repositioned anywhere along the boundary layer to acquire frequency information at a new point. Increasing the number of measurements is straight forward by simply adding more fibers and photomultiplier tubes. As an example, a bundle of fiber optics could be used in conjunction with this diagnostic to track the evolution of these second-mode instability waves in the boundary layer.

A key contribution of this thesis is the simplification of the development process for focused schlieren and deflectometry diagnostic tools. The source grid is an important component but is complicated to make properly. A new method for creating a custom source grid was introduced in this thesis. Source grids of any dimension can quickly and accurately made by printing the grid as a vinyl decal and adhering it to a sheet of Lexan®. The most important component is the cutoff grid, which is responsible for the diagnostic's sensitivity to density gradients, the depth of field, and over all image quality. A new method was introduced using

pulsed light sources for exposing film to create negatives of the source grid. Using lithographic film for creating cutoff grids is required for best performance of the focused schlieren system. Deflectometry was improved by streamlining the process of mounting equipment and optimizing the signal to noise ratio. Previous work using deflectometry have used dry ice which was shown in this work to significantly improve the signal to noise ratio of this diagnostic.

These contributions to hypersonic research through the improvement of the techniques behind focused schlieren and deflectometry are summarized as follows:

- Developed a new non-intrusive method for measuring second-mode instability waves
- Demonstrated the utility of using focused schlieren for imaging flow phenomena such as second-mode instability waves
- Developed a new technique for creating scalable source grids with opaque lines
- Developed an improved method for creating high contrast cutoff grids using a pulsed light and lithographic film
- Applied new techniques for improving the deflectometry signal to noise ratio

5.3 Future Research

Focused schlieren and deflectometry successfully measured and imaged second-mode instability waves in the hypersonic boundary layer; however there are several areas of improvement for this diagnostic. The focused schlieren system sensitivity

could be improved by increasing the light intensity. This allows for the system to be cutoff more while maintaining the illumination at a usable level for imaging purposes. The current system featured optics that were fixed in location due to the test constraints. A rigid, portable stand alone diagnostic could improve the flexibility and performance of this diagnostic. This system would allow for the component spacing to be optimized for improving the image quality and sensitivity. Another advantage of a stand-alone system is that it could easily be moved to allow for a larger field of view or for specific regions to be more easily examined.

In addition to improving the focused schlieren and deflectometry diagnostic, new applications for this diagnostic should be investigated. The narrow depth of field of focused schlieren makes it a suitable candidate for being used for particle image velocimetry (PIV). This method uses PIV software, with a pair of focused schlieren images that were taken several microseconds apart, to create a velocity map of the flow. This application could be extremely valuable for hypersonic testing because it current PIV techniques are not practical due to the extremely small particle size required to faithfully follow the flow. This would improve the diagnostic be increasing the amount of quantitative information that this diagnostic provides.

A future application of deflectometry in hypersonic flow could be increasing the number of measurement locations. This could allow for phenomena, such as second-mode instability waves, to be examined as they move along the surface of the model. If these fibers are spaced closely enough, velocity information could be gathered. The data from each sensor is correlated to determine the velocity based upon the time delay and spacing of the fiber optics. An extension of this would be to

see if a high-speed (on the order of 1 MHz) ICCD camera could be used to acquire similar information as the deflectometry diagnostic. Currently, deflectometry is capable of providing very precise frequency information. However, acquiring further information on the amplitude of density fluctuations would be invaluable and needs to be investigated.

This research has shown focused schlieren and deflectometry to be a very promising technique. This diagnostic is capable of imaging density gradients in a wind tunnel with a narrow region of sharp focus. The deflectometry diagnostic has shown itself extremely well suited to measuring the frequencies of different flow phenomena non-intrusively. These diagnostic tools will be a useful addition to the tools available to experimental researchers to further the development of aerospace technologies.

Appendix A

Matlab FFT script

```
% FFT Program by Colin VanDercreek with code from Matthew Borg of AFRL
clear all
close all
clc
tic

num_wind=100; %Number of windows in signal
col={'b','r','g','k'};
%Locate Data
[temp_raw_name,temp_raw_location] = uigetfile('*.txt','Select the Raw D
if isequal(temp_raw_name,0)
    disp('User selected Cancel')
else
    disp(['User selected', fullfile(temp_raw_name, temp_raw_location)])
end
temp_prompt = {'Sample Rate [Samples/s]:','Low Pass Filter [Hz]:'};
temp_dlg_title = 'Data Aquisition Characteristics';
temp_num_lines = 1;
temp_def = {'5000000s','3000'};
temp_characteristics = inputdlg(temp_prompt,temp_dlg_title,temp_num_lin
temp_characteristics_string=char(temp_characteristics);
temp_characteristics=str2num(temp_characteristics_string);
Sample_Rate=temp_characteristics(1); %Samples per second
lowpass_filter=temp_characteristics(2);

%Create Pathway to file so that it can be loaded into Matlab
temp_raw_data_name=strcat(temp_raw_location,temp_raw_name);

%Load data
temp_raw_data=dlmread(temp_raw_data_name);
temp_L=length(temp_raw_data);
t=1:length(temp_raw_data);
nfft=4096;%round(length(pcb_temp)/num_wind);
sf = Sample_Rate;
% Perform FFT
h=spectrum.welch('blackman',nfft,30);
```

```
spect=psd(h,temp_raw_data,'Fs',sf);

a=semilogy(spect.freq/1000,spect.data);
%hold on
set(a,'linewidth',2)
power=spect.data;
temp=axis;
axis([0 2000 10E-12 power(1)])
b=xlabel('Frequency (kHz)');
c=ylabel('psi^2/Hz');
d=title('Run 29, L = 1.5"');

%legend('x/L=0.298','x/L=0.361','x/L=0.423','x/L=0.486')
set(gcf,'color','white')
set(gca,'fontsize',16)
set(b,'fontsize',16)
set(c,'fontsize',16)
set(d,'fontsize',16)

toc
freq = spect.freq;
data = spect.data;
```

Bibliography

[1] J. D. Anderson. *Hypersonic and High Temperature Gas Dynamics*. AIAA, 2000.

[2] T. W. Robarge and S. P. Schneider. Laminar boundary-layer instabilities on hypersonic cones: Computations for benchmark experiments. 35th Fluid Dynamics Conference, AIAA Paper 2005-5024, June 2005.

[3] D. Marren, M. Lewis, and L. Q. Maurice. Experimentation, test, and evaluation requirements for future airbreathing hypersonic systems. *Journal of Propulsion and Power*, 17(6):1361–1365, 2001.

[4] A. Pope. *Wind-Tunnel Testing*. John Wiley & Sons, 2 edition, 1954.

[5] R. H. Korkegi. *Hypersonic Aerodynamics*. Training Center for Experimental Aerodynamics, Course Note 9 1962.

[6] T. Roediger, H. Knauss, M. Estorf, S. P. Schneider, and B. V. Smorodsky. Hypersonic instability waves measured using fast-response heat-flux gauges. *Journal of Spacecraft and Rockets*, 46(2):266–273, March - April 2009.

[7] S. P. Schneider. Hypersonic laminar-turbulent transition on circular cones and scramjet forebodies. *Progress in Aerospace Sciences*, 40:1–50, 2004.

[8] K. M. Casper, S. J. Beresh, J. F. Henfling, R. W. Spillers, B. Pruett, and S. P. Schneider. Hypersonic wind-tunnel measurements of boundary-layer pressure fluctuations. AIAA 39th Fluid Dynamics Conference, AIAA Paper 2009-4054, June 2009.

[9] A. J. Smits, M. Pino Martin, and S. Girimaji. Current status of basic research in hypersonic turbulence. Number AIAA 2009-151. 47th AIAA Aerospace Sciences Meeting, 2009.

[10] D. Sahoo, M. J. Ringuette, and A. J. Smits. Experimental investigation of a hypersonic turbulent boundary layer. Number AIAA 2009-780. 47th AIAA Aerospace Sciences Meeting, 2009.

[11] A. J. Smits, K. Hayakawa, and K. C. Muck. Constant-temperature hot-wire anemometer practice in supersonic flows. Number AIAA 1983-0050. AIAA 21st Aerospace Sciences Meeting, 1983.

[12] S. Garg and G. S. Settles. Measurements of a supersonic turbulent boundary layer by focusing schlieren deflectometry. *Experiments in Fluids*, 25:254–264, 1998.

[13] H. Schardin. Schlieren methods and their applications. *Egrebnisse der Exakten Naturwissenschaften*, 20(303-439), 1942.

[14] G. S. Speak and D. J. Walters. Optical considerations and limitations of the schlieren method. Technical Report R & M 2859, British Aeronautical Research Council, 1954.

[15] J. Brackenridge and J. Peterka. Criteria for quantitative schlieren interferometry. *Applied Optics*, 6(4):731–735, 1967.

[16] S. S. McIntyre, E. Stanewsky, and G. S. Settles. An optical deflectometer for the quantitative analysis of turbulent structures. International Congress on Instrumentation in Aerospace Simulation Facilities, CH3028-8/91/0000-003, October 1991.

[17] P. T. Tokumaru and P. E. Dimotakis. Image correlation velocimetry. *Experiments in Fluids*, 19(1):1–15, 1995.

[18] J. Weiss and N. Chokani. Integration properties of the focusing schlieren deflectometer. Number AIAA 2006-2810. 25th AIAA Aerodynamic Measurement Technology and Ground Testing Conference, 2006.

[19] R. W. Fish and K. Parnham. Focussing schlieren systems. Technical Report Technical Report No. I.A.P. 999, Aeronautical Research Council, 1951.

[20] L. R. Boedeker. Analysis and construction of a sharp focussing schlieren system. Masters thesis, Massachusets Institute of Technology, July 1959.

[21] L. M. Weinstein. An improved large-field focusing schlieren system. AIAA 29th Aerospace Sciences Meeting, AIAA Paper 91-0567, January 1991.

[22] L. M. Weinstein. Large-field high-brightness focusing schlieren system. *AIAA Journal*, 31(7):1250–1255, July 1993.

[23] F. S. Alvi and G. S. Settles. A sharp-focusing schlieren optical deflectometer. AIAA 31st Aerospace Sciences Meeting and Exhibit, AIAA Paper 93-0629, January 1993.

[24] S. H. Collicott and T. R. Salyer. Noise reduction properties of a multiple-source schlieren source. AIAA 24th Fluid Dynamics Conference, AIAA Paper 93-2917, 1993.

[25] S. P. Cook and N. Chokani. Quantitative results from the focusing schlieren technique. Number AIAA 93-0623. 31st Aerospace Sciences Meeting, 1993.

[26] E. Gartenberg, L. M. Weinstein, and E. E. Lee. Aerodynamic investigation with focusing schlieren in a cryogenic wind tunnel. *AIAA Journal*, 32(6):1242–1249, June 1994.

[27] G. L. Pellet, W. L. Roberts, L. G. Wilson, W. M. Humphreys, S. M. Bartram, L. M. Weinstein, and K. M. Issac. Structure of hydrogen-air counterflow diffusion flames obtained by focusing schlieren, shadowgraph, piv, thermometry, and computation. Number AIAA 94-2300. 25th AIAA Fluid Dynamics Conference, 1994.

[28] M. J. Hargather, M. J. Lawson, G. S. Settles, L. M. Weinstein, and S. Gogineni. Focusing-schlieren piv measurements of a supersonic turbulent boundary layer. Number AIAA 2009-69. 47th AIAA Aerospace Sciences Meeting, 2009.

[29] D. R. Jonassen, G. S. Settles, and M. D. Tronosky. Schlieren "piv" for turbulent flows. *Optics and Lasers in Engineering*, 44:190–207, 2006.

[30] F. A. Jenkins and H. E. White. *Fundamentals of Optics*. McGraw-Hill, 3rd edition, 1957.

[31] B. P. Petitjean, K. Viswanathan, D. K. McLaughlin, and P. J. Morris. Space-time correlation measurements in subsonic and supersonic jets using optical deflectometry. AIAA 28th Aeroacoustics Conference, AIAA Paper 2007-3613, 2007.

[32] M. J. Doty and D. K. McLaughlin. Two- point correlations of density gradient fluctuations in high speed jets using optical deflectometry. 40th AIAA Aerospace Sciences, January 2002.

[33] G. S. Settles. *Schlieren and Shadowgraph Techniques*. Springer-Verlag, 2001.

[34] J. D. Kim and S. O. Park. Unstead characteristics of hypersonic forward facing cavity flow. AIAA 18th Applied Aerodynamics Conference, AIAA Paper 2000-3925, 2000.

[35] J. W. Hosch and J. P. Walters. High spatial resolution schlieren photography. *Applied Optics*, 16(2), February 1977.

[36] T. J. Juliano, R. Segura, M. P. Borg, K. M. Casper, M. J. Hannon, B. M. Wheaton, and S. P. Schneider. Starting issues and forward-facing cavity resonance in a hypersonic quiet tunnel. Number AIAA 2008-3735. AIAA 38th Fluid Dnamics Conference, 2008.

[37] T. Salyer, S. H. Collicott, and S. P. Schneider. Feedback stabilized laser differential interferometry for supersonic blunt body receptivity experiments. Number AIAA-2000-0416. AIAA 38th Aerospace Sciences Meeting, 2000.